Anatoly Surzhikov
Elena Lysenko

Creation and Accumulation of Radiation Defects in Single Crystals of Magnesium Oxide

Research Aims and Methodology

Springer

Creation and Accumulation of Radiation Defects in Single Crystals of Magnesium Oxide

Anatoly Surzhikov · Elena Lysenko

Creation and Accumulation of Radiation Defects in Single Crystals of Magnesium Oxide

Research Aims and Methodology

Springer

Anatoly Surzhikov
Tomsk Polytechnic University
Tomsk, Russia

Elena Lysenko
Tomsk Polytechnic University
Tomsk, Russia

Edited by
Alexander Rogachev
Research Institute of Physics and Chemistry
Francisk Skorina Gomel State University
Gomel, Belarus

Olga Galtseva
Tomsk Polytechnic University
Tomsk, Russia

ISBN 978-3-031-60206-1 ISBN 978-3-031-60207-8 (eBook)
https://doi.org/10.1007/978-3-031-60207-8

This Springer imprint is published by the registered company Springer Nature Switzerland AG
The registered company address is: Gewerbestrasse 11, 6330 Cham, Switzerland

Preface

Oxides of alkaline earth metals (OAEM) occupy a special place among structural materials as the main raw material in the production of high-quality insulation from ceramics and glass. There is also a great interest in the research of SCM determined by the use of these materials as scintillators for the registration of nuclear radiation, thermoluminescent dosimeters, active elements of optical quantum generators and storage devices, the front wall of thermonuclear reactors, through-pass insulators of nuclear power plants. For the practical use of products made of OAEM in irradiation conditions, it is necessary to solve the fundamental problem of radiation materials science—the establishment of the structure of radiation defects, the mechanisms of their creation and the laws of accumulation. To date, some success has been achieved in this direction. However, the main results relate to the area of low and medium levels of radiation excitation. For such levels of excitation, extremely high radiation intensity has been reliably established.

However, the range of problems that can be solved with the use of powerful radiation installations is determined: generation of nanosecond ultrahigh-frequency (microwave) pulses, collective acceleration of charged particles, the implementation of a controlled fusion reaction and the creation of high-power lasers. In this edition, the questions posed for the SCM were solved using the example of single crystals of magnesium oxide.

By the beginning of the authors' work, the structure of the color centers induced by radiation in magnesium oxide, the positions of the maxima of the optical absorption and luminescence bands, as well as the values of their half-widths and the temperature range of stability were sufficiently established. There is practically no information about the location of internode ions in magnesium oxide crystals, and methods for their registration have not been worked out. These data are particularly important, since the efficiency of the accumulation of radiation defects depends to a certain extent on the efficiency of fixing displaced ions in the crystal lattice.

It is considered established that the creation of radiation defects in magnesium oxide occurs as a result of elastic collisions of incoming particles with crystal-forming particles and the knocking out of the latter into the internodes. However, all studies confirming this point of view were carried out using low and medium levels of arousal.

The effect of high absorbed radiation energy capacities on the formation and accumulation of radiation defects in magnesium oxide crystals has not been practically studied. It is quite realistic to expect specific radiation-stimulated phenomena with such excitations. In the field of radiation defect formation of solids under the action of powerful radiation fluxes, it is realistic to expect the implementation of new mechanisms for generating radiation defects, the possibility of creating Frenkel defects in solids at high excitation densities due to the decay of multiparticle electronic excitations.

As for systems with a dominant shock mechanism for generating radiation defects at low and medium levels of excitation, in particular magnesium oxide, the collective interaction of elementary excitations can lead to non-elementary processes of creating Frenkel defects. Prior to the preparation of this monograph, there were only separate, scattered publications in the periodical press on all the issues raised.

Tomsk, Russia

Anatoly Surzhikov
Elena Lysenko

Introduction

Alkaline earth metal oxides (AEMO) occupy a special place among structural materials as the main raw material in the production of high-quality insulation from ceramics and glass.

Great interest in the research of AEMO is also determined by the use of these materials as scintillators for detecting nuclear radiation, thermoluminescent dosimeters, active elements of optical quantum generators and memory devices, the front wall of thermonuclear reactors, and bushing insulators of nuclear power plants.

It is necessary to solve the fundamental problem of radiation materials science: to establish the structure of radiation defects, the mechanisms of their creation and the laws of accumulation for the practical use of products made of AEMO under irradiation conditions.

To date, some progress has been made in this direction. However, the main results relate to the region of low and medium levels of excitation by radiation, the extremely high radiation resistance of AEMO crystals has been reliably established for such excitation levels.

However, a range of problems is defined that can be solved with the use of powerful radiation facilities: generation of nanosecond microwave pulses, collective acceleration of charged particles, the implementation of a controlled thermonuclear fusion reaction and the creation of high-power lasers.

The questions posed for AEMO were solved on the example of magnesium oxide single crystals in this monograph.

The structure of the color centers induced by radiation in magnesium oxide, the positions of the maxima of the optical absorption and luminescence bands, as well as the values of their half-widths and the temperature range of stability, were quite fully established by the beginning of the work of the author.

There is practically no information about the place of fixing of interstitial ions in magnesium oxide crystals, and methods for their registration have not been worked out.

These data are of particular importance, since the efficiency of accumulation of radiation defects depends to a decisive extent on the efficiency of pinning displaced ions in the crystal lattice.

It is considered established that the creation of radiation defects in magnesium oxide occurs as a result of elastic collisions of incident particles with crystal-forming particles and knocking out of the latter into interstices.

However, all studies supporting this view have been done using low and middle levels of arousal.

The effect of high powers of absorbed radiation energy on the formation and accumulation of radiation defects in magnesium oxide crystals has not been practically studied. It is quite realistic to expect specific radiation-stimulated phenomena under such excitations.

It is realistic to expect the implementation of new mechanisms for the generation of radiation defects, the possibility of creating Frenkel defects in solids at high excitation densities due to the decay of many-particle electronic excitations in the field of radiation defect formation of solids under the action of powerful radiation fluxes [1].

The collective interaction of elementary excitations can lead to non-impact processes of the creation of Frenkel defects with regard to systems with a dominant impact mechanism of generation of radiation defects at low and middle levels of excitation, in particular, in magnesium oxide.

Contents

Chapter 1
Structure, Properties, Point Defects and Radiation Defect Formation in Magnesium Oxide Crystals

Contents

The interpretation of any processes occurring in a solid under radiation exposure should be based on the available information on the fundamental properties of the substance under study, on a clear definition of the boundaries within which it is legitimate to transfer any ideas developed for a different type of solid. To this end, this section briefly considers the main crystal-physical properties, the band structure, and the dominant types of defects in the crystal lattice of MgO single crystals.

A. Surzhikov and E. Lysenko, *Creation and Accumulation of Radiation Defects in Single Crystals of Magnesium Oxide*, https://doi.org/10.1007/978-3-031-60207-8_1

1.1 Structure and Properties of MgO Crystals

1.1.1 Crystal Physical Properties

MgO crystals are divalent structural analogues of alkali halide crystals (AHC) and have a face-centered cubic lattice of the NaCl type (space group Fm3m), representing the densest cubic packing of O_2 ions, the octahedral voids of which are occupied by Mg^{2+} ions.

Magnesium oxide belongs to the class of ionic compounds with a charge of crystal-forming ions close to 2.

At the same time, quantum mechanical calculations and X-ray spectral measurements of the electron density indicate an ion charge of $2 = 1.01$ [2], which allows some authors to refer MgO to covalent compounds [2] or to intermediate between ionic and covalent crystals [3].

Apparently, such a divergence of points of view can be explained by the large diffuseness of the oxygen valence electron cloud, as a result of which the oxygen charge turns out to be close to 1. In this case, the electrons do not localize on Mg^{+2} (with its transformation into Mg^{+l}), and belong oxygen orbitals.

1.1.2 Energy Electronic Structure of MgO

The Brillouin zone is a cuboctahedron with characteristic points $G(Q_h)$, $\Delta(C_{4v})$, $\Delta(C_{3v})$ $\sum(C_{2v})$, $X(D_{4h})$. $L(D_{3d})$, $K(C_{2v})$ in face-centered cubic lattices of the NaCl type. The lower valence band is formed from the 2S orbitals of oxygen. The upper valence band is formed from the 2P-orbitals of oxygen with the participation of the 3S-orbitals of magnesium. The conduction band consists of Mg 3S orbitals. The width of the band gap is determined by the energy gap at the point G (transition $G_{15} - G_1$).

The spectra ε_1 and ε_2 (the real and imaginary parts of the permittivity) in the region of fundamental absorption at this scheme describes the centers of absorption and reflection.

Peaks at 7.689, 7.715, 7.752 and 7.768 eV are distinguished in the reflection spectra at the fundamental absorption edge [1]. Peaks are observed (according to the ε_2 spectrum) at 10.8, 13.3, 16.8, 17.3, 20.5 eV, corresponding to interband transitions in the shorter wavelength region.

Peaks in the region of 7.7 eV are attributed to exciton transitions at the G-point of the Brillouin zone ($G_{3/2}$ and $G_{1/2}$ are excitons). The peak at 22 eV (determined from the characteristic losses) is due to the excitation of plasma oscillations [5]. The value of the fundamental absorption edge is obtained (at 77 K) 7.77 eV by subtracting the exciton structure. This value can be taken as the band gap.

The calculated values of the width of the valence band of MgO differ significantly from the corresponding values in AHC.

Width of valence band is 5.0 eV [6] within the framework of the cluster model; it is 7.0 eV [7], according to other calculations. The width of the valence band was determined as 8.5 eV [8] from X-ray spectroscopy data (based on the width of the K-band of oxygen). On the whole, the valence band width averaged over various data can be assumed to be 7 eV.

As indicated above, the maximum found in the region 7.77 eV in the spectra ε_1 and ε_2 is attributed to the excitation of exciton states at the G-point of the Brillouin zone.

It was possible to establish the doublet structure of this maximum, due to the spin–orbit splitting of the exciton. The components of the doublet at 7.69 eV and 7.76 eV correspond to the hole component of the exciton with $j = 3/2$ and $j = 1/2$, respectively [1, 5]. The strength of the transition oscillator in the doublet is estimated to be 0.035 and 0.017, respectively. The calculated binding energy of the $G_{3/2}$—exciton according to the Wannier model is 80 meV [5], which is much less than the corresponding value for AHC. The Bohr radius of the exciton is about 30.5 Å, i.e. it is more by 15 times the interion distance.

MgO X-ray excitons are much more thermally stable. In particular, an exciton arises with $r \approx 1$ Å and the binding energy is estimated at 0.5 eV upon excitation of an electron from the $L_{II,III}$—level of Mg [9]. In this case, a sharp maximum of X-ray absorption appears at 54.0 eV (α is absorption).

The calculated data on the effective mass of holes and excitons at various points of the Brillouin zone are found in accordance with the large width of the valence band [7]. The average value of the effective mass of a hole in the flux of the valence band is 0.77 m_o (m_o is the mass of a free electron). The isotropic mean effective mass is $0.76 \cdot m_o$. The effective mass of the optical exciton is significantly small, amounting to $0.38 \cdot m_o$.

Elementary electronic excitations in MgO are highly mobile having such a small effective mass. Hole and exciton self-trap effects, characteristic of AHC, are not observed in MgO crystals. Indeed, it was not possible to detect the molecular ion m_2^{3-} (relaxed hole) by the electron paramagnetic resonance (EPR) method [10, 11]; studies of the edge luminescence of MgO showed the absence of self-trapped states of G-excitons [12, 13].

More detailed studies of the short-wavelength luminescence of MgO made it possible to isolate the luminescence band at 6.9 eV, which is identified with the radiative annihilation of relaxed single-center excitons [14].

It was found that the states of free and relaxed excitons are separated by a potential barrier with a height of about 40 meV; relaxation of excitons occurs at temperatures above 80 K. The high mobility of holes appears in electrotransport processes at low temperatures; it is reflected in the appearance of peaks of thermally stimulated conductivity at destruction of hole centers [15].

1.1.3 Thermodynamic Equilibrium Defects

Thermodynamically equilibrium defects are Schottky pairs in most ionic dielectrics. Harding determined the formation energy of a Schottky defect, which varied within (3.4–4.0) eV in a cycle of works on the study of self-diffusion of Mg [16–18]. Probably the most reliable value is 3.8 eV [17].

The processes of ion transfer in MgO, as in AHC, are associated primarily with the migration of cationic vacancies. Using the method of labeled atoms, the migration energy of cationic vacancies was determined to be 1.56 eV [17].

This result agrees well with data on the immobility of cation vacancies in magnesium oxide at temperatures below 500 K [19–22]. The calculation results differ significantly from the experimental data on the migration energy of cationic vacancies [23–24]. The cation vacancy migration energy is 2.1 eV in the bulk of the crystal and 1.2 eV on the surface (face (110)), according to the calculation.

The energy of formation of anionic and cationic Frenkel pairs was also calculated [25–27]. The obtained values turned out to be anomalously high and amount to 17.3 eV for an anionic and 7.3 eV for a cationic Frenkel pair. The high formation energies of Frenkel pairs are probably one of the reasons for the increased radiation resistance of magnesium oxide crystals.

The main properties of MgO single crystals are considered in this section. It should be noted that MgO single crystals are qualitatively identical to alkali halide crystals in fundamental characteristics as the ionicity of the chemical bond, the structure of the crystal lattice, the mechanism of ionic electrotransfer and the type of micro- and macrodefects, although the quantitative values of some parameters have more large values (charge of ions, lattice energy, activation energy of ionic electrotransfer).

It is also necessary to emphasize an essential feature of MgO crystals, which is the large width of the valence band.

Therefore, magnesium oxide is characterized by a high mobility of holes and the absence of the effect of their autolocalization.

1.2 Color Centers of MgO Crystals

Various types of point defects are formed in the process of irradiation in oxides of alkaline earth metals (AEM), which are called color centers by analogy with AHC, although many of them are optically inactive. It is generally accepted that point defects in oxides are divided into electronic, hole and interstitial centers, since AEM oxides are identical to AHC in structure and type of chemical bonding.

1.2.1 Electronic Color Centers

Vacant anion sites in the crystal lattice of magnesium oxide have a positive charge close to 2; therefore, the formation of two types of the simplest electronic color centers associated with the localization of one or two electrons on an anion vacancy is possible. These defects are analogues of the F-color centers in AHC and are designated F^+ and F, respectively. The EPR spectrum of the F^+-color center in magnesium oxide was first deciphered in 1957 [28].

It is possible to assume the formation of aggregate centers of the M and R type due to the coagulation of the F-centers by analogy with AHC in magnesium oxide. However, there are no reports of such defects.

Interaction of charged F^+-centers with cationic vacancies is possible in magnesium oxide crystals in contrast to AHC.

In 1961, the appearance of a line similar in characteristics to the signal from the F^+-center in the EPR spectrum of irradiated magnesium oxide crystals with a certain anisotropy of the g-factor [28] was registered, which indicates a violation of the cubic symmetry of the F^+-color center. This defect is called F_c^+ and is an association of an F^+-center and a cation vacancy [29, 30].

The formation in magnesium oxide crystals of an associate of their two F^+-centers and a cationic vacancy (the F_{2t}-center) also seems to be realistic. The existence of such a center was shown by theoretical calculations in [30] and by the EPR method in [32].

1.2.1.1 Optical Absorption

In 1964, Wertz et al. [33] found that the optical absorption band with a maximum at about 5.0 eV correlates with the EPR signal of F^+-centers during thermal annealing of neutron-irradiated magnesium oxide crystals.

Subsequently, an analysis of the change in the absorption coefficient at the maximum of this absorption band during neutron irradiation and thermal annealing confirmed this correlation. It was believed for a long time that the maximum of the optical absorption band of F^+-centers in MgO crystals falls at 5.0 eV [34–36]. The oscillator strength of F^+-centers was experimentally obtained and is 0.8 for MgO crystals irradiated with neutrons [34].

However, the results obtained in [37] cast doubt on such an interpretation of the optical absorption band with a maximum at about 5.0 eV.

The authors studied the optical absorption spectrum and the EPR spectrum in magnesium oxide crystals irradiated with neutrons and additively colored in magnesium vapor. Very good agreement was found between the concentrations of F^+-centers, determined from the EPR spectra and from the absorption coefficient in the band with a maximum of about 5.0 eV for MgO crystals irradiated with neutrons. On the other hand, a very intense band is about 5.0 eV is observed for additively colored

crystals in optical absorption spectra of them, the EPR signal of the F^+-centers is insignificant.

Thus, it can be considered that the optical emission band for the emission of magnesium oxide crystals by neutrons with a maximum value of about 5.0 is due to the absorption of F^+-color centers. In additively colored crystals, insignificant F^+-centers are distinguished, which are absorbed in this region of distribution by any (not F^+) diamagnetic centers. The F-center can be such a center because:

1. F-center should be the main electronic center for reasons of general electrical neutrality in additively colored magnesium oxide crystals.
2. Theoretical estimates of the energy of optical transitions in the F-center for MgO crystals give a value close to 5.0–5.4 eV [38] and 5.05 eV [39].

Therefore, it is reasonable to assume that the optical absorption bands of the paramagnetic F^+ and diamagnetic F-color centers in magnesium oxide crystals practically coincide in position and shape.

This assumption was directly confirmed in [40], whose authors observed the $F \rightarrow F^+$ phototransition similar to that which was carried out for calcium oxide [41].

Most of the color centers are present in the F-state when an additively colored magnesium oxide crystal is in thermodynamic equilibrium. Emission of light from the F-absorption band leads to the transfer of electrons to the conduction band, some of which are captured by impurity centers, as a result of which a decrease in the absorption coefficient in F-band and increase its value in the F^+-band.

F^+-centers are not covered for additively colored magnesium oxide crystals in the EPR spectrum within the sensitivity of the method. The absorption density maximum at a sample temperature of 298 K corresponds to the photon energy of 5.01 eV; the half-width of this band is 0.77 eV. Observations of the resonance of the F^+-centers are observed after the crystal is illuminated by light from the F bands. The position of the maximum absorption concentration is added to 4.92 eV; the half-width becomes 0.62 eV.

A study [40] showed that the shift of the maximums of optical absorption bands of F^+ and F-color centers and the change in their half-widths in the temperature range (77–300) K content is insignificant and does not exceed of 5%.

Using the value of the oscillator strength of 0.8 for the F^+-center [34], the authors of [40, 42] obtained a value close to unity for the oscillator strength of the F-center (1.25 [42] and 0.7 [40]).

The maximum destruction of F_c^+-centers was found of 3.6 eV at a light photon energy, when magnesium oxide crystals were bleached by monochromatic light with a wavelength in the range (2500–6500) Å [40]; therefore, it can be roughly considered responsible for the absorption band with a maximum of about 3.6 eV F_c^+-centers. There are no data on the optical absorption of F_{2t}-centers.

1.2.1.2 Luminescence of Electronic Color Centers

It is possible, by exciting the crystal with light from the F-band, to determine the parameters of the luminescence bands of these centers, knowing the position of the optical absorption bands of the F-type color centers.

Such an experiment was carried out in [42]. In the photoluminescence spectrum of magnesium oxide crystals irradiated at 80 K with high-energy (2 meV) electrons, intense luminescence was observed in the band with a maximum of about 3.13 eV when illuminated with light from the absorption band of F-centers. The half-width of the band was 0.6 eV.

To verify the responsibility for this luminescence band of F-type color centers, the authors studied the change in the luminescence intensity in the band with a maximum at 3.13 eV and the change in the optical absorption coefficient in the F-band with an increase in the absorbed radiation energy of high-energy electrons.

It was found that the intensity of the luminescence band increases monotonically with an increase in the absorption coefficient in the F-band, which confirms the responsibility for the luminescence in the band with a maximum at 3.13 eV of the F-type color centers.

To determine specifically which of the color centers (F^+ or F) corresponds to the luminescence in the band with a maximum at 3.13 eV, it is essential to recall that neutron irradiation leads to the accumulation of predominantly E^+-centers in magnesium oxide crystals, and the additive coloring of F-centers.

Based on this, the authors studied the photoluminescence spectra (illumination from the F-absorption band) of MgO crystals irradiated with neutrons and additively colored in magnesium vapor [40].

It turned out that, the photoluminescence spectrum exhibits luminescence in a band with a maximum at 3.16 eV for crystals irradiated with neutrons at room temperature. The half-width of the band is 0.66 eV. The position of the luminescence band maximum shifts to 3.22 eV at half-width of 0.59 eV at 77 K.

Only luminescence is observed in the band with a maximum at 2.4 eV (half-width is 0.65 eV) in the photoluminescence spectrum of additively colored magnesium oxide crystals. The spectra obtained at room temperature and liquid nitrogen temperature differed insignificantly.

The luminescence in the band with a maximum at 2.4 eV was also manifested in the thermoluminescence spectra, when additively colored crystals that experienced the $F \rightarrow F^+$ phototransition were subjected to heating [40]. In such a process, electrons thermally released from localized states are captured by F^+-centers, forming F-centers in an excited state.

Thus, the emission band with a maximum at 2.4 eV can be attributed to the emission of F-centers.

To observe the luminescence band of F-centers in additively colored crystals, the color density must be substantially greater than the density of capture centers; otherwise the color centers will be transformed into the F^+ state.

There are no data on the luminescence of F_c^+ and F_{2t}.

1.2.1.3 Thermal Stability

In order to determine the thermal stability of electronic color centers in magnesium oxide crystals, the study of the change in the intensity of the absorption band with a maximum at 5.0 eV and the intensity of the luminescence of F-color centers and the measurement of the concentration of F^+-centers were carried out by the EPR method in MgO crystals irradiated with high-energy electrons and additively colored in magnesium vapor, depending on the annealing temperature [43].

The intensity of the luminescence band and the intensity of the EPR signal of F^+-centers at each annealing temperature were measured after the crystal was exposed to light in the ultraviolet region of the spectrum for additively colored crystals.

Since additive coloring generates only F-centers in magnesium oxide, such treatment with UV light leads to the maximum concentration of paramagnetic F^+-centers. It was found that in a crystal irradiated with high-energy electrons, the optical absorption intensity in the F band, the luminescence intensity, and the EPR signal of the F-color centers coincide simultaneously until they almost completely disappear at a temperature of 800 K; this decrease corresponds to this temperature range and is observed at temperatures of 1200 K for additively colored crystals.

These experiments were verified in [42] and similar results were obtained.

The results of such thermal annealing of irradiated and additively colored crystals lead to very interesting conclusions: negative ion vacancies in magnesium oxide crystals remain immobile up to temperatures of 1200 K; the annealing of F^+-centers at lower temperatures observed in irradiated crystals occurs due to the release of interstitial oxygen ions and their recombination with immobile anion vacancies.

The F_c^+-centers in magnesium oxide are extremely thermally stable; they are detected in the EPR spectra after annealing at 1300 K [10].

1.2.2 Hole Color Centers

The hole color centers in magnesium oxide, formed on the basis of cationic vacancies, should probably be a mirror image of electronic color centers.

The simplest hole center is a hole localized on a cation vacancy. It is denoted by the symbol V^- in magnesium oxide. The capture of the cation vacancy of the second hole leads to the formation of a V-center.

In 1959, Wertz [44] discovered for the first time in neutron-irradiated crystals two paramagnetic axial centers with a tetragonal axis along the ⟨100⟩ direction, but with different spins (1/2 and 1) and assigned them to V^- and V-centers, respectively. The optical absorption band in the spectral region of about 2.3 eV, induced in these crystals, was also associated by Wertz with the absorption of these hole centers [45].

This assumption was confirmed by the results of work [46], in which a correlation was established between the amplitudes of the EPR signal of V^-, V-centers and the optical absorption value in the band with a maximum at 2.3 eV during irradiation of magnesium oxide crystals with high-energy (2 meV) electrons. The authors of

this work obtained the value of the oscillator strength of V^- and V-centers (0.1–0.2) combining EPR and optical studies, and the value of the half-width is about 0.96 eV.

Experiments using EPR and double electron-nuclear resonance unambiguously confirmed the correlation between the absorption coefficient in the band with a maximum at about 2.3 eV and the intensity of the EPR signal of V^- and V-color centers [48].

One can expect the existence of an association of an anionic and cationic vacancy with a localized hole and the localization of a hole on the association of an anionic and two cationic vacancies by analogy with electronic color centers in magnesium oxide crystals.

The EPR method has so far managed to detect a defect of the second type, called V_4. However, their concentration is extremely low and amounts to 1% of the number of F centers [49]. Absorption bands due to aggregate hole centers have not been identified either.

Some authors [10, 46] noted the absence of a band with a maximum at 2.3 eV in the optical absorption spectrum of irradiated magnesium oxide crystals. The low concentration of V-centers can be explained by the capture of holes by impurity ions. This seems quite possible at significant levels of contamination of magnesium oxide samples.

Hole color centers in magnesium oxide single crystals in addition to cationic vacancies can also form on other defects that have a negative effective charge with respect to the crystal lattice. Such defects are impurity ions of other valences, isolated or near the cation vacancy.

V_{OH} [47, 50, 51]-, V_{OD} [5147, 52, 54]-, V_F [55–57]-, V_{Al} [55, 57]-, [Li] [58]-, [Na]° [59, 60]-centers have been detected and studied using EPR and electron nuclear double resonance (ENDR), infrared spectroscopy, optical absorption, luminescence and magnetic circular dichroism.

The listed color centers have, as well as V^- and V-centers, axial symmetry; their tetragonal axis is located in the ⟨100⟩ direction. The models of these hole color centers have been established with full reliability.

Attention is drawn to the fact that for all V-type color centers, which include a cationic vacancy, very similar properties are observed.

The [Li]°- and [Na]°-centers differ substantially from other hole centers in magnesium oxide. This is understandable, since in this case the oxygen ion, on which the hole is localized, is located in the immediate vicinity of the impurity ion and, therefore, is perturbed by it. In other cases, the main perturbation is caused by the cation vacancy.

The optical parameters of hole color centers are given in Table 1.1.

It is shown that the destruction of hole color centers is carried out by thermal release of holes. In this case, hole recombination luminescence is observed in the visible and near infrared regions of the spectrum. The impossibility of a detailed study of the luminescence of hole color centers is due to the same value of the maxima of the optical absorption bands (~ 2.3 eV).

Table 1.2 shows data on the thermal stability of hole color centers are given.

Table 1.1 Optical parameters of hole color centers in magnesium oxide single crystals

Center	Position of the absorption band maximum, eV	Absorption band half-width, eV	Transition oscillator strength
V^-	2.33 [61]	0.97 [61, 62]	0.1–0.2 [46, 61, 63]
V	2.3 [61]	0.95 [61]	0.24 [61]
V_{oh}	2.23 (77 K) [62] 2.21 (295 K) [62] 2.19 [64]	0.88 [61], 0.94 [62]	0.1 [62]
V_F	2.33 [61]	0.97 [61]	–
V_{al}	2.32 [64]		–
[Li]°	1.83 74.75 [64, 65]	1.0 [58], 1.1 [66]	0.09 [58]
[Na]°	1.58 [60]	0.7–0.8 [60]	–

Table 1.2 Value of the half-life temperature of hole color centers in single crystals of magnesium oxide

Center	V^-	V	V_{OH}	V_F	V_{Al}	[Li]°	[Na]°
Temperature value (T, [K])	420 [72] 400 [71]	345 [72] 350 [70]	300 [50] 335 [72]	320 [69] 335 [72]	365 [67] 370 [72]	230 [72] 210 [68]	190 [72] 190 [60]

1.2.3 Impurity Color Centers

In view of the significant contamination of magnesium oxide crystals, the formation of color centers in them is possible with the direct participation of impurity ions.

However, the identification of the optical absorption and luminescence bands of these centers is significantly hindered by the change in their valence state as a result of irradiation.

Thus, in [10], the transitions are shown $Ti^{4+} \rightarrow Ti^{3+}$; $V^{3+} \rightarrow V^{2+}$; $Cr^{3+} \rightarrow Cr^{2+}$; $Fe^{1+} \leftarrow Fe^{2+} \rightarrow Fe^{3+}$; $Co^{2+} \rightarrow Co^{l+}$; $Ni^{2+} \rightarrow Ni^{3+}$; $Ru^{2+} \rightarrow Ru^{l+}$; $Pd^{2+} \rightarrow Pd^{3+}$ when studying the states of impurity ions in MgO crystals by the EPR method before and after irradiation with accelerated electrons, gamma and X-rays,

The valence state of some impurity ions of transition metals can also be changed by high-temperature calcination of crystals in various media.

For example, it was found in [73] that the calcination of magnesium oxide crystals in a reducing atmosphere (hydrogen, carbon monoxide) or in vacuum at a temperature of 1600 K converts 99% of iron into the Fe^{2+} state.

Calcining crystals in an oxidizing atmosphere at the same temperature converts 70% of all iron to the Fe^{3+} state in contrast.

The positions of optical absorption bands have been reliably established only for iron ions of all the impurity color centers in magnesium oxide.

The absorption band of Fe^{2+} ions is located in the near infrared region of the spectrum at 10,000 A (10,850 cm^{-1}) [74]. The strength of the oscillator is 7.3×10^{-6} [75]. Since irradiation with ionizing radiation and calcination in an oxidizing

atmosphere lead to the transfer of iron ions in magnesium oxide crystals to the Fe^{3+} state; the optical absorption bands with maxima at 4.3 and 5.7 eV were attributed to the absorption of Fe^{3+} ions [76]. This assumption was confirmed in [46] by the correlation of the change in the impurity iron concentration, determined by chemical analysis, and the absorption intensity in the bands with a maximum at 5.7 and 4.3 eV, as well as by the use of magnetic circular dichroism and EPR methods [77].

Decomposition into Gaussian components of the ultraviolet region of the spectrum for neutron-irradiated magnesium oxide crystals at 4 K gave half-widths of 0.73 eV and 0.96 eV for optical absorption bands with maxima at 4.3 eV and 5.7 eV, respectively [78].

The oscillator strength of the optical transition in Fe^{3+} at 4.3 eV was determined by joint measurements of the intensity of the EPR signal and the intensity of the absorption band with a maximum at 4.3 eV and was found to be 3.8×10^{-2} [75].

It was found by EPR method that Fe^{3+} ions are partially associated with charge-compensating cationic vacancies in magnesium oxide crystals and, possibly, with impurity ions of monovalent metals; as a result of which the defect symmetry decreases to axial and orthorhombic [49]. However, the effect of charge compensators on the optical absorption of Fe^{3+} ions has not been studied.

A number of weak optical absorption bands with maxima at 5.31, 5.68 and 5.94 eV were found for neutron-irradiated magnesium oxide crystals [78], and in the spectral region (5.6–6.0) eV for crystals irradiated with heavy ions [79]. Comparing the intensity of optical absorption in this part of the spectrum with the concentrations of impurity ions, the authors do not exclude the possibility that absorption of Al and Si takes place. Absorption is considered possible in the region of ~ 6 eV for Cr^{3+}, V^{3+}, and Mn^{4+} [10].

The luminescence of impurity color centers has been most thoroughly studied for activated MgO powder phosphors [80]. An intense luminescence band is observed with a maximum at 5.3 eV in the X-ray luminescence spectrum of the MgO-Al powder,

The introduction of F^-, Cl^- and Si^{3+} ions into magnesium oxide leads to the appearance of intense luminescence in the region of 5.1 eV. Luminescence with a maximum of about (5.8–5.9) eV occurs when magnesium oxide is activated by Li or Na ions; luminescence is characteristic in the region of 6.9 eV for the MgO-Ca phosphor.

A distinctive feature of the observed radiation is its strong quenching in the temperature range corresponding to the effective destruction of hole color centers [80, 81]. The authors of these works showed that the luminescence in the ultraviolet region of the spectrum of these phosphors is intense at the stages of annealing of electronic defects and is absent at the stages of annealing of hole defects; on the basis of this, the short-wavelength luminescence was associated with the recombination of electrons with hole centers V_{Al}, [Li]°, [Na]°, V_F, V_{Cl}, V_{Si}, V_{Ca}, We are dealing with indirect activation of magnesium oxide by impurity ions in the phosphors described above. Radiative transitions occur in oxygen ions perturbed by vacancies and impurity ions, which are not directly photoexcited [80].

Ultraviolet luminescence does not appear in MgO-OH when electrons recombine with V_{OH}-centers. Instead, an intense glow is observed in the blue region of the spectrum. During the interaction of electrons with V_{OH}-centers, the energy is easily transferred to the OH^- ions that are part of the recombination centers, which give rise to their characteristic blue glow [80].

The MgO-Sn phosphors are characterized by luminescence in the band with a maximum at 2.9 eV, which manifests itself both upon direct excitation of Sn^{2+}-centers and in the region of intrinsic absorption [81]. Recombination glow can occur both during recombination of electrons with Sn^{3+} and holes with Sn^{1+}-centers. The efficiency of electron recombination luminescence is the same at 80 and 300 K; the efficiency of hole recombination luminescence decreases during the transition from 80 to 300 K, which is associated with thermal ionization of Sn^{1+}-centers.

A number of narrow luminescence bands from 2.51 to 2.58 eV are observed in relatively pure magnesium oxide crystals at 77 K under the influence of X-ray irradiation. Comparison of these bands with the glow bands in magnesium oxide crystals with an admixture of nickel allowed them to be associated with Ni^{2+} ions. The decrease in the intensity of the glow with the time of X-ray irradiation is consistent with the ideas about the conversion of Ni^{2+} to Ni^{3+} under the influence of irradiation [10].

The role of Cr^{2+} and Fe^{2+} ions as luminescence centers in the red and blue regions of the spectrum is considered to be established, respectively [81, 82].

$$Cr^{2+} + \overline{e} \rightarrow Cr^{3+*} \rightarrow Cr^{3+} + hv \text{ (red radiation)}; \tag{1.1}$$

$$Fe^{2+} + p \rightarrow Fe^{3+*} \rightarrow Fe^{3+} + hv \text{ (blue radiation)}. \tag{1.2}$$

1.2.4 Interstitial Defects

There is little direct evidence of the existence of interstitial ions in magnesium oxide crystals. This would not be surprising if radiation disturbances accumulated in the form of Schottky defects, since these defects correspond to the removal of an ion from a regular lattice site to the crystal surface. Therefore, the presence of these defects can be judged indirectly by an increase in the macroscopic size of the crystal with a constant size of the unit cell.

If Frenkel defects are formed, then due to the displacement of ions into the internodes, both the macroscopic size of the crystal and the size of the unit cell should increase. In this case, with a disordered distribution of point defects with isotropic distortion, the change in the volume of the crystal and the parameter of the crystal lattice should occur in the same way.

Changes in the lattice parameter Δa and the volume ΔV of a magnesium oxide crystal were compared with changes in the concentration of intrinsic radiation defects

with a dose of fast neutron irradiation [49]. The irradiation products were recorded by optical methods and the EPR method.

It is found that the change in Δa is comparable to the change in ΔV at a flux of up to 3×10^{19} neutrons·cm^{-2}. This fact indicates the presence of the same number of isolated vacancies and interstitial ions in the crystal.

The correlation found by the authors between the change in Δa, ΔV and the kinetics of accumulation in this range of irradiation doses of F-centers indicates the predominant accumulation of radiation defects in magnesium oxide crystals in the form of Frenkel anion pairs (FAP).

The MgO crystal lattice is tightly packed. The maximum spherical volume of the interstitial space has a radius of 0.30 Å, which is significantly less than the ionic radii of Mg^{+2} and O^{2-} ions [80]. An unfavorable geometric factor makes it difficult to form stable interstitial defects in perfect sections of the crystal.

Therefore, it can be expected that most interstitial centers will contain some additional defects (vacancies, impurities). Indeed, it was noted that with an increase in the Fe impurity content, the accumulation rate of F-type centers increases [3, 83]. In this connection, an assumption is made about the capture of interstitial oxygen on impurities with an excess positive charge relative to the lattice. A similar conclusion is made when studying the EPR of Fe^{+3} ions [84].

The capture of interstitial oxygen on monovalent anion-substituting impurities, in particular on F, was detected by the EPR method in [85, 86]. The $(OF)^{2-}$ molecule is centered on the anionic node and becomes mobile at T ~ 45 K.

Interesting data on stable interstitial defects in MgO were obtained in [71]. The crystals were irradiated with neutrons at 338 K with doses of $(9 \times 10^{16}$–$10^{17})$ neutron·cm^{-2}. EPR spectra and optical absorption in the F-band were measured; three new groups of lines attributed to N_I, N_{II} and N_{III} centers were found in the EPR spectra measured at 77 K.

The authors propose a model of H-centers in the form of an O_2^--molecule placed in an anionic vacancy and associated with a cationic vacancy. The O_2^--molecule is formed when oxygen ions displaced into internodes form a chemical bond with anions located in the lattice nodes. The composition of the N_{III}-center, in addition to the vacancy of the cation, includes an additional defect, the nature of which has not been established; most likely it is an impurity ion.

An additional confirmation of the interstitial nature of H-centers can be their absence when irradiated with MgO X-rays and gamma rays, which, as is known, do not create Frenkel pairs. Another argument can be the data on pulsed annealing.

After a short-term annealing the samples (t = 5 min), the EPR spectrum of the V- and H-centers was measured and the optical absorption in the F-band. It is established that the fracture temperatures of the H-centers are in full accordance with the annealing temperature of the F-centers.

Similar centers have also been found in crystals of SrO [87] and CaO [88].

In the work on transmission electron microscopy [89], it was shown that interstitial clusters can be observed in magnesium oxide crystals irradiated with fast neutrons up to 3×10^{19} neutrons·cm^{-1}. Clusters were observed as formations about 30 Å in size.

The study of the motion of these formations under an electron microscope and the study of thermal annealing allowed the authors to conclude that the clusters consist of interstitial dislocation loops lying in the (110) plane. A detailed analysis showed that these loops have the form of two layers of ions embedded in a packing sequence; alternating rows consist of equal amounts of Mg^{2+} and O^{2-} ions.

The data of the work [90] are very interesting, the authors of which are trying to give their identification of optical absorption bands with maxima at 5.7 eV and 4.3 eV as associated with optical transitions on the anionic vacancy and interstitial oxygen ions.

Since an absorption band appears in deformed crystals with a maximum at 5.7 eV and is absent at 4.3 eV, these absorption bands are attributed to various defects.

Assuming, by analogy with AHC [91], that anionic vacancies are created during crystal deformation. Authors believe that in irradiated crystals the optical absorption in the band with a maximum at 5.7 eV corresponds to the absorption of anionic vacancies. Taking into account the symbatic behavior during X-ray and thermal annealing of optical absorption bands with maxima of 5.7 and 4.3 eV, these bands are attributed to complementary defects and based on this, the optical absorption band with a maximum at 4.3 eV binds to interstitial oxygen ions.

The author explains the correspondence between the change in the intensity of the optical absorption band with a maximum of 4.3 eV and the change in the EPR signal of Fe^{3+} ions by the role of impurity Fe^{3+} ions as a stabilizer of interstitial oxygen.

The authors see confirmation of the hypothesis about the capture of internode oxygen ions by iron ions in the appearance in the EPR spectrum, in addition to signals associated with Fe^{3+} ions in an octahedral environment, of two weak lines arranged symmetrically relative to the central line of the Fe^{3+} ion (transition—1/2 $\rightarrow$ 1/2) and in direct proportion between the change in the intensity of these lines and the absorption coefficient in the band with a maximum at 4.3 eV [92].

If anionic vacancies and interstitial oxygen ions are created in magnesium oxide crystals at irradiated with X-rays, then the appearance of F-centers should also be observed, which the authors did not observe. Therefore, such an interpretation of the optical absorption bands with maxima at 5.7 and 4.3 eV is incorrect.

Secondly, it was reported in [76] that these bands are associated with Fe^{3+} ions, and then in [77], directly using the effects of magnetic circular dichroism and electron spin resonance, it was proved that these absorption bands correspond to charge transfer processes on Fe^{3+} ions.

However, the hypothesis of the intercostal oxygen ion capture by impurity ions Fe^{3+} seems very attractive.

Confirmation of this hypothesis is the results of work [93], in which the dependences of the absorption coefficient in the F-band on the dose of irradiation with neutrons and high-energy electrons of magnesium oxide crystals with different concentrations of iron impurity ions were investigated (5×10^{-2} to 6×10^{-3})%. It is shown that samples containing more impurity iron ions are stained more efficiently; the presence of Fe^{3+} impurity increases the rate of formation of F-centers.

A similar result of an increase in the concentration of F-centers with an increase in the concentration of impurities was obtained for other materials, for example, crystalline copper [94].

1.3 Radiation Defect Formation in Magnesium Oxide Crystals

The most important stage of radiation damage to solids is the displacement of atoms or ions from the nodes of the crystal lattice. The energy required for displacement can be obtained by an atom either as a result of interaction with the force field of an incoming fast particle, or as a result of the decay of electronic excitation. In the first case, the transition time of the atom to the interstitial position (10^{-14}–10^{-15} s) is significantly less than the period of thermal vibrations of the lattice. Therefore, the displacement mechanism is called shock. In the second case, the displacement occurs in a time comparable to the period of thermal oscillations, and the displacement efficiency increases with increasing duration of localization of electronic excitation. The mechanisms of this group are called non-basic.

Shock and non-shock mechanisms differ significantly in the amount of the minimum energy that needs to be communicated to the ion for its displacement from the lattice node. This energy Ed is called threshold energy.

The shock mechanism is universal and is implemented in all types of condensed media when irradiated with high-energy particles or quanta. More stringent conditions are imposed on the implementation of non-standard mechanisms, of which the following should be noted:

1. It is necessary that the energy of electronic excitation exceeds the threshold energy of displacement.
2. The decay of the electronic excitation into a Frenkel pair is possible when the excitation lifetime in a fixed unit cell exceeds the characteristic time corresponding to the effective period of thermal oscillations of the lattice. This condition is well fulfilled for AHC; therefore, the most fully non-elementary mechanisms have been studied on silk-haloid systems.

On the other hand, the impact mechanism has been studied in detail in metals for which the role of non-impact mechanisms is negligible.

MgO crystals occupy an intermediate position between ionic AHC and covalent semiconductors. It is an ionic compound according to the type of chemical bond and the band gap width; it is a semiconductor according to the values of the valence band width and the exciton binding energy.

It is known that the shock mechanism of generation of radiation defects dominates in semiconductors, while the exciton mechanism is predominant in ion AHC.

Unconditional interest is the study of the mechanisms of joining defects in crystals with intermediate properties.

1.3.1 Creation of Radiation Defects in the Anionic Sublattice of Magnesium Oxide Single Crystals

The work of Sibley and Chen [95] is a pioneering work on elucidating the mechanism of radiation defect formation in the anionic sublattice of single crystals of magnesium oxide. The authors compared the effect of electron and neutron irradiation on the efficiency of accumulation of F-centers in MgO crystals at room temperature.

It was found that with equal integral radiation fluxes, the intensity of the F-band in the optical absorption spectra during neutron irradiation is 50 times higher than during electron bombardment.

Since the primary energy losses of neutrons due to the large mass and lack of charge occur only during elastic scattering on the target nuclei, and electrons, in addition, transfer part of the energy to the electronic subsystem, the above result is explained by the decisive role of elastic collisions in the formation of Frenkel anion pairs in magnesium oxide crystals.

The efficiency of accumulation of radiation defects in the case of the ionization process of defect formation should be insensitive to changes in the energy of particles falling on the material.

On the other hand, in the case of elastic collisions, a pronounced dependence on the energy of the bombarding particles should be observed, since in order to displace an atom or ion from a regular lattice node, it must receive a certain amount of energy from the incident particle. It is necessary for displacement that the incident particle has energy $E \geq Ed$, where Ed is the displacement energy.

Thus, the displacement energy of an atom or ion can be determined experimentally by reducing the energy of incident particles to a level at which the formation of defects is not recorded in the case of a shock mechanism of radiation defect formation.

Such an experiment was carried out in [96] for magnesium oxide crystals irradiated with accelerated electrons at liquid nitrogen temperature. The threshold electron energy value of 0.33 meV was established, below which the efficiency of accumulation of F-centers decreases sharply.

True is that an insignificant number of F-centers is still observed at electron energy values below the threshold, but since their concentration does not change. It is most likely that the formation of F-centers in this area of electron energies is due to the localization of electrons in pre-radiation anionic vacancies.

Since, no change in the efficiency of accumulation of F-centers was detected even at high doses of irradiation with electrons with an energy less than 0.33 meV, then it is possible to estimate the value of the threshold energy of the non-adiabatic displacement of the oxygen ion in the interstitial with the formation of a stable F-center taking into account the indicated value of the electron energy beyond the threshold [94, 107]

$$E_d = \frac{2(E + 2mc^2)E}{Mc^2}, \tag{1.3}$$

where E is the kinetic energy of the incident particle (0.33 meV); m is the mass of the electron; M is the mass of the O^{2-} ion.

Such an estimate leads to threshold energy of oxygen ion displacement of ~ 60 eV.

It is interesting to note that this value is close to the calculated value of the threshold separation energy of the charged components of the Frenkel anion pair in MgO (~40 eV) [98]. Therefore, it is possible that the separation of the charged components of the Frenkel anion pair is the limiting stage of the formation of a stable defect.

The profiles of the distribution of F-centers and the number of displaced oxygen ions in elastic collisions along the $^{20}Ne^{+}$ ion track were compared [79, 99]. The calculation was carried out according to the Lindhard theory for elastic scattering of heavy ions. The profiles of the F-centers were measured at room temperature. The authors obtained a good qualitative agreement of the calculated and experimental profiles obtained, which also serves as evidence in favor of the shock mechanism of radiation defect formation in the anionic sublattice of magnesium oxide.

However, due to powerful cascades, the crystal lattice in the irradiated region significantly overheats and deforms which intensifies annealing processes and makes it difficult to identify the possible contribution of non-failure mechanisms.

Therefore, the use of heavy ions initiating thermal wedges is undesirable when emitting radiation defecation mechanisms.

Henderson and Bowen [49], assuming the shock mechanism of the formation of F-centers during neutron bombardment of MgO, calculated the kinetic curve of their accumulation. It was believed that annealing of Frenkel anionic pairs occurs only when the interstitial ion statistically enters the instability zone of vacancies. The calculated and experimental accumulation curves almost completely coincide with the linear size of the instability zone 9a (a is the lattice parameter).

The experiment was carried out at room temperature. The absence of other types of annealing of Frenkel pairs seems unlikely, since there is evidence of high mobility of interstitial ions in magnesium oxide at low temperatures [43].

Confirmation of the shock mechanism of the creation of radiation defects in the anionic sublattice of magnesium oxide are also the results of work [95], in which the effect of the intensity of irradiation with high-energy electrons on the efficiency of accumulation of F-centers was studied.

It was found that with a threefold change in the beam current density ($0.5 \div 1.5$ $\mu A \cdot cm^{-2}$); the concentration of F-centers for crystals of a given purity depends only on the irradiation time.

The works of A. S. Kuznetsov, N. V. Yaek, A. V. Sprat [90] are devoted to the study of the possibility of implementing non-elementary mechanisms of radiation defect formation in the anionic sublattice of magnesium oxide.

The authors identified optical absorption bands with maxima at 5.7 eV and 4.3 eV as optical transitions in the anionic vacancy and interstitial oxygen, respectively. Taking into account the significant increase in absorption in these bands with an increase in the X-ray irradiation time of magnesium oxide crystals, a hypothesis was put forward about the effective participation of ionization mechanisms in the creation of Frenkel anion pairs (FAP) in MgO.

However, defects oriented by ⟨100⟩ are responsible for the optical absorption band with a maximum at 5.7 eV according to the data of [100], when magnesium oxide crystals are deformed; therefore it is incorrect to attribute this absorption band to anionic vacancies.

The following fact serves as an objection to the proposed identification of optical absorption bands and the hypothesis created on this basis about the failure of FAP generation in magnesium oxide crystals under X-ray irradiation. If the increase in the optical absorption of MgO crystals in bands with maxima at 5.7 and 4.3 eV under the action of X-rays is indeed associated with the appearance of anionic vacancies and interstitial oxygen ions (in the form of analogues of α and I-centers in alkaline halide crystals (AHC)), then an increase in the coefficient must also be observed absorption in the F-band. The authors did not observe this.

It should be noted that as early as 1957 and 1958 [101, 102], a change in the absorption coefficient in the F-band in magnesium oxide crystals was reported when they were irradiated with X-ray and ultraviolet radiation.

However, the authors do not analyze the origin of anionic vacancies at all.

We will compare the curves of the increase in the number of F-centers created in magnesium oxide and KCl crystals by ultraviolet radiation to clarify this issue.

The process of accumulation of F-centers can be divided into two stages For KCl [103]. At the first stage, which quickly tends to saturation, defects that exist in the crystal before irradiation are involved. At the second stage, only their own radiation defects appear, the number of which increases linearly over a wide range of irradiation time.

The accumulation of F-centers for MgO is carried out in a single, rapidly saturated stage, obviously associated with the presence of pre-radiation vacancies [104].

The fact that the phenomenon of autolocalization of excitons and holes has not yet been detected in these crystals proves in favor of the shock mechanism of radiation defect formation in MgO. No signal from the O_2^{3-} molecule was observed in the electron paramagnetic resonance (EPR) spectrum in magnesium oxide. They are probably unstable, which excludes the possibility of two-center autolocalization of holes and excitons. The hole zone in MgO is large (~ 5 eV) [105] and the criterion of single-center autolocalization in the form of O-centers in regular nodes of the magnesium oxide lattice is probably also not fulfilled [106].

All of the above confirms the dominant role of the shock mechanism of radiation defect formation in the anionic sublattice of magnesium oxide.

However, there is information in the literature, the explanation of which is difficult from this point of view.

Earlier, an interesting result was obtained - the efficiency of the accumulation of F–centers sharply decreases in the temperature range (140–200) K when studying the temperature dependence of the accumulation of F-centers in the process of high-intensity proton irradiation of magnesium oxide crystals.

The scattering cross-section and the transmitted energy do not depend on temperature in elastic collisions; therefore a decrease in the efficiency of the accumulation of F-centers should be observed only at the temperatures of their thermal destruction.

Therefore, it remains to be assumed that during low-temperature high-intensity proton irradiation, in addition to the shock mechanism of radiation defect formation, another ionization mechanism participates in magnesium oxide crystals. In this case, the decline in the efficiency of the accumulation of F-centers can be explained by a decrease in the rate of generation of primary FAP.

Similar results were obtained in [107]. The authors interpret them as a result of an increase in the take-off range of the FAP components that occur during irradiation at lower temperatures.

The profiles of radiation defect formation in magnesium oxide crystals under irradiation with various ions were experimentally determined and the results obtained were comparable with the theoretical profiles calculated for the case of a shock mechanism for creating radiation defects [108].

It turned out that in the case of light ions, whose energy is spent mainly on ionization processes, the experimentally obtained profiles of radiation defect formation do not repeat the theoretical profiles.

In particular, the efficiency of the formation of radiation defects was higher than predicted by theoretical calculations.

Based on these results, the authors concluded that ionization mechanisms are involved in the processes of radiation defect formation in the anionic sublattice of magnesium oxide crystals.

The hypothesis of shock generation of F-centers in magnesium oxide crystals is confirmed by the work [109], in which the results of measuring the kinetics of accumulation of F-centers in MgO crystals under proton irradiation and the results of calculating the number of FAP formed by elastic scattering of protons on the nuclear subsystem of magnesium oxide crystals are compared using the classical Thompson model.

Calculations were performed using the radiation parameters used during the experiment.

It turned out that the experimentally observed concentrations of F-centers at the temperature of liquid nitrogen significantly exceed the calculated number of FAP. The calculations did not take into account the effects of focusing and channeling of fast particles, as well as annealing processes, which should lead to an even greater discrepancy with the experiment. There is a good agreement between the calculation and the experiment at temperatures close to room temperature.

Consequently, the mechanism of formation of radiation defects only through elastic collisions cannot explain the concentration of F-centers observed in experiments at low temperatures in magnesium oxide crystals.

1.3.2 Creation of Radiation Defects in the Cationic Sublattice of Magnesium Oxide Single Crystals

There is information in the literature that at first glance seems to confirm the determining role of the ionization mechanism of radiation defect formation in the cationic sublattice of MgO.

These are:

1. The accumulation of hole color centers in identical concentrations during isodose irradiation with electrons, gamma rays and X-rays [56].
2. The cross-section of the formation of hole centers in MgO crystals is $(10^2 \div 10^3)$ barn [110], which is incompatible with the threshold energy of the nonadiabatic displacement of the magnesium ion into the internode by elastic collisions (64 eV) [56].
3. There is no dependence of the efficiency of defect accumulation on proton energy [22].

However, it should be noted that the hole color centers in MgO crystals are created only in crystals containing impurity ions Al, F, Na, Li, H, etc., the presence of which itself implies the presence of pre-radiation cation vacancies.

Therefore, the hole color centers are observed in the form of V_{Al}, V_F, [Na], [Li], V_{OH} etc. The formation of hole color centers V and V^- in MgO crystals by radiation is also possible only in impurity samples containing hydrogen (deuterium) [50, 111, 112]. Impurity H^+ ions, due to their small size, are placed in the interstitial, where a covalent bond is formed between them and oxygen ions. These OH-molecules, together with nearby cationic vacancies that compensate for the effective charge of the hydrogen ion, form the V_{OH}-center.

It turned out that when the crystal is irradiated with electrons or high-energy quanta, hydrogen ions become mobile and leave the V_{OH}-centers, leaving single cationic vacancies [50, 111, 112].

All this indicates the inconsistency of the claims about the possibility of the decay of electronic excitations to structural defects in the cationic sublattice of magnesium oxide. The observed hole color centers are formed on pre-radiation cation vacancies.

Moreover, there are numerous facts according to which cationic vacancies are not created even when magnesium oxide crystals are irradiated with high-energy electrons and neutrons [50, 95, 111]. The absence of cationic vacancies in MgO when irradiated with heavy ions [99], which produce excitations in the nuclear subsystem of materials, indicates the extraordinary radiation resistance of the cationic sublattice. It is believed to be due to the high mobility of interstitial cations, which leads to their rapid recombination with cationic vacancies with the restoration of a defect-free crystal structure [28, 99].

Currently, the only generally recognized method for creating cationic vacancies in magnesium oxide is the cultivation of crystals with the addition of suitable inovalent impurities, the effective charge of which is compensated by cationic vacancies.

Chapter 2
Objects and Methods of Research Used in the Study

Contents

The work used single crystals of magnesium oxide grown by melting in an electric arc.

Table 2.1 shows the content of the main impurities in the crystals used.

The study of the processes of generation of radiation defects and determination of their lifetime in magnesium oxide crystals at high power absorbed radiation energy was carried out on the installation of pulsed optical spectroscopy with nanosecond time resolution.

Correlation curves of annihilation radiation of positrons in magnesium oxide were taken at a facility to study the angular distributions of annihilation gamma quanta.

The pulse electron accelerator "Pulse-I" of the Tomsk Polytechnic University was used as a source of high radiation exposure densities to study post-effects in irradiated crystals. The electron energy in the beam E = 0.135 meV, the duration of the irradiation pulse t = 10^{-8} s; the beam current density j = (50–1000) A.

Irradiation of crystals with high-energy protons was carried out on a cyclotron of Tomsk Polytechnic University.

A. Surzhikov and E. Lysenko, *Creation and Accumulation of Radiation Defects in Single Crystals of Magnesium Oxide*, https://doi.org/10.1007/978-3-031-60207-8_2

Table 2.1 The content (mass) of the main impurities in single crystals of magnesium oxide of various origin

	Ca	Si	Al	Fe	Mn	Ag	Sn	Cu	Cr
MgO (I)	1.2×10^{-1}	3.5×10^{-1}	1.5×10^{-2}	2×10^{-2}	–	3×10^{4}	–	$3\,3 \times 10^{-3}$	–
MgO (II)	–	–	6×10^{-6}	2×10^{-4}	7×10^{-6}	–	–	–	6×10^{-6}
MgO (III)	10^{-2}–10^{-3}	1×10^{-1}	10^{-2}–10^{-3}	10^{-2}–10^{-3}	–	–	10^{-2}	10^{-3}–10^{-4}	–
MgO (IV)	10^{-2}–10^{-3}	10^{-2}–10^{3}	10^{-2}–10^{-3}	10^{-3}–10^{-4}	10^{-4}–10^{-5}	–	–	–	$0.5 \times 10^{-4\,-4}$

An industrial X-ray machine URS-55 (45 kV; 20 mA) was used for X-ray irradiation.

Stationary measurements of the optical absorption spectra of magnesium oxide crystals were performed on the SF-4A spectrophotometer.

Crystal calcination and annealing were carried out in air in an electric resistance furnace (300–1800) K. The temperature was controlled by a Pt − PtRo thermocouple and a potential.

The spectra of photostimulated luminescence of pre-irradiated crystals were measured under stationary optical excitation in the region of the F-absorption band. The source of excitation was a mercury lamp DRT-250. The light of the required length was allocated by the SF-4A monochromator. The spectral composition of the crystal glow was studied using a SF-4 monochromator, photomultipliers FEU-79 and FEU-39, an amplifier and an automatic potentiometer.

2.1 Installation of Pulsed Optical Spectroscopy

An experimental setup manufactured at Tomsk Polytechnic University was used to study the processes of formation and destruction of radiation defects in magnesium oxide crystals.

The installation allows photovoltaic spectral-time measurements of optical absorption and luminescence induced by radiation in the materials under study.

Parameters of the experimental setup are below:

spectral measurement range is (200–800) nm;
the measurement time interval is (7×10^{-9}–10^{-3}) s;
time resolution is 7×10^{-9} s;
the temperature range of measurements is (78–600) K.

Schematically, the essence of the installation is as follows: the luminous flux from the light source is directed using a quartz lens through a sample, a quartz lens and a monochromator to a photomultiplier, the electrical signal from which is recorded by an oscilloscope. Under the influence of radiation generated by the accelerator, the sample is colored and the anode current of the photomultiplier changes in time proportionally to the induced color. Based on the results of measurements at different wavelengths of probing light, the full spectrum of optical absorption of the sample can be restored.

A pulsed electron accelerator with fixed beam parameters is used as a radiation source in the installation: the average electron energy is 200 keV; the irradiation duration is 5×10^{-9} s; the particle flux density is 1 kA cm^{-2}.

The output of the accelerated electron beam is carried out through an aluminum foil with a thickness of 20 μm into the pumped volume of a cryostat for optical studies mounted on the output flange of the accelerator.

The energy spectrum of accelerated electrons was measured using a foil charge spectrometer [113]. The time and current characteristics of the accelerated electron

pulse were controlled using a measuring transformer, pre-calibrated with current pulses calibrated in amplitude and duration.

As sources of probing light during measurements in the time interval (10^{-9}–10^{-3}) s, the installation uses ISP-500 pulsed xenon lamps and a light source structurally similar to the Podmoshensky's light source.

The power supply scheme of pulsed light sources is based on the isolation of a quasi-rectangular current pulse from the time dependence of a high-capacity discharge.

A photoelectronic multiplier FEU-97 with and without sodium salacylate is used to register light signals and convert them into electrical ones.

To increase the anode current of the photomultiplier, a pulsed supply of increased voltage to a low-resistance divider is used in the installation. The switching power supply unit of the power supply generates a rectangular high-voltage pulse with a duration of 12 ms and an amplitude of up to 5 kV with a total divider resistance of 70 Ohms.

Linearity control of the recording system was carried out using a calibration multi-stage attenuator. The light source in this case was radiation from a pulse lamp. The light-ampere characteristic of the FEU-97 is linear in the range of values of the anode current of 0.1–0.5 A with a pulsed supply voltage of 2.7 kV (Fig. 2.1).

The error in measuring the signal amplitude was determined from comparing the results of multiple measurements of the amplitude of light pulses supplied to the photomultiplier from the LED AL-102B, powered by amplitude-calibrated pulses from the generator G5-9. The maximum spread of the results did not exceed 3%.

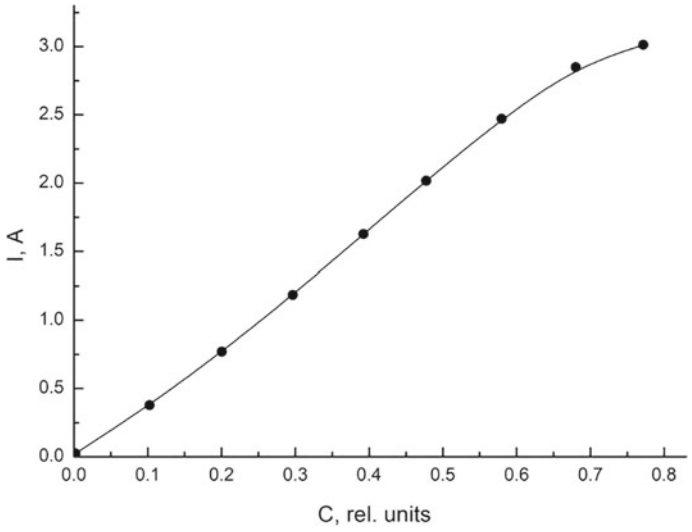

Fig. 2.1 Dependence of the anode current of the FEU-97 (I) on the illumination (C) of the photocathode

The estimation of the error in the measurements of time intervals was carried out by comparing the true shape of the calibration pulse signal with the reproducible measuring circuit. The results of such a comparison for the FEU-97 generally coincide with the passport data. Its time resolution, estimated from the leading edge of the anode current pulse, is (5–7) $\times$ 10^{-9} s.

The optical measurement scheme used in the installation is designed in such a way as to ensure the maximum luminous intensity of the system. The angle between the probing light beam and the irradiated surface of the sample is 7°.

Due to this, the length of the optical path of the probing light in the colored volume increases by more than 10 times, compared with the magnitude of the optical path at normal beam incidence.

The design of the cryostat for optical studies allows the sample to be positioned in accordance with the optical scheme described above and optical measurements to be carried out in the temperature range (78–600) K.

The temperature of the sample is controlled using a chromel—alumel thermocouple and a PP-63 potentiometer.

The sequence of operation of the installation blocks is as follows.

When the set value of the charging voltage of the capacitor bank of the pulse voltage generator (PVG) of the accelerator is reached; the matching circuit of the digital voltmeter VK7-10A is triggered and includes a circuit for starting the probing light source. At the same time, a synchronization unit is started, from the output of which a synchro pulse delayed for the time of the light source ignition (200 ms) is removed, which ensures the operation of the switching power supply unit of the power supply unit. The same pulse, delayed by 2 ms by the passive delay line LZO-20-600 (until the operating parameters of the FEU are stabilized), also ensures the launch of the accelerator PVG and, at the same time, the oscilloscope scan generator.

A large spread of the accelerated electron flux density from pulse to pulse (10%) leads to a significant error in optical measurements. Reducing this error by statistical methods to 5% leads to the need for a 12-fold repetition of measurements. The reduction of the error of a single measurement to 5% was obtained by normalizing the results of optical measurements by the integral radiation dose.

The sensitivity of the photoelectronic multiplier, the optical absorption and scattering of light on the elements of the optical path change significantly with the change in the wavelength of the radiation under study.

These factors do not play a role in measuring optical absorption spectra, since the optical density is the ratio of the intensities of probing light of a certain wavelength that passed through the sample before and after the start of the irradiation pulse. It is necessary to take into account these factors when measuring luminescence spectra.

Therefore, the calibration of the optical path for spectral sensitivity was carried out. As a light source with a known continuous spectrum, an incandescent temperature wide-range TRSh-2850 was used.

The spectral intensity of the radiation density of the TRSh-2850 lamp is calculated by [114]

$$r(\lambda, T) = r_s(\lambda, T)\varepsilon(\lambda, T), \tag{2.1}$$

where ε (λ, T) is the grayness coefficient of tungsten from [141]; $r_s(\lambda, T)$ is the intensity of the spectral density of blackbody radiation, defined as

$$r_s(\lambda, T) = C_1\lambda^{-5}(e^{C_2/\lambda T} - 1)^{-1}, \tag{2.2}$$

where C_1, C_2 are the first and second radiation constants; T is the color temperature (2850); λ is the wavelength of light.

The optical path is graded directly after determining the spectral intensity of the radiation density of the TRSH-2850 lamp. To do this, the TRSH-2850 lamp is placed in a cryostat in place of the sample in the installation. The power supply of the PMU-97 is carried out from a stationary power source VS-23, the signal from the PMU is recorded by the microammeter M-95.

The calibration values of the optical path are the quotients of dividing the current value according to the M-95 microammeter at λ_i by the intensity of the radiation density at the same wavelength λi of the TRSH-2850 calibration lamp.

The error in determining the calibration values of the optical path was estimated from a sevenfold measurement of the strength of the anode current of the photomultiplier and is no more than 2%.

2.2 Installation for Studying the Angular Distributions of Annihilation Gamma Quanta

The installation is designed to measure the angular distributions of 2 γ-annihilation decays of positrons in solids. The most informative experimental method for studying 2 γ-annihilation is the method of measuring the angular distributions of annihilation gamma quanta [31].

The block diagram of the installation is shown in Fig. 2.2.

The main units of the installation are an isotope and sample attachment unit, radiation detectors, a collimator system, “Cedar” electronic device and a digital typewriter BZ-15.

The installation has the following operating parameters:

The activity of the $Na^{22}(ß^+,\gamma)$ positron source is 0.37 GBq;
The angular resolution of the installation is (0.5–0.8) mrad;
The distance from the sample to the gamma-quantum detector is 1300 mm;
Collimator width is (0.5–1.0) mm;
Collimator height is 70 mm;
The alignment and parallelism of collimators is not worse 0.1 mrad.

The experimental equipment used satisfies the basic technical conditions required for such type of installations as follows from the review of the state of measuring equipment for the study of the angular correlation of annihilation gamma quanta [115].

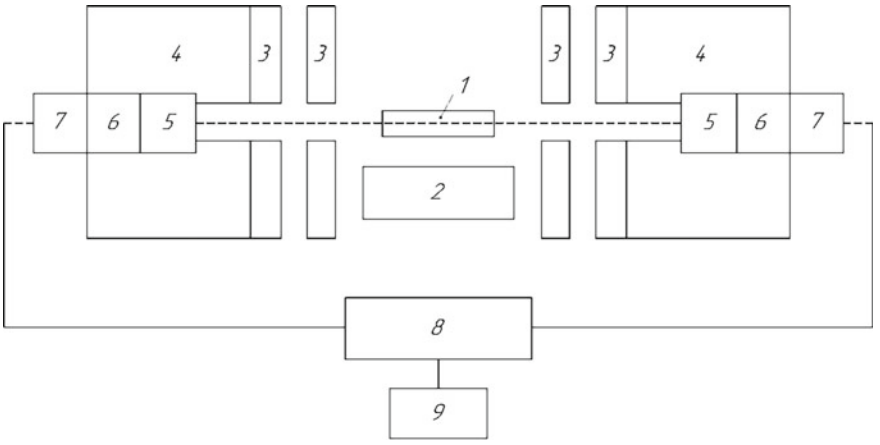

Fig. 2.2 Block diagram of an installation for measuring correlation curves of annihilation gamma quanta, where 1 is a sample; 2 is an isotope; 3 is collimators; 4 is lead houses; 5 is a scintillator; b is a FEU; 7 is a cathode repeater; 8 is an "Cedar" electrode device; 9 is a digital typewriter

2.2.1 Radiation Detectors

Radiation detectors are designed to register the annihilation gamma quanta emitted during the annihilation of positrons in the sample under study. Scintillation counters based on the FEU-52 are used as detectors. A thallium-activated NaI crystal serves as a scintillator. The detectors are placed in lead houses. One of the detectors with its collimator together can move with the help of a rotary device in a horizontal plane in both directions relative to the main horizontal axis of the installation. The second detector is stationary.

2.2.2 Collimator System

The collimator system includes four collimators, two of which are located directly in front of the detectors and serve for collimation of annihilation gamma quanta, having a small deflection angle relative to 180°. The other two are located in front of the isotope and serve to shield the source (it eliminates the possibility of radiation from the isotope entering the detectors).

2.2.3 Isotope and Sample Attachment Unit

A special design cage made of plexiglass is placed directly on the lead holder of the isotope, in the vertical guide of which the sample holder is installed. The sample

is fixed in a special slot of the holder and together with it is pressed by a spring to the plane of the horizontal slot of the clip. The isotope-sample distance was selected experimentally and is 3 mm in order to make optimal use of the positron beam.

2.2.4 Source of Positrons

The source of positrons is the radionuclide $Na^{22}(\beta^+,\gamma)$ with an activity of 0.37 GBq. The half-life of this isotope is 2.58; the maximum energy of positrons in the main decay branch is 0.54 meV. The diameter of the working spot is 10 mm.

2.2.5 The "Cedar" Electrode Device

The "Cedar" electronic device is designed for automatic control of the experimental installation and recording device, discrimination of signals coming through two channels, counting the number of pulses in a given time interval on each channel, or coinciding in time on both channels, indication of the measurement result, information interface with a digital typewriter.

2.2.6 Measurement Error

Since the correlation curves of annihilation radiation $N(\theta)$ are measured using a coincidence scheme, the overall measurement error will be determined by the statistical error in registering true coincidences and the error caused by the background of random coincidences [116].

Due to the low load of both input channels of the matching scheme used, $\Delta\tau \approx 1$ mseconds, i.e. when $n_1\ \Delta\tau \ll 1$ and $n_2\ \Delta\tau \ll 1$. The total speed of counting matches is

$$N(\theta) = N\theta_{true} + T(\theta)_{ran} \quad \text{for, } \Delta\tau \tag{2.3}$$

The average number of matches for time t is

$$\overline{N}(\theta) = \overline{N}(\theta)_{true} + N(\theta)_{ran}, \tag{2.4}$$

relative fluctuation of the number of coincidences due to the applicability of Poisson's law in this case is

$$\delta_{N(\theta)} = 1/[N(\theta)]^{1/2}. \tag{2.5}$$

Thus, the measurements are carried out in two stages. At the beginning, the background of random coincidences is measured for time t. In our case, this measurement is

$$N_{backgr} = T(\theta > \theta_{\max}), \tag{2.6}$$

where $\theta_{max} = 20$ mrad.

Then the total effect of $N(\theta)$ is measured and $N(\theta)_{true}$ is determined from (2.5). The time for selecting statistics is determined from the required accuracy of measuring correlation curves (at least 1%).

2.2.7 *Calculation of Positron Absorption in Single Crystals of Magnesium Oxide*

Information on the distribution of the density of thermalized positrons over the depth of the sample under study is particularly needed to interpret the data on the annihilation of positrons in matter when studying the structure of defects in single crystals, to assess the sensitivity of the positron spectroscopy method and to exclude the influence of annihilation gamma quanta from the substrate material.

Currently, the characteristics of the passage of electrons and positrons in matter are being studied in detail by machine modeling methods.

It is possible to satisfactorily calculate the characteristics of the scattered electron flux and particle runs in comparison with experimental data When using calculation models and known cross sections of elementary processes (scattering and energy losses) [117, 118].

There are practically no such experimental data for positrons due to the difficulty of registering them and the lack of suitable sources with high radiation intensity.

Therefore, in many cases, including ours, the necessary information about the integral and differential distributions of the positron flux in a substance can be obtained only by calculations.

The calculated depth distribution of positron annihilation centers in magnesium oxide crystals from a standard $Na^{22}(\beta^+, \gamma)$ source on a glass substrate is presented by curve 1 (Fig. 2.3). The calculations took into account the energy spectrum of positrons.

It is necessary, of course, to compare the obtained result with experimental data to assess the reliability of the calculation model. There is practically no such data for positrons.

Therefore, according to the model used, calculations of the deep distribution of the absorbed energy of accelerated electrons with energy of 0.135 meV in magnesium oxide crystals were also carried out (curve 2) and compared with experimentally measured values (Fig. 2.4).

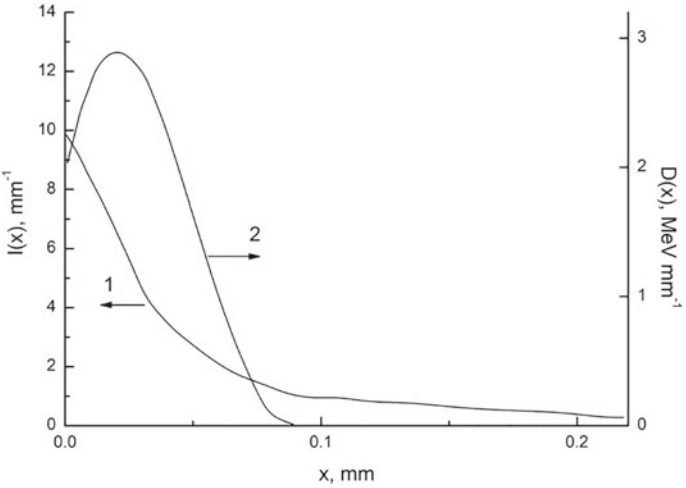

Fig. 2.3 Calculated depth distribution in magnesium oxide crystals of positron annihilation centers from $Na^{22}(ß^+, \gamma)$ radionuclide (1) and absorbed electron energy with an energy of 0.135 meV (2)

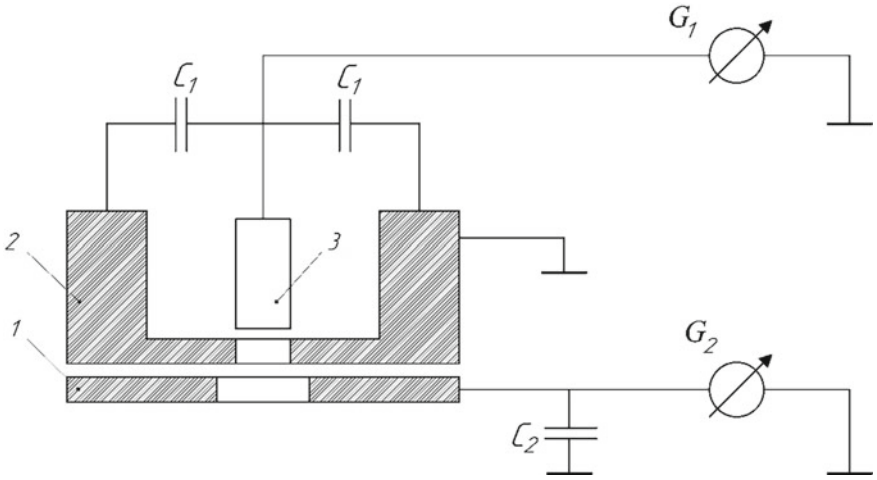

Fig. 2.4 The scheme of calibration of the monitor by the current density of the accelerated electron beam, where 1 is a collimator; 2 is a monitor; 3 is a Faraday cylinder; G1, G2 are model and calibrated galvanometers, respectively

A good agreement between the experiment and the calculation was found, which confirms the reliability of the calculation model used.

Analysis of the calculations shows that 80% of the positrons from the number of protons emitted by the $Na^{22}(^{\beta+},\gamma)$ source towards the studied sample annihilate in the magnesium oxide crystal layer with a thickness of 80 μm. On the other hand,

electrons with energy of 0.135 meV are absorbed in a magnesium oxide crystal with a thickness of 80 μm.

Thus, the basic information about the crystal structure defects obtained by the positron annihilation method comes from layers of magnesium oxide crystals irradiated with electrons with an energy of 0.135 meV.

When studying the electronic structure of various kinds of defects, including radiation defects, in real crystals by the method of positron annihilation, it is possible to study a given area of samples by selecting an appropriate source.

A given area of samples can be investigated by selecting the appropriate source in real crystals by the method of positron annihilation when studying the electronic structure of various kinds of defects, including radiation.

2.3 Dosimetry of the Radiation

The absorbed radiation energy of accelerated particles in magnesium oxide crystals was determined by calculation using Equation

$$D_{cr} = K\frac{Ejt}{dq}, \tag{2.7}$$

where E is the average energy of particles in the beam, [eV]; j is the beam current density, [A · cm^{-2}]; t is the irradiation time, [c]; d is the thickness of the colored crystal layer, [cm]; q is the particle charge, [Kl]; K is the conversion coefficient of eV · cm^{-3} to Gr, equal to magnesium oxide 4.5×10^{-17}.

Thus, it is necessary to determine the values of j, t, E, d to calculate the absorbed radiation energy of accelerated particles in single crystals of magnesium oxide.

2.3.1 High-Current Electron Beam

Information about the current density of the beam j was obtained using a Faraday cylinder placed in place of the crystal under study and connected to a set of low-inductive capacitors and an M-95 microammeter. The time constant of the electrical circuit is significantly less than the time constant of the deflecting galvanometer system. In this case, the galvanometer operates in ballistic mode, and its deviations are proportional to the charge of the electron beam introduced into the Faraday cylinder.

To carry out operational control of the electron flux density at the moment of each irradiation pulse, a monitor is placed in front of the collimator during experiments. Calibration of the monitor according to the electron beam current density is carried out according to the scheme shown in Fig. 2.4.

The principle of calibration consists in carrying out the readings of the model galvanometer G1 included in the Faraday cylinder circuit (3) in accordance with the readings of the galvanometer G2 in the monitor circuit. Galvanometers operate in ballistic mode.

The error in measuring the electron flux density by the monitor is determined by the error of a single measurement of the Faraday cylinder galvanometer and the monitor galvanometer, as well as a random error associated with the fluctuation of the electron beam. The error was calculated according to the method described in [119, 120]. The galvanometer of the Faraday cylinder was graduated by the charge Q of a capacitor with a capacity of C Q = CU, where U is the charge voltage. Then the error of measuring the electron flux density j for the Faraday cylinder is determined by the accuracy class of measuring devices of capacitance, voltage, diameter of the collimating hole, as well as by the random error associated with fluctuations in the switching circuit.

The error in measuring j by a Faraday cylinder galvanometer with a confidence probability, $\alpha = 0.95$ is 3.5%. The error in measuring the electron flux density by the monitor galvanometer with a confidence probability $\alpha = 0.95$ in the measurement range used does not exceed 3%.

The average electron energy in the beam E was determined from the spectral energy distribution of electrons for the accelerator used and was 0.135 meV during the experiments.

The electron energy spectrum is shown in Fig. 2.5 and is typical for this class of accelerators.

The spectrum was obtained using a charge spectrometer, which is a system of foils arranged in a vacuum along the beam one after the other [113]. The electron energy

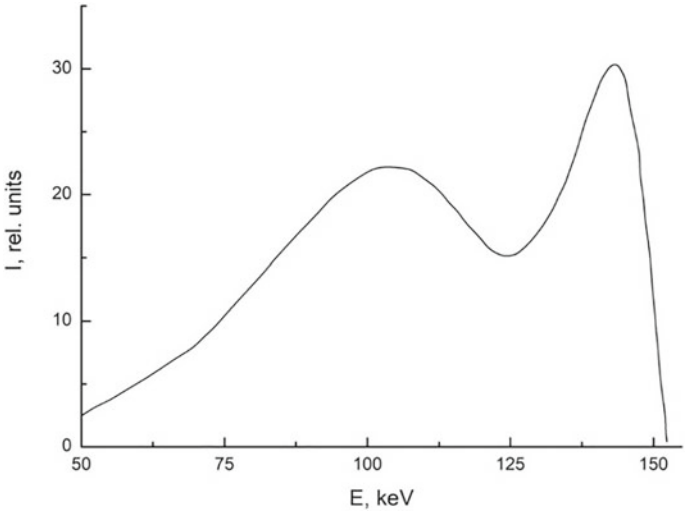

Fig. 2.5 Energy spectrum of electrons in the beam [174]

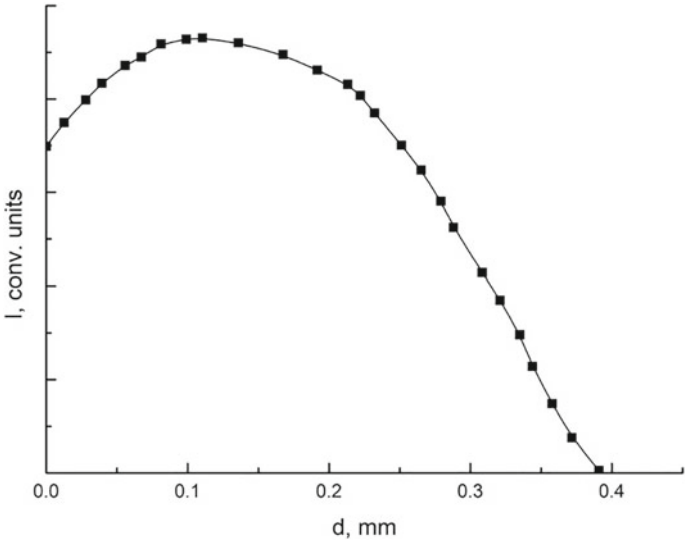

Fig. 2.6 Color distribution over the thickness of the magnesium oxide crystal after irradiation with a high-current electron beam up to 3×10^6 Gy ($j = 600$ A $\cdot$ cm^{-2})

spectrum was constructed by measuring the charge on each of the spectrometer foils after the end of the irradiation pulse.

The error in restoring the spectrum is due to errors in measuring the distribution of charges and the error of the method of restoring the spectral distribution of the charge. The average quadratic error with 3% accuracy of the initial data is 20%.

The thickness of the colored layer of the magnesium oxide crystal was determined using the MF-2 microphotometer after irradiation with five pulses of accelerated electrons and is 80 μm (Fig. 2.6).

The duration of the radiation pulse was measured by a Faraday cylinder and I2-7 m of small time intervals. The pulse duration was 10^{-8} during the experiments.

Thus, $t = 10^{-8}$ s, $E = 0.135$ meV and $j = 10$ A cm^{-3} at $d = 80$ μm; the power of the absorbed electron radiation energy in magnesium oxide is 28.5×10^{10} Gr $\cdot$ min^{-1} according to the Eq. (2.7).

2.3.2 High-Energy Protons

The parameters of the proton beam during the experiments were strictly fixed and according to the data of the cyclotron operation service.

The thickness of the colored layer of the magnesium oxide crystal d with the beam parameters used was determined using the MF-2 microphotometer and for protons with an energy of 10 meV was 340 μm (Fig. 2.7).

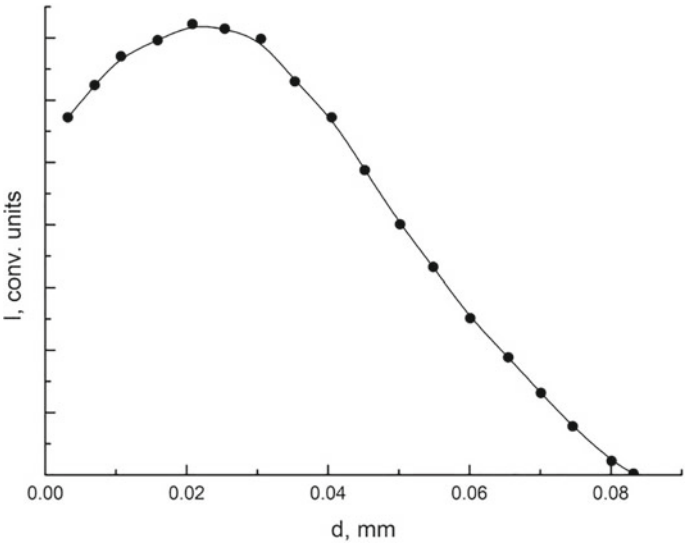

Fig. 2.7 Color distribution over the thickness of the magnesium oxide crystal after irradiation with protons up to 10^7 Gy

2.3.3 Absorbed X-ray Radiation Energy

The absorbed energy of X-ray radiation in MgO crystals was determined from the following expression [37]

$$D_{cr} = \frac{(\mu/\rho)_{cr}}{(\mu/\rho)_d} D_d, \tag{2.8}$$

where $(\mu/p)_{cr}$ and $(\mu/p)_d$ are the mass coefficients of attenuation of the radiation energy by the crystal and the dosimeter; D_d is the radiation energy absorbed by the dosimeter.

A KNO_3 chemical dosimeter similar to the Fricke ferrosulfate dosimeter [122] was used to determine D_d with a constant radiation yield of 1.6 ions per 100 eV of absorbed energy.

The power of the radiation energy absorbed by the dosimeter turned out to be equal to 219 Gr · min^{-1}.

The mass attenuation coefficients of the crystal and the dosimeter were calculated according to the formula for chemical compounds [123] by averaging the mass attenuation coefficients of the constituent atoms or ions with weights corresponding to their mass content in each element of the substance, i.e.

$$(\mu/\rho) = \sum_i n_i (\mu/\rho)_i, \tag{2.9}$$

where n is the mass fraction of the ith—element with the mass attenuation coefficient $(\mu/p)_i$.

The value $(\mu/p)_i$ depends on the quantum energy of the incident X-rays. Therefore, it seems necessary to determine the effective energy of the quantum of X-ray radiation of the URS-55 installation used by us (45 kV, 20 mA).

It is known that the law of X-ray power attenuation can be written as [39]

$$I_i = I_0 e^{-\mu x}, \tag{2.10}$$

where i_i is the radiation power behind the absorber layer with thickness x_i; I_0 is the radiation power without an absorber; μ is the linear attenuation coefficient.

Therefore, it is always possible to determine the linear, and, consequently, the mass attenuation coefficients of the radiation used from the experimental dependence on the Eq. (2.10).

The use as an absorber of a material with a known law of variation of the attenuation coefficient from the radiation energy will make it possible to establish the value of the effective quantum energy of the X-ray radiation used.

Figure 2.8 shows the dependence of the attenuation of the power of the radiation we use on the thickness of the aluminum absorber measured using the DRG2-01 dosimeter.

The mass attenuation coefficient determined from the obtained dependence turned out to be equal to 1.2 $cm^2\ g^{-1}$, which corresponds to the effective energy of the X-ray quantum of 28 keV [123].

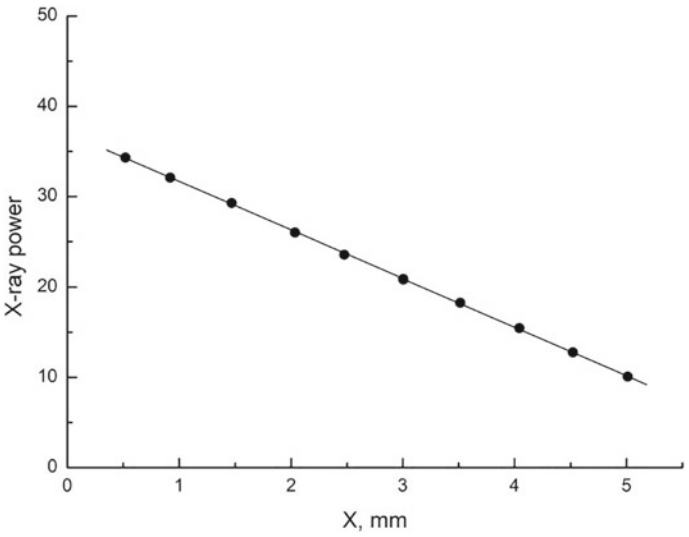

Fig. 2.8 Dependence of the change in the X-ray power of the URS-55 installation (45 kV, 20 mA) on the thickness of the aluminum absorber

The values (μ/ρ) of K, N, O, Mg for the established energy range of the X-ray radiation we use are taken from [123].

It is obtained what $(\mu/\rho)_{KNO_3} = 1.975\ cm^2\ g^{-1}$; $(\mu/\rho)_{MgO} = 0.646\ cm^2\ g^{-1}$, taking into account the mass fraction of elements in the compounds according to the Eq. (2.9),

The power of the X-ray radiation energy absorbed by the crystal is determined ($W_{cr} = 71.6\ Gr \cdot min^{-1}$), knowing the mass absorption coefficients of the crystal and the dosimeter and the value of D_d, according to the Eq. (2.8).

2.4 Additional Optical Absorption of Irradiated MgO (I) Crystals

The content of this section assumes the solution of two tasks:

1. The possibility of creating stable F-type color centers in MgO crystals under irradiation (without clarifying the causes of the origin of anionic vacancies).
2. Establishment of the structure of electronic color centers (F^+ or F) in case of their accumulation.

The position of the maxima of the optical absorption bands of the F-type color centers in magnesium oxide crystals has been reliably established as 4.92 eV (F^+) and 5.01 eV (F) at 298 K [31–33].

Therefore, the creation of stable electronic color centers under the influence of irradiation can be judged by the change in the optical density in the spectral region of 5.0 eV.

The close position of the maxima of the optical absorption bands of the F^+ and F-color centers makes it difficult to identify them by optical absorption spectra.

However, the glow of the F^+ and F-centers is manifested in different parts of the spectrum. The maximum of the glow band of F^+ centers is located at 3.15 eV (298 K) and F-centers is located at 2.4 eV (298 K) [31–33].

Therefore, information about the structure of electronic color centers in magnesium oxide crystals can be obtained from the position and intensity of the luminescence bands when the irradiated crystal is excited by light from the F-absorption band.

Figures 2.9 and 2.10 show typical optical absorption spectra of an MgO (I) crystal in the region of (3.7–5.6) eV after irradiation with a high-current electron beam and protons.

As follows from the figure, irradiation of MgO crystals with a high-current electron beam leads to the appearance of a complex spectrum of additional optical absorption.

Although crystal irradiation leads to an increase in the optical density in the F-absorption band (~ 5.0 eV), nevertheless, the complexity of the spectrum of additional optical absorption makes it necessary to analyze the possible causes of its appearance.

In general, the additional optical absorption of magnesium oxide crystals during irradiation may be due to:

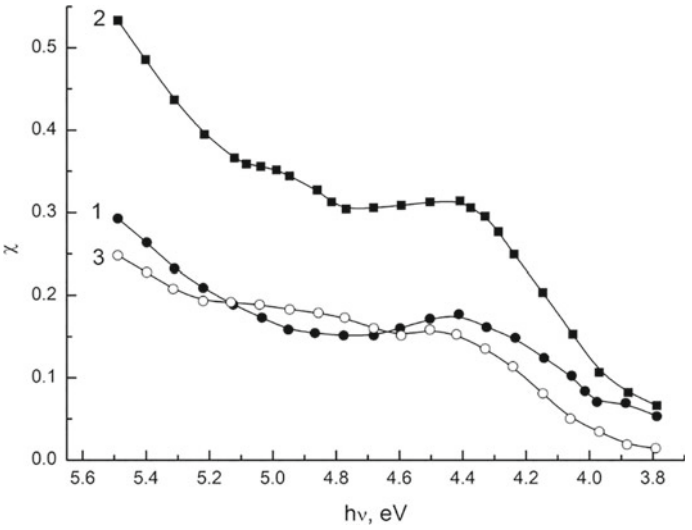

Fig. 2.9 Optical absorption spectra of the MgO (I) crystal, where 1 is the initial one; 2 is irradiated with a high-current electron beam (800 A = cm^2, 9.5 = 10^6 Gy); 3 is the difference between spectra 2 and 1 (additional optical absorption)

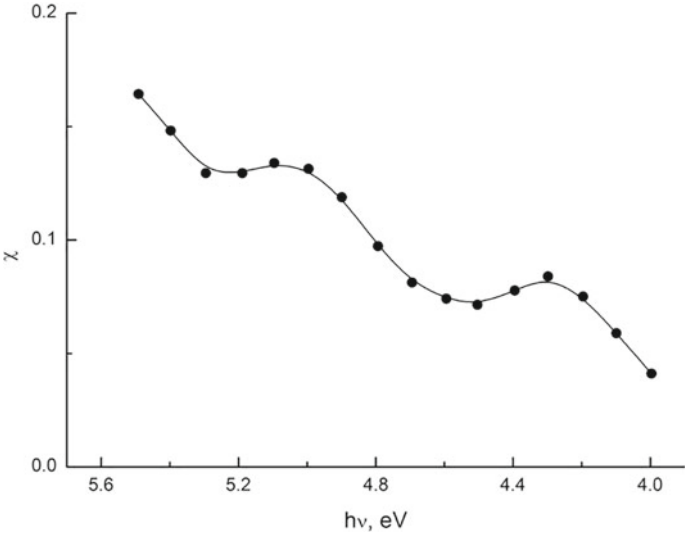

Fig. 2.10 Spectrum of additional optical absorption of an MgO (I) crystal irradiated with protons up to $6 \cdot 10^6$ Gy

1. Impurity color centers.
2. Color centers based on their own defects of the crystal lattice (both pre-radiation and those created during irradiation).

Due to the significant contamination of MgO (I) crystals, it is possible to form color centers in them with the direct participation of impurity ions.

Let's analyze this possibility taking into account the impurities detected by spectral analysis in the studied crystals.

When studying the states of impurity ions by the EPR method before and after irradiation of magnesium oxide crystals with electrons, y- and X-rays, the possibility of changing the charge state of ions Ti, V, Sg, Fe, Ru, Pd, Co, Ni, Mn was shown [10].

Only the crystals under study contain iron ions (Table 2.1) from the listed elements; therefore, we will consider possible manifestations of iron ions in the spectrum of additional optical absorption of MgO (I).

The position of the maximum absorption band of Fe^{2+} ions is reliably established at 1.2 eV [74], which is far from the region we are studying. Therefore, Fe^{2+} ions are eliminated from further consideration.

It is known that irradiation of magnesium oxide crystals with ionizing radiation leads to the appearance of optical absorption bands with maxima at 4.3 and 5.7 eV [76]. The linear correlation between the change in the absorption intensity in these bands during irradiation and the concentration of impurity iron ions [46], as well as the use of magnetic circular dichroism and EPR methods [77] allowed to reliably establish the responsibility of Fe^{3+} ions for absorption bands with maxima at 4.3 and 5.7 eV.

Absorption in the region of 5.7 eV is non-elementary. Thus, in [79, 80], a number of weak optical absorption bands were detected for magnesium oxide crystals irradiated with neutrons and heavy ions in the (5.6–6.0) eV spectral region. Comparing the intensity of optical absorption in this part of the spectrum with the concentrations of impurity ions, the authors do not exclude the possibility that there is absorption of Al, Si.

Ca, Si and Ag ions remained unobserved from the impurities present in the studied crystals.

Impurity ions Ca^{2+}, which isoelectronic to Mg^{2+}, slightly distort the electronic structure of magnesium oxide. Therefore, the possible optical effects associated with these ions located near the fundamental absorption are masked by interband transitions.

We could not find any information from all the abundance of literature on magnesium oxide about the absorption of impurity ions Si and Ag, which is probably due to their weak optical activity.

Thus, the impurities present in MgO (I) optical crystals cannot cause the appearance of an additional optical absorption band with a maximum at 5.0 eV in the spectrum.

Interstitial anions, cations and cationic and anionic vacancies can act as intrinsic defects of the crystal lattice with the participation of which the formation of color centers is possible under irradiation.

Magnesium oxide crystals are characterized by a shock mechanism for generating radiation defects at low and medium levels of radiation exposure [73, 95, 96, 99]; radiation-stimulated effects under the action of X-rays are caused by pre-radiation defectiveness [10].

Non-irradiated magnesium oxide crystals are characterized by Schottky disorder (removal of ions from regular nodes of the crystal lattice onto the crystal surface) [10]. Therefore, there is a certain amount of anionic and cationic vacancies in all crystals of magnesium oxide before irradiation; while there are no interstitial anions and cations.

As our experiments have shown, irradiation of MgO (I) crystals with X-rays leads to the appearance of additional optical absorption in the 5.0 eV region (Fig. 2.11).

Based on the above, the absorption band with a maximum at 5.0 eV in the spectrum of additional optical absorption of MgO (I) crystals may be due to the formation of color centers with the participation of anionic or cationic vacancies, but not interstitial anions and cations.

The capture of holes and electrons, respectively, on cationic and anionic vacancies leads to the creation of hole and electron color centers.

However, firstly, the maxima of the optical absorption bands of the hole color centers are located in the region of 2.3 eV [44–45], which is far from the spectral region we are studying.

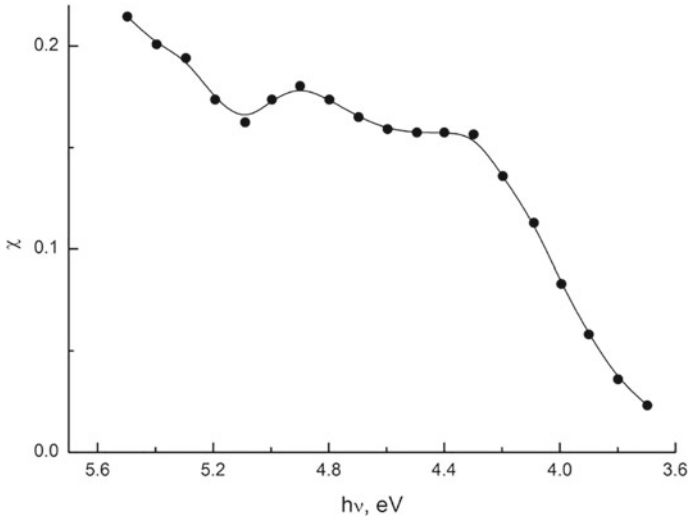

Fig. 2.11 The spectrum of additional optical absorption of an MgO (I) crystal with a thickness of 250 μm after irradiation with X-rays up to 2×10^5 Gy

Secondly, due to the small value of the forces of the transition oscillator in the hole centers of coloring (0.1–0.2) [46, 58] their registration by optical absorption spectra is difficult.

Thus, the appearance in the spectrum of additional optical absorption of magnesium oxide crystals after irradiation with a high-current electron beam and protons of the absorption band in the region of 5.0 eV is due to the formation of color centers on anionic vacancies (F-type color centers).

The photoluminescence spectra of crystals after irradiation were studied in order to establish the structure of the electronic color centers (F^+ or F) formed in MgO (I) crystals when irradiated with a high-current electron beam and protons, (Fig. 2.12, curves 1,2).

The appearance in the photoluminescence spectrum of a glow in the band with a maximum at 3.15 eV and the absence of a glow in the region of 2.4 eV indicates the predominant formation of magnesium oxide crystals when irradiated with protons and a high-current electron beam of electronic color centers in the form of F^+.

Thus, the spectrum of additional optical absorption of MgO crystals irradiated by protons and a high-current electron beam in the (3.7–5.0) eV region consists of two elementary bands with maxima at 4.3 ($Fe3^+$) and 4.92 eV (F^+).

The decomposition of the complex spectrum of additional optical absorption into components was performed in order to verify this conclusion.

The values of the half-widths of the absorption bands of F^+—color centers with a maximum at 4.92 eV and Fe^{3+} ions with a maximum at 4.3 eV in magnesium oxide

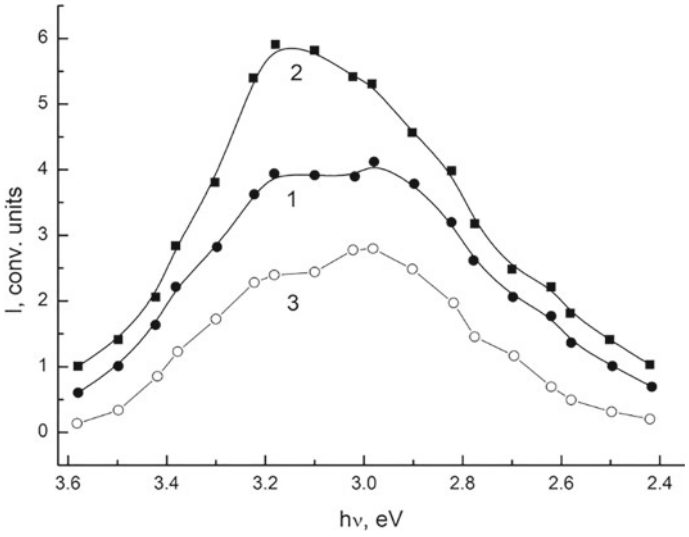

Fig. 2.12 Photoluminescence spectra of irradiated MgO (I) crystals, where 1 is by a high-current electron beam up to 9.5×10^6 Gy ($j = 800$ A $\cdot$ cm^{-2}); 2 is by protons up to 18×10^6 Gy; 3 is by X-rays up to 2×10^6 Gy

crystals have been reliably established and are, respectively, 0.62 eV (298 K) [40] and 0.73 eV (4 K) [78].

Therefore, in the case of responsibility for absorption bands with a maximum at 4.3 and 4.92 eV in crystals of MgO (I) ions of Fe^{3+} and F^{+} centers irradiated by protons and a high-current electron beam, there should be a coincidence between the above values of the half-widths of the absorption bands and those isolated during spectrum decomposition.

The decomposition of the additional optical absorption spectrum into elementary components was carried out under the assumption of the Gaussian shape of the absorption bands [101, 102]

$$\alpha_i = \alpha_m e^{\frac{-4\ln 2}{W^2}(E_i - E_m)^2}, \tag{2.11}$$

where α_i is the value of the optical density corresponding to the value of the photon energy E_i; α_m is the value of the optical density at the maximum of the absorption band E_i; W is the half-width of the absorption band.

Decomposition, which begins with the separation of the absorption band with a maximum at 4.3 eV, is carried out for a crystal irradiated with a high-current electron beam (Fig. 2.9). The graphical dependence $\ln \alpha_i = (E_i - E_m)^2$ is constructed from the low-energy decay of the optical density (3.6–4.1) eV (Fig. 2.13), from which the numerical values α_m and W are determined.

The value α_m corresponds to the value α_i at $E_m = E_i$, i.e. at $(E_i - E_m,)^2 = 0$; the value of the half-width W is determined through the angle of inclination β of the

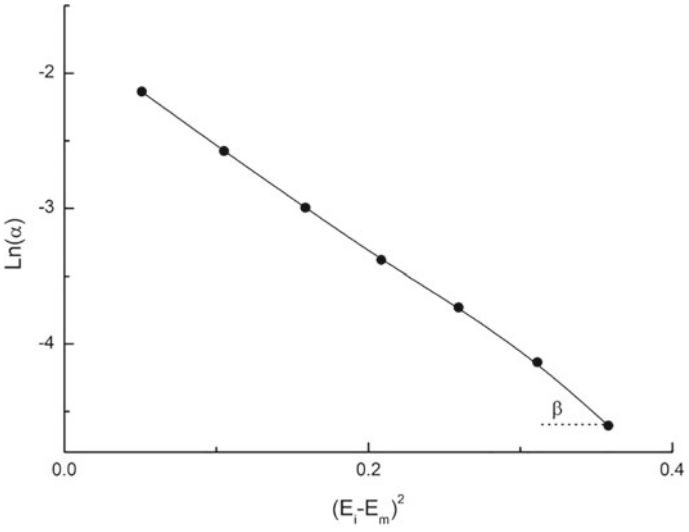

Fig. 2.13 Spectrum of additional optical absorption of an MgO (I) crystal irradiated with a high-current electron beam (j = 800 A см$^{-2}$) up to 3.5 × 10^6 Gy, with deduction the absorption band with a maximum at 4.3 eV

graphical dependence

$$tg\beta = \frac{4 \ln 2}{W^2}. \tag{2.12}$$

It turned out that the half-width of the absorption band with a maximum at 4.3 eV is close to the value of the half-width of the absorption band of Fe^{3+} ions at 4 K (0.73 eV) and is 0.66 eV.

Taking into account, certain values of α_m and W according to the Eq. (2.11), an absorption band with a maximum at 4.3 eV is constructed, which is graphically subtracted from the spectrum of additional optical absorption.

The entire procedure described above is performed under the condition $E_m =$ 4.92 eV for the resulting remainder (Fig. 2.14).

Processing of the results allowed us to establish the value of the half-width (0.61 eV) of the absorption band with a maximum at 4.92 eV, which practically coincides with the known value of the half-width of the absorption band of F^+-centers (0.62 eV).

The correspondence of the values of the half-width of the absorption bands determined by us, with maxima at 4.3 and 4.92 eV, to the known values of the half-width of the optical absorption bands of Fe^{3+} ions and F^+ centers confirms the responsibility of Fe^{3+} ions and F^+ centers for absorption in bands with maxima at 4.3 and 4.92 eV in the spectrum of additional optical absorption of MgO (I) crystals, irradiated by a high-current electron beam.

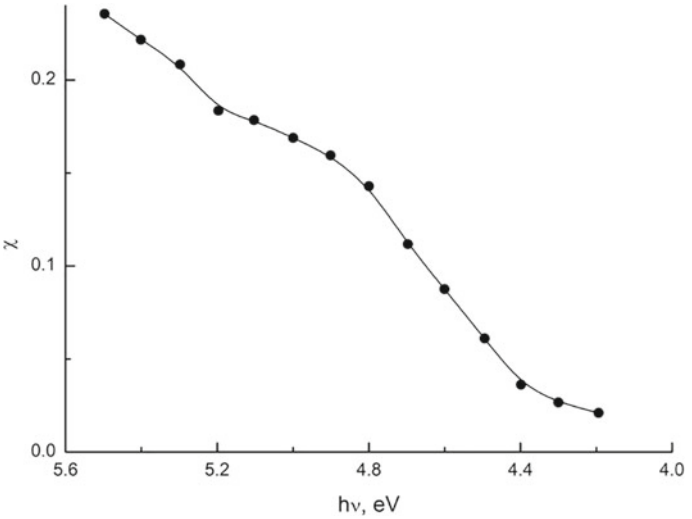

Fig. 2.14 Determination of the absorption band parameters with a maximum at 4.3 eV for a magnesium oxide crystal irradiated with a high-current electron beam (j = 800 A cm^{-2}) up to 9.5 × 10^6 Gr

Thus, irradiation of MgO (I) crystals by a high-current electron beam leads to the formation of F^+ electronic color centers.

In addition to the high-current electron beam, other types of radiation were used in the work, namely X-rays and high-energy protons, irradiation of which MgO (I) crystals leads to the appearance of additional optical absorption (Figs. 2.10 and 2.11) similar to that shown in Fig. 2.9 for a crystal irradiated with a high-current electron beam.

Therefore, it was necessary to conduct studies of the photoluminescence spectra of crystals subjected to these effects.

It turned out that, as with irradiation with a high-current electron beam, and with irradiation with X-rays and high-energy protons, F^+-centers are mainly created in MgO (I) crystals (Fig. 2.12).

Chapter 3
Formation of Radiation Defects in MgO Crystals Under High-Temperature Proton Irradiation

Contents

High-temperature irradiation refers to the irradiation of crystals at temperatures close to 300 K in this section. Protons have a mass intermediate between the masses of electrons and heavy ions and have a high ionizing ability comparable to the result of exposure to high-current electron beams.

At the same time, the proton energy is sufficient for the development of cascade processes of elastic collisions.

Therefore, when irradiating MgO crystals with protons, there is a fundamental possibility of implementing both shock and non-shock mechanisms of defect formation. This is also indicated by the results of work [125], where it was found that with a decrease in the mass of ions implanted in MgO, the efficiency of the formation of radiation defects increased. The defect formation efficiency exceeded the value predicted by the theory of atomic collisions for H^+ and Ne^+ ions.

There is a need to specify the mechanism of ion displacement that dominates during high-temperature irradiation of MgO crystals in connection with the above.

Experimental investigation of this issue is the main task of this chapter.

The methodically set task was solved by studying the spatial distribution of radiation defects in the proton track.

At the same time, we proceeded from the fact that for light charged ions there is a possibility of strict analytical calculation of energy losses for elastic collisions and for ionization and excitation of target atoms [97, 126, 127].

A. Surzhikov and E. Lysenko, *Creation and Accumulation of Radiation Defects in Single Crystals of Magnesium Oxide*, https://doi.org/10.1007/978-3-031-60207-8_3

It is possible to establish a functional relationship between the concentration of defects created and proton energy losses comparing the experimentally measured distribution profile of radiation defects with the calculated data.

The impact mechanism of defect formation will lead to a linear relationship between the number of defects created and the amount of energy loss due to elastic collisions.

The implementation of the decay mechanisms of binary electronic excitations should correspond to a quadratic or close to quadratic dependence of the number of defects created on the magnitude of proton energy losses for ionization and excitation of target atoms.

3.1 Kinetics of the Change in the Intensity of the Absorption Band with a Maximum at 4.92 eV

It was shown in the previous chapter that the absorption bands with maxima at 4.3 and 4.92 eV induced by irradiation with protons, high-current electron beam and X-rays are identified respectively with the absorption of impurity ions of Fe^{3+} and F^{+}-centers.

However, the questions of the origin of anionic vacancies on which F^{+}-centers are formed during irradiation remains open.

Therefore, below we present the results of an experimental study of the kinetics of changing the intensity of the band with $hv_m = 4.92$ eV when irradiating MgO (I) crystals with protons with energy E = 9.3 meV.

Figure 3.1 shows the kinetics of change in the intensity of the band with $hv_m =$ 4.92 eV when crystals are irradiated by protons (curve 1, lower scale) and X-rays (curve 2, upper scale).

The kinetics of band growth goes through two stages: a fast initial and a slow linear one in the case of proton irradiation. During X-ray irradiation of crystals, the kinetic dependence has a nonlinear form and is saturated at approximately the same level as the rapid initial stage of the kinetic curve for proton irradiation.

The completion of the rapid growth stage of the band intensity with $hv_m = 4.92$ eV is accompanied by saturation of the absorption band intensity of Fe^{+3} ions (Fig. 3.2) and the almost complete disappearance of the EPR signal from Cr^{3+} ions.

These data indicate that the fast stage of the kinetic curve for the 4.92 eV band is associated with the radiation recharge of defects existing in the crystal before irradiation.

Indeed, the capture of electrons on the pre-radiation vacancies of anions, with the formation of F-type centers, as well as on Cr^{3+} ions with their recharging of Cr^{3+}, should be accompanied by the capture of holes on Fe^{+2} ions and their oxidation to the Fe^{+3} state.

It is obvious that the duration of these redox reactions will coincide. This explains the simultaneous saturation of the intensity of the absorption band of Fe^{+3} ions, the

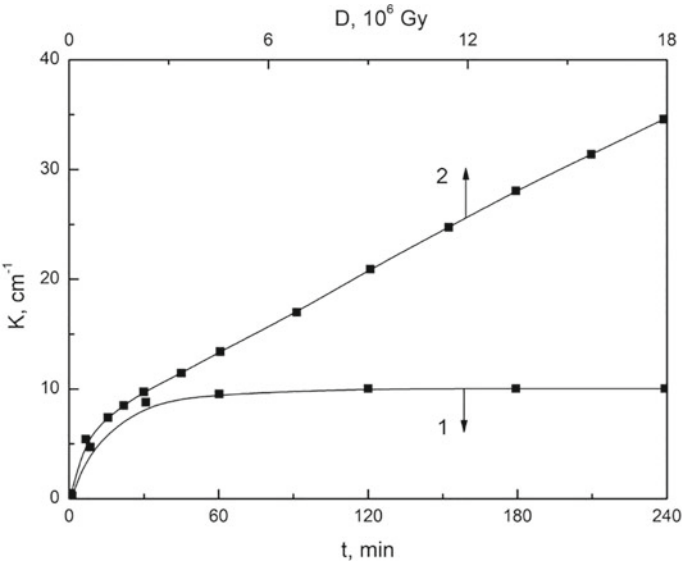

Fig. 3.1 Kinetics of the change in the intensity of the band with $hv_m = 4.92$ eV in MgO (I) under irradiation by protons (1) and X-rays (2)

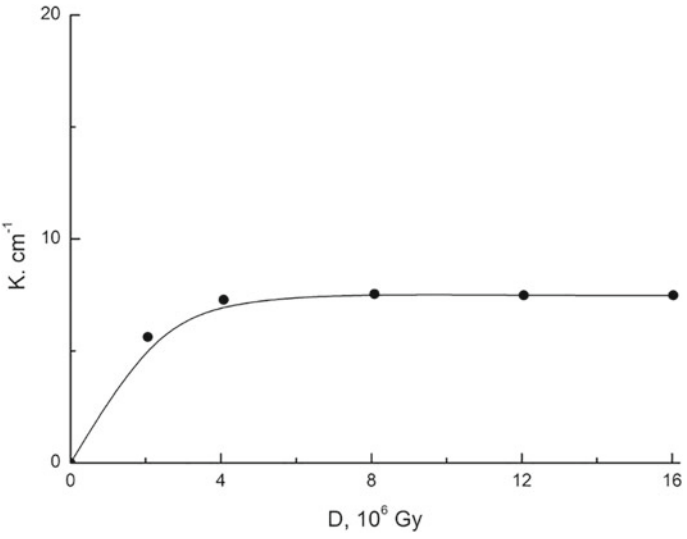

Fig. 3.2 Kinetics of the change in the intensity of the band with $hv_m = 4.3$ eV in MgO (I) under irradiated by protons with an energy of 9.3 meV

disappearance of the EPR signal from Cr^{3+} ions and the completion of the fast stage in the kinetic curve for the 4.92 eV band.

The behavior of the kinetic curve is more significant for the band with hv_m = 4.92 eV after the completion of the fast stage. A linear increase in the intensity of the band occurs only under proton irradiation and is not observed during crystal X-ray irradiation. It is known that X-rays irradiation does not generate new crystal lattice defects in MgO crystals, whereas high-energy particles are capable of causing anion displacement [10].

Therefore, the linear increase in the intensity of the band observed in the experiment with hv_m = 4.92 eV should be associated with the radiation generation of F^+-color centers.

We performed an experiment to prove this position, the idea of which is based on the difference in the thermal stability of radiation-generated F-centers and defects of pre-radiation origin. It is known that the thermal stability of radiation-generated F and F^+-centers is relatively high and is due to the thermal stability of interstitial defects [71].

The destruction of interstitial defects and annealing of the F-band is observed at temperatures exceeding (590–625) K. Annealing of defects of a pre-radiation nature is mainly due to the thermal stability of V-type hole centers and is observed at temperatures not exceeding 450 K [128]. In particular, the EPR signal from Cr ions is completely restored at a temperature of 450 K [128].

Therefore, if the irradiated samples are annealed at a temperature exceeding the stability of the hole centers, but not higher than the temperature of destruction of interstitial defects, then defects created by radiation will remain in the crystal.

The MgO (I) samples were irradiated under the same conditions with protons with E_o = 9.3 meV. The radiation doses for the samples were different. All samples were annealed at a temperature of 475 K for 30 min after irradiation; the intensity of the absorption band was measured at 4.92 eV. The dependence of the intensity of the band with hv_m = 4.92 eV on the radiation dose obtained using this procedure is shown in Fig. 3.3.

It can be seen that this dependence strictly reproduces the linear stage of the accumulation curve shown in Fig. 3.1 (curve 1). This experiment proves that at the linear accumulation stage, defects whose thermal stability coincides with the stability of interstitial anions are responsible for the band with hv_m = 4.92 eV. It is obvious that such defects are the centers of coloring.

The studies presented in this section on the kinetics of changes in the intensity of the absorption band with hv_m = 4.92 eV allow us to conclude that F^+-color centers of MgO crystals created by radiation are mainly responsible for optical absorption in this spectral region at doses exceeding 3×10^6 Gy (the dose required for saturation of the rapid stage).

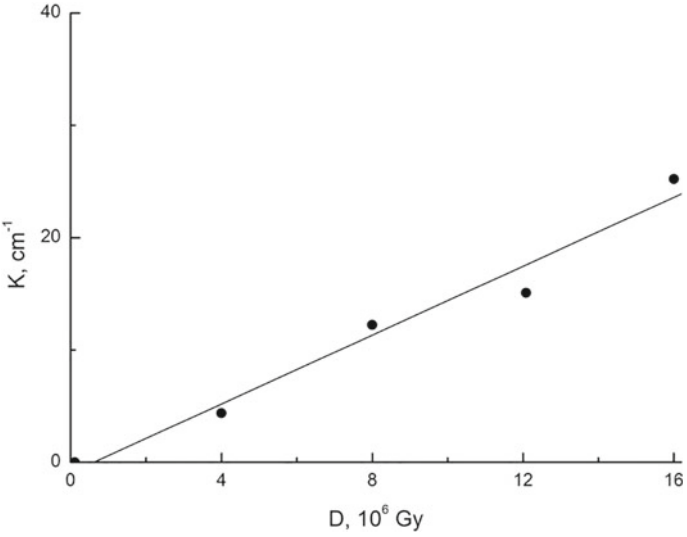

Fig. 3.3 Dose dependence of the intensity of the optical absorption band with $hv_m = 4.92$ eV in MgO (I) crystals after irradiation with protons with E = 9.3 meV and annealing at 475 K for 30 min

3.2 Photo Luminescence of Irradiated MgO (I) Crystals

The radiation accumulation of F^+-color centers, identified by us with a linear increase in the intensity of the optical absorption band with $hv_m = 4.92$ eV, should be accompanied by the accumulation of anionic interstitial defects in the crystal.

The detection of interstitial defects in proton-irradiated MgO (I) crystals would be a direct proof of the radiation generation of Frenkel anion pairs.

Therefore, the results of photoluminescence studies of irradiated MgO (I) crystals will be considered below, the main purpose of which was to prove the radiation generation in proton tracks of anionic interstitial defects of magnesium oxide [129]. Additionally, the task was pursued to clarify once again the type of F-centers created in MgO (I) crystals under proton irradiation.

We used of the luminescent method for recording interstitial defects of magnesium oxide is based on the data of [130], where changes in the cathodoluminescence spectrum of MgO crystals were detected depending on the type of ions implanted in the sample.

In particular, it was found that the cathodoluminescence spectrum of untreated crystals in the visible and near-infrared regions represents two groups of bands of approximately equal intensity. The center of the short-wave group is at λ ~ 440 nm (blue luminescence), the long-wave group is located at λ ~ 700 nm (red luminescence).

Implantation of Mg^{+2} ions into the crystal led to a relative increase in blue luminescence, while implantation of oxygen caused a sharp increase in the intensity of red glow.

If we take into account that, the accompanying defect has the same character due to the proximity of the masses of the embedded ions, then the observed changes in the spectra should be associated with the formation of interstitial defects, which include either magnesium or oxygen, respectively.

We also used a method for comparing the effects of X-ray and proton irradiation on the spectral composition of MgO luminescence when developing a technique for luminescent registration of radiation interstitial defects. This method is based on the well-known fact that Frenkel defects in the magnesium oxide lattice are generated when exposed to a stream of high-energy particles and are not created during X-ray excitation.

The samples were irradiated with protons with energy of 10 meV and a particle flux density of 1.7×10^{15} m^{-2} s^{-1}. X-ray irradiation was performed on the URS-55A installation in the mode at $U_{tr} = 45$ kV and $I_{tr} = 20$ mA. The irradiation and measurement of the spectra were carried out at room temperature.

Photoluminescence of crystals, both before and after irradiation, was excited in the wavelength range (220–340) nm. The highest excitation efficiency (without correction for the density of the exciting light flux) was achieved at $\lambda_b = 254$ nm. Therefore, in the future, the excitation of luminescence was always produced by light with $\lambda_b = 254$ nm.

The luminescence spectrum of unradiated crystals is shown in Fig. 3.4.

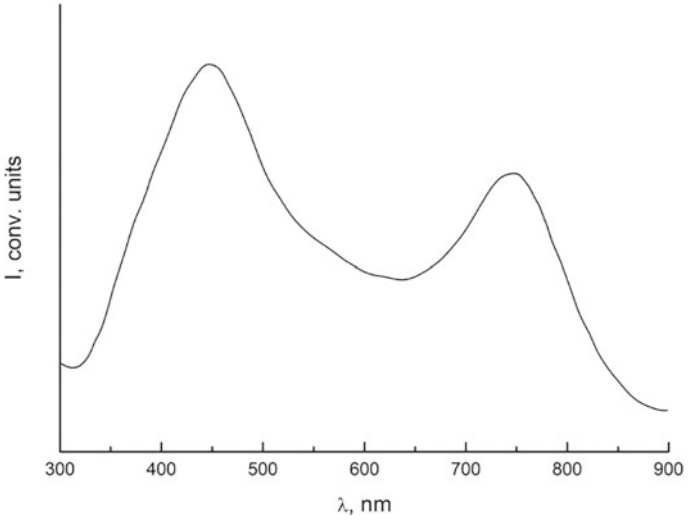

Fig. 3.4 Photoluminescence spectrum of MgO (I) crystals before irradiation ($\lambda_b = 254$ nm)

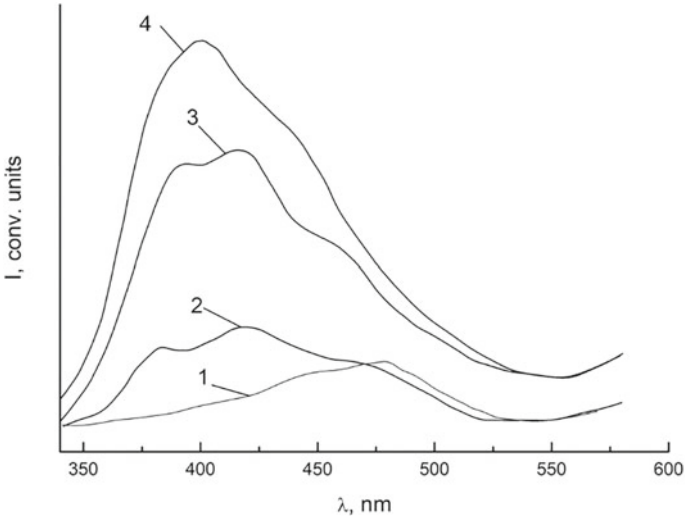

Fig. 3.5 Blue photoluminescence spectra of MgO (I) crystals before and after irradiation with protons with an energy of 9.3 meV (λ_b = 254 nm), where 1 is before irradiation; 2 is dose 4.3×10^6 Gy; 3 is dose 1.72×10^7 Gy; 4 is dose 2.1×10^7 Gy

It is obvious that it is practically identical to the cathodoluminescence spectrum of untreated MgO crystals obtained in [130] and also represents two bands with maxima at 460 nm and 730 nm.

The overall effect of proton irradiation is as follows. Radiation bands with maxima at 390 nm and (420–430) nm appear in the spectrum of blue luminescence, the intensity of which increases with increasing radiation dose (Fig. 3.5, curves 2–4).

The intensity of the red luminescence band also increases; its maximum is shifted to the long-wavelength region of the spectrum (Fig. 3.6, curves 1, 3).

The reason for the shift of the maximum of the red luminescence band was established using the following experiment.

The radiation spectrum of the X-ray sample was measured (Fig. 3.7, curve 1).

Then the same sample was additionally irradiated with protons and the radiation spectrum was measured again (Fig. 3.7, curve 2).

Then the difference of the spectra was plotted, which is a regular Gaussian curve with a maximum at 760 nm and a half-width of 0.3 eV (Fig. 3.7, curve 3).

It is obvious that the observed changes in the red luminescence spectrum under proton irradiation are associated with the appearance and growth of the radiation band with λ_m = 760 nm. Note that the intensity of the new red luminescence component correlates with the optical density at the maximum of the F^+-band of absorption [129].

Annealing of the crystal at 880 K causes the disappearance of luminescence at 760 nm. Subsequent X-ray examination of the sample does not restore it [109].

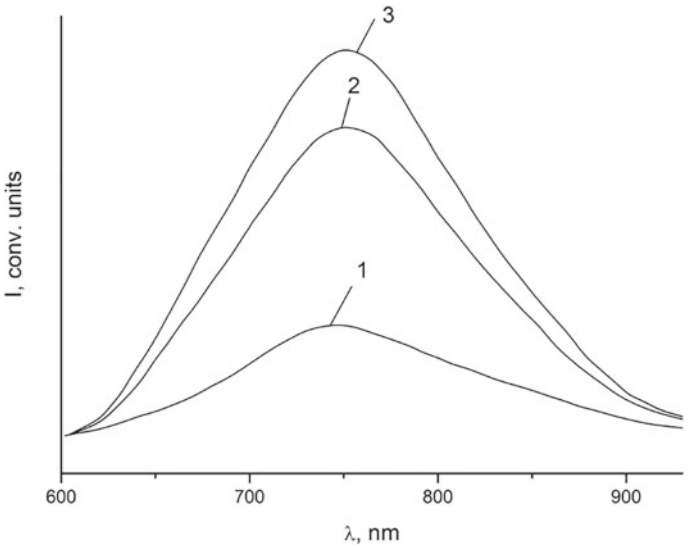

Fig. 3.6 Red photoluminescence spectra of MgO(I) crystals after irradiation with protons with an energy of 9.3 meV ($\lambda_b = 254$ nm), where 1 is dose 4.3×10^6 Gy; 2 is dose 1.3×10^6 Gy; 3 is dose 1.72×10^7 Gy

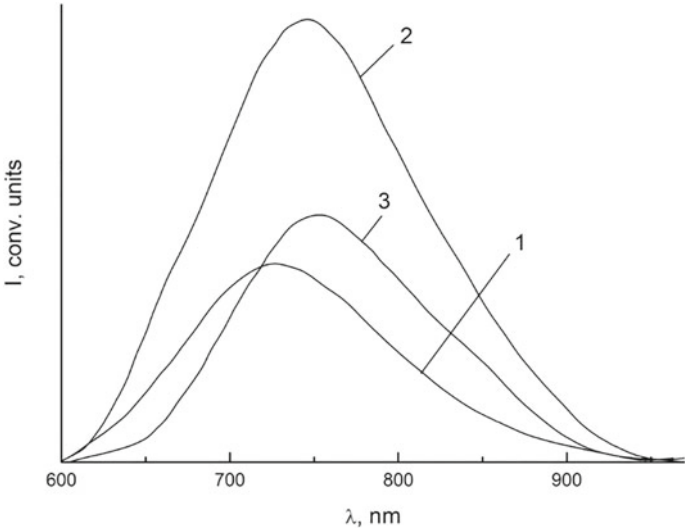

Fig. 3.7 Red photoluminescence spectra of MgO (I) crystals after irradiation with protons with an energy of 9.3 meV ($\lambda_b = 254$ nm), where 1 is the crystal was irradiated with X-rays for 20 min; 2 is the crystal after X-ray irradiation was irradiated with protons with an energy of 9.3 meV at a dose 4.3×10^6 Gy; 3 is the difference between spectra 1 and 2

Analyzing the data presented above, we set ourselves the task of identifying radiation bands associated with new defects in the crystal lattice, and, above all, with defects that include interstitial atoms or ions.

It is obvious that such defects, and, consequently, the radiation bands accompanying them, can occur only after proton irradiation, which, unlike X-rays, can generate Frenkel pairs.

Consider the radiation bands that most effectively arise after proton irradiation.

1. The band with $\lambda_m = 390$ nm. This band has been repeatedly observed in irradiated with high-energy particles, as well as in additively colored crystals [38, 40, 42] and is quite reliably identified with radiative transitions in the F^+-centers of MgO coloring.

We associate the radiation observed by us in the region of 390 nm with the radiation of F^+-centers taking into account the fact that photoluminescence in our case was excited in the F^+-band of absorption.

It should be noted that we did not observe the radiation of F-centers ($\lambda_m = 517$ nm [42]) in our experiments, although the absorption band of F-centers practically coincides with the absorption of F^+-centers and light with $\lambda_b = 254$ nm should excite them equally.

Probably, proton irradiation, as well as neutron irradiation, mainly generates F^+-color centers.

2. The band with $\lambda_m = 760$ nm. Its relationship with the defect that is created only with high-energy irradiation follows from the very procedure for isolating this band.

The linear correlation of the band with $\lambda_m = 760$ nm with the number of accumulated F^+-centers, the irreversible annealing of this band at the destruction temperatures of F^+-centers, the superimposition of the maximum position of the band on the spectral range of the radiation of oxygen embedded in MgO, allows us to identify this radiation band with a defect that includes interstitial oxygen.

3. The band with $\lambda_m = 430$ nm. Radiation with a maximum at 430 nm was observed by a number of authors when studying the spectra of photo-, thermo-, and cathodoluminescence of deformed crystals [107, 115, 116]. It is shown that the intensity of this band correlates with the degree of deformation of the MgO crystal and that the radiation centers are not dislocations, but point defects or their small aggregates [131].

It is assumed that these centers can be either aggregates of vacancies [131] or defects including interstitial magnesium [130, 132]. Apparently, it is impossible to exclude a compromise model of the center in the form of a small vacancy aggregate that localized interstitial magnesium on itself.

The presence of a band with $\lambda_m = 430$ nm in proton-irradiated crystals and its apparent dependence on the radiation dose allow us to conclude that complex centers similar to defects of deformation origin may occur during elastic collisions of protons.

Since the glow with $\lambda_m = 430$ nm was excited in our case by light with $\lambda_b = 254$ nm, it can be assumed that the absorption band of these defects is located in the short-wavelength region of the spectrum.

Indeed, this conclusion is consistent with the fact that the maximum band of the spectrum of photoexcitation of radiation with $\lambda m = 430$ nm is detected at $\lambda = 235$ nm [133].

Summarizing the results presented above, we can conclude that:

1. Exposure to light from the absorption region of F-type centers initiates radiative transitions only in single-electron F^+-centers in proton-irradiated crystals. On this basis, it can be concluded that F^+-centers mainly accumulate during proton irradiation.
2. There is a radiation band with $\lambda_m = 760$ nm, which can be identified with anionic interstitial defects in the photoluminescence spectra of crystals irradiated with protons. Consequently, F^+-centers accumulated during irradiation are created on radiationally created anionic vacancies.
3. The presence in the radiation spectra of a band with a maximum at 430 nm indicates the generation of radiation defects by protons, the structure of which is similar to point defects of deformation origin.

3.3 Proton Energy Losses in MgO (I) Crystals

This section of the paper presents the calculation of the energy dependence of linear proton energy losses in magnesium oxide crystals and experimental results on the spatial distribution of proton energy in a crystal.

These data are necessary to construct a spatial distribution of linear energy losses of a particle in order to compare the distribution of energy losses with the distribution profile of radiation defects in the next section of the work.

Since proton tracks are almost straight-line, we mean what spatial distribution is the distribution of measured values (particle energy, optical absorption intensity, etc.) over the depth of the irradiated volume.

3.3.1 Calculation of Proton Energy Losses Due to Ionization and Elastic Collisions

Energy losses of heavy charged particles in a substance occur as a result of their interaction with electrons and nuclei of target atoms.

The energy spent on ionization and excitation of the target atoms is attributed to ionization losses; energy dissipated in the sample during elastic collisions with nuclei is attributed to losses on elastic collisions.

Energy losses due to inelastic collisions with nuclei, braking radiation, etc. are negligible for heavy charged particles with energy of less than 10 meV [133].

Ionization energy losses of a particle occur if its kinetic energy exceeds the kinetic energy of ionization E_i. E_i is 1.8 keV with respect to protons inhibited in MgO crystals (the band gap is 7.8 eV).

Consequently, protons excite the electronic subsystem of the crystal almost to complete deceleration.

A quantitative measure of ionization energy losses is the value of linear energy losses, which can be calculated using the Bethe-Bloch Equation [133].

The Bethe-Bloch Equation has the form for heavy charged particles with atomic number Z, mass M and energy E ($E > 0.5$ meV)

$$\left(\frac{dE}{dx}\right) = \frac{2\pi e^4 N_e Z^2 M}{mE} \ln \frac{4mE}{MJ}, \tag{3.1}$$

where e and m are the charge and mass of the electron; N_e is the concentration of electrons in the sample; J is the average ionization and excitation potential of the target atoms.

The average ionization and excitation potential J for binary compounds can be calculated by the Equations [169]

$$J = kZ_{eff}, \ln Z_{eff} = \frac{Z_1 \ln Z_1 + Z_2 \ln Z_2}{Z_1 + Z_2}, \tag{3.2}$$

where Z_1 and Z_2 are the atomic numbers of the anions and cations of the compound.

We obtain Z_{eff} equal to 10.2 for magnesium oxide. The coefficient k is a function of the effective atomic number of the compound and for $Z_{eff} = 10.2$ it can be equal to 13 eV. Therefore, the value of J for MgO crystals according to (3.2) is equal to 133 eV.

The electron density is determined by the Equation

$$N_b = \frac{4(Z_1 + Z_2)}{a^3}, \tag{3.3}$$

where a is the crystal lattice parameter.

We get $N_e = 1.08 \times 10^{24}$ cm^{-3} taking, a = 4.2 Å [1].

Substituting the calculated values of J and N_e in (3.1) and expressing $\left(\frac{dE}{dx}\right)_i$ in [MeV cm^{-1}], E is in [MeV], we get

$$\left(\frac{dE}{dx}\right)_i = \frac{258.8 \ln 16.4E}{E}. \tag{3.4}$$

Proton energy losses due to elastic collisions are determined by the interaction potential of the proton with crystal-forming ions.

According to (2.8) and (2.9), the boundary energy of Coulomb scattering of protons in MgO is (120 ÷ 100) eV. Consequently, the condition of Coulomb interaction of protons with the nuclei of target atoms is fulfilled at particle energies exceeding 10 keV.

Linear energy losses due to elastic collisions are described by the Equation in the Coulomb interaction of colliding particles [97]

$$\left(\frac{dE}{dx}\right)_C = \frac{4\pi a_0^2 N_0 Z_1^2 Z_a^2 M_1 E_k^2}{M_2 E} \ln\left(\frac{T_m}{E^*}\right), \tag{3.5}$$

where E^* is the minimum recoil energy; Z_a is the atomic number of the ion.

Since we are interested in collisions leading to displacement of ions, the value of E can be assumed to be equal to the threshold energy of displacement E_d. The experimentally obtained value of D is 60 eV for oxygen ions [96] and 62 eV for magnesium ions [110].

The total proton energy losses due to elastic collisions for MgO crystals are equal to the sum of the losses in the cationic and anionic sublattices of the crystal according to the Bragg additivity rule [127, 133]. Substituting the numerical values of the quantities included in (3.5), we obtain the equations:

1. Elastic losses in the cationic sublattice

$$\left(\frac{dE}{dx}\right)_C^{Mg} = \frac{2.12 \times 10^{-2} \ln 2560E}{E}, \tag{3.6}$$

2. Elastic losses in the anionic sublattice

$$\left(\frac{dE}{dx}\right)_C^{O} = \frac{1.41 \times 10^{-2} \ln 3683E}{E} \tag{3.7}$$

3. Total losses on elastic collisions

$$\left(\frac{dE}{dx}\right)_C = \frac{1.41 \times 10^{-2}}{E}(1.5 \ln 2560E + \ln 3683E). \tag{3.8}$$

The energy loss values in (3.6)–(3.8) are expressed in [MeV cm^{-1}], the proton energy is in [MeV].

Expressions (3.6) and (3.8) define the energy dependences of the efficiency of creating cationic and anionic defects in elastic collisions of a proton with crystal-forming ions (with the exception of the final section of the track, when the proton energy becomes below 10 keV).

At the same time, the energy of elastic collisions transmitted to the cationic sublattice is higher by 1.5 times than the corresponding value for the anionic sublattice.

The energy spent on the excitation and ionization of the target atoms is more than higher by 10^3 times than the energy loss due to elastic collisions; it follows from the comparison of (3.4) and (3.8). Therefore, compounds in which the decay of electronic excitations does not lead to the birth of defects are radiation-resistant.

3.3.2 Proton Energy Distribution Over the Depth of Irradiated MgO (I) Crystals

A sharp increase in energy losses due to elastic collisions with a decrease in proton energy causes an uneven distribution of atoms displaced along the length of the track because of elastic collisions.

It is necessary to express the Eqs. (3.6)–(3.8) through the distance from the considered section of the particle track to the irradiated crystal surface in order to be able to compare the experimentally obtained distribution profile of radiation defects with the calculated distribution of energy losses for elastic collisions.

It is necessary to know the distribution of proton energy over the depth of the irradiated object to do this.

Therefore, the results of experimental determination of the proton energy distribution over the depth of irradiated crystals will be considered below.

We found the energy distribution of protons by measuring the energy of particles passing through MgO (I) crystals of various thicknesses. Samples with a size of 5 $\times$ 5 mm were cut out of the ingot and etched in heated to 350 K nitric acid to a predetermined thickness within (20–350) μm.

KC1 crystals were used as proton energy detectors. It is known that proton irradiation of KC1 crystals causes the appearance of a colored layer with a sharp boundary caused by the creation of optically active radiation defects. The thickness of the colored layer corresponds to the proton path and depends on their initial energy.

The "mileage-energy" dependence for protons is measured with high accuracy and with its help for most silk-haloid crystals; it is easy to find the initial energy of the particle from the thickness of the colored crystal layer [169].

Since the detecting crystals were located behind the MgO (I) crystals, the initial proton energy in this case corresponded to the energy of the particle after passing through a crystal layer equal to the thickness of the sample.

MgO samples and KCl detecting plates were placed in an irradiation cassette. The cassette was a plane-parallel lead plate with a thickness of 10 mm, having 10 collimating holes with a diameter of 2 mm.

MgO (I) samples with different thicknesses were glued with epoxy resin opposite the holes on the side of the cassette facing the proton beam. The KCl plates were fixed with a spring clip on the opposite side of the cassette. Then the cassette was mounted on the flange of the cyclotron ion conduit perpendicular to the axis of the proton beam.

The irradiation was carried out by protons with an initial energy of 5.1 meV for 10 min, which was sufficient for the appearance of a well-visible colored layer in the crystal KCl. The experiment was repeated 5 times with the replacement of detecting crystals.

The thickness of the MgO samples and the thickness of the colored layers in the KCl crystals were repeatedly measured using an ISA-2 microscope. The measurement results were averaged; a confidence interval for a probability of 0.99 was calculated according to the method [134].

Figure 3.8 shows the dependence of the proton energy obtained in this way on the thickness of the MgO sample passed by the proton. KCl crystals placed behind MgO samples with a thickness of more than (136.0–1.5) μm were not stained. In this regard, the energy distribution curve was extrapolated to a run length equal to 136 μm.

The measurement results were approximated by a power function by the method of least squares

$$E(x) = 0.33(R_0 - x)^{0.56}, \tag{3.9}$$

where x is the distance [microns] from the track section under consideration to the irradiated surface of the sample; $E(x)$ is the proton energy [MeV] at a distance of x from the sample surface; R_0 is the proton mileage [microns].

Equation (3.9) can be used for arbitrary initial proton energies not exceeding 10 meV, with the substitution of the corresponding value of the path R_Q. It is easy to calculate the energy of a particle at any distance from the crystal surface with its

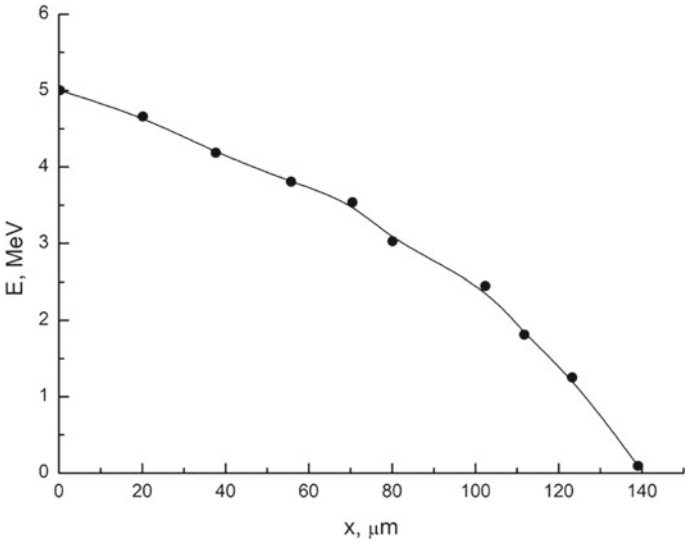

Fig. 3.8 The distribution of protons over the thickness of MgO (I) crystals ($E_o = 5.1$ meV)

help; it is possible to find the value of the required type of energy loss substituting the found value in (3.4), (3.6)–(3.8).

3.4 Distribution of F^+-centers by Depth of MgO (I) Crystals Irradiated with Protons

The main task of this section of the work was to solve the question of the dominant mechanism of anion displacement under conditions of proton bombardment of MgO (I) crystals at a temperature of 300 K.

The answer to this question can be obtained by comparing the experimental profile of the distribution of radiation defects with the spatial distribution of proton energy losses.

The energy losses of the particle are calculated with high accuracy by the Eqs. (4.4), (4.6)–(4.8) in a wide energy range of the retarding proton, which is ~ 90% of the initial energy (at E ≅ 10 meV); the deep distribution of energy losses is easily restored using the proton energy distribution obtained in the previous section in the crystal.

Microphotometric measurements of the absorption spectra of irradiated crystals were performed at different distances from the irradiated surface of the sample.

The samples were irradiated with protons with $E_0 = 9.3$ meV and a beam current of 4.1×10^{-4} A·m^{-2} at a dose of 7×10^6 Gy.

The optical absorption induced by irradiation was found as the difference between the absorption spectra measured at a given depth and the spectrum obtained at a depth of 700 μm, significantly exceeding the thickness of the colored layer.

The spectra of additional staining of crystals obtained in this way at different distances from the irradiated surface are shown in Fig. 3.9. Analysis of these spectra showed that their component composition includes Gaussian bands with maxima at 4.92 and 4.3 eV.

Figure 3.9 clearly shows that the most significant changes in intensity (as we move away from the irradiated crystal surface) are experienced by a band with $h_{vm} = 4.92$ eV, which we identify with the absorption of F^+-centres.

This fact is clearly illustrated in Fig. 3.10, which shows the difference between the spectra measured at depths of 320 and 350 μm and which coincides in shape with the F^+-band of absorption.

The intensity distribution curves of the bands over the depth of the irradiated volume were constructed after decomposition of the spectra into components: for the F^+-band (Fig. 3.11, curve 1) and for bands with $h_{vm} = 4.3$ eV (Fig. 3.12, curve 1) and $h_{vm} = 5.63$ eV (Fig. 3.12, curve 2). The presented curves indicate a fundamental difference in the nature of the defects responsible for the F^+-band and for the band with $h_{vm} = 4.3$ eV.

Indeed, since the radiation dose exceeded the value required to complete the radiation oxidation of iron ions (Fig. 3.2), the uniform distribution of the intensity

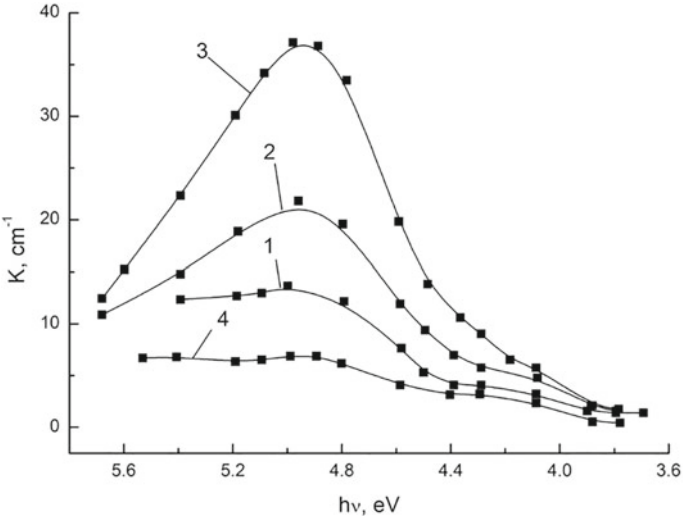

Fig. 3.9 Spectra of additional optical absorption of MgO (I) crystals at different distances from the irradiated surface of the sample, where 1 is at X = 100 μm; 2 is at X = 320 μm; 3 is at X = 350 μm; 4 is at X = 400 μm

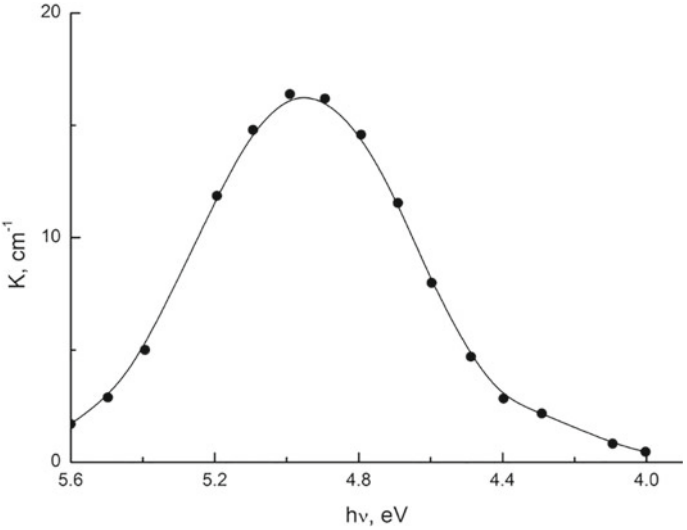

Fig. 3.10 The difference in the absorption spectra of the MgO (I) crystal irradiated by protons with $E_0 = 9.3$ meV, measured at a depth of 320 and 350 μm

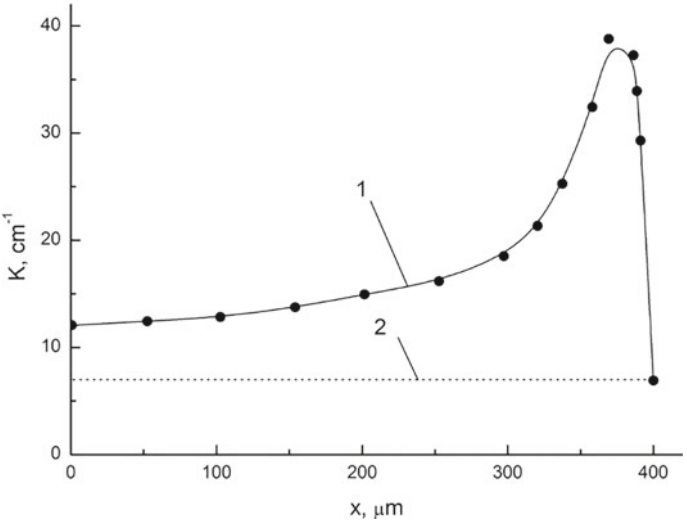

Fig. 3.11 Intensity distribution of the F^+-band over the thickness of the MgO (I) crystal irradiated with protons with an energy of 9.3 meV (1) and the constant component of the distribution (2)

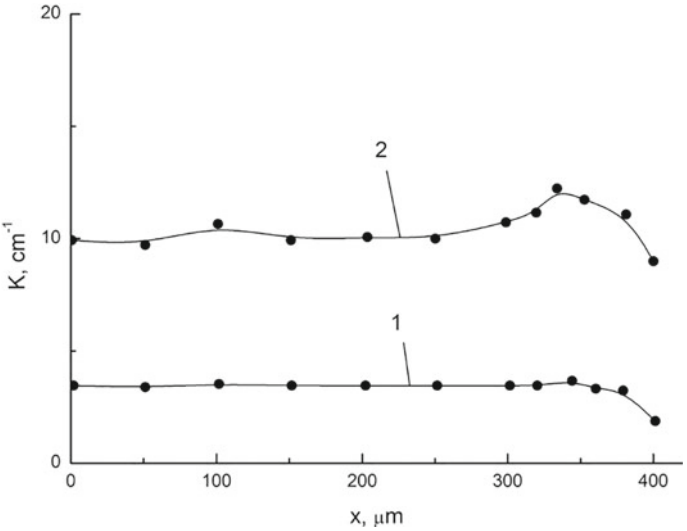

Fig. 3.12 The thickness distribution of the MgO (I) crystal of optical absorption with $h_{vm} = 4.2$ eV (1) and 5.63 eV (2) after irradiation with protons with an energy of 9.3 meV

of the band with $h_{vm} = 4.3$ eV reflects the uniformity of the distribution of impurity iron ions in the crystal.

Thus, this result is consistent with the identification of the band with $h_{vm} = 4.3$ eV with optical transitions in Fe^{+3} ions.

On the other hand, the pronounced heterogeneity of the distribution of F^+-centers indicates a different mechanism of their creation, which is clearly different from the mechanism of recharging of pre-radiation defects of the crystal lattice.

We compared the intensity distribution of the F^+-band with the distribution of proton energy losses on elastic collisions in the anionic sublattice to determine the mechanism of creation of F^+-centers.

The proton energy was found at a given distance from the irradiated crystal surface for this purpose, according to Eq. (3.9); energy losses were calculated according to Eq. (3.7).

Figure 3.13 shows the dependence of the intensity of the F^+-band obtained in this way on the proton energy losses due to elastic collisions. The left and right arrows indicate, respectively, the positions of the track sections on the surface (x = 0) and at a depth of 320 μm.

It is clearly seen from the presented curve that the intensity of the F^+-band with high accuracy corresponds to the elastic energy losses of the proton on the overwhelming part of the proton path length (at least 85% of the path length). The linear dependence is transformed into a nonlinear one only in the final part of the track in the region of the maximum of the band intensity distribution.

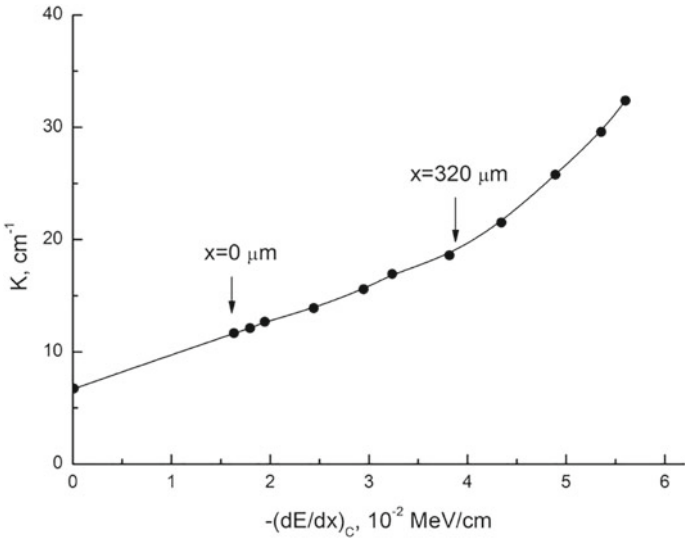

Fig. 3.13 Dependence of the intensity of the F^+-band of optical absorption on the linear loss of proton energy on elastic collisions

This result indicates the direct connection of the process of creating F^+-centers with the elastic scattering of protons on crystal-forming ions.

Considering the intensity distribution curve of the band with $h_{vm} = 5.63$ eV over the depth of the irradiated volume (Fig. 3.12, curve 2), it is necessary to emphasize its intermediate form relative to the distribution curves of F^+-centers and Fe^{+3} ions.

This fact is additional evidence that defects of various nature are responsible for the band with $h_{vm} = 5.63$ eV, some of which are generated by radiation, others are not.

Let's consider some features in the nature of the dependence presented in Fig. 3.13.

1. The presence of a constant component is characteristic. If we continue the linear section of the curve to the zero value of the energy loss (dashed curve), then the constant component in the intensity of the F^+-band, independent of the proton energy loss, is cut off on the ordinate axis. This value, equal to 7 cm^{-1}, is in accordance with the saturation level of the intensity of the band with $h_{vm} =$ 4.92 eV at the fast stage (Fig. 3.1, curve 1). The constant component in the distribution of F^+-centers is carried out symbatically to the distribution of Fe^{+3} ions and is shown in Fig. 3.11, curve 2.

The difference between curves 1 and 2 (Fig. 3.12) is shown in Fig. 3.14 (curve 1).

This curve represents the distribution of F^+-centers formed on vacancies created by radiation, while the constant component obviously reflects the distribution of defects responsible for the initial rapid stage of kinetic dependence.

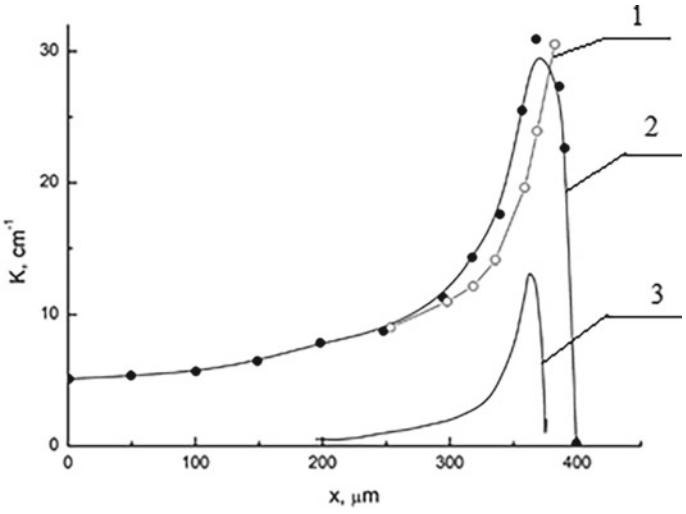

Fig. 3.14 Intensity distribution of the F^+-band over the thickness of MgO (I) crystals irradiated with protons with an energy of 9.3 meV, where 1 is the experimental curve (without a constant component); 2 is the curve normalized to the initial value and adjusted in accordance with the distribution of proton energy losses for elastic collisions; 3 is the difference between curves 1 and 2

2. The increase in the intensity of the band outstrips the increase in losses due to elastic collisions in the final section of the proton path. Therefore, there is no correlation between the calculated and experimental defect distribution profiles in this area.

This fact can be presented more clearly if we explicitly construct the intensity distribution profile of the F^+-band calculated by the shock mechanism and compare it with the experimental one.

The calculated values of linear energy losses were normalized to their initial value at $X = 0$ for this purpose. The distribution of normalized energy losses is shown in Fig. 3.15, curve 1. Then the initial intensity of the F^+-band without a constant component was multiplied by the corresponding normalized values of energy losses as weight multipliers. Thus, the relative measurements of energy losses and the intensity of the F^+-band were brought into line.

The theoretical distribution of the intensity of the F^+-band (according to the shock mechanism model) is shown in Fig. 3.14, curve 2.

It can be seen that, basically, the distribution of F^+-centers corresponds to the distribution of defects created as a result of elastic proton scattering from a comparison of curves 1 and 2, Fig. 3.14.

However, the number of accumulated F^+-centers significantly exceeds the number of F^+-centers created in elastic collisions in the region of the distribution maximum. For example, the excess corresponds to ~ 55% of the calculated value at $X = 350$ μm.

The observed discrepancy between the experimental and calculated data cannot be explained by the calculation error taking into account the good correlation of the

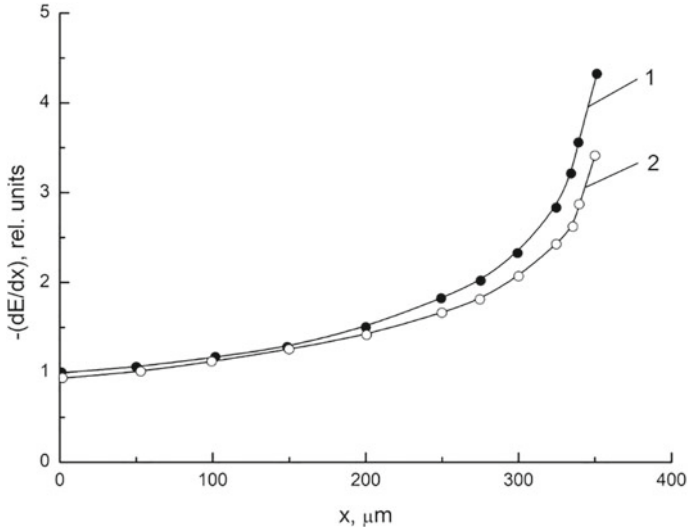

Fig. 3.15 Normalized by initial values (at $X = 0$) distributions of linear proton energy losses over the thickness of MgO (I) crystals ($E = 9.3$ meV), where 1 is for elastic collisions; 2 is for ionization and excitation of atoms

calculated and experimental data over the overwhelming length of the track (~ 85% of the mileage) and that the range of applicability of the equations used extends to the proton energy of 1 meV (X = 360 μm).

Probably, a similar discrepancy was observed in [132], when MgO crystals were irradiated with light ions. Therefore, this effect cannot be considered accidental.

The convergence of the calculated and experimental data did not change when using Eq. (3.8) for total proton energy losses due to elastic collisions, i.e. taking into account, the energy transfer to the cation sublattice does not change the defect distribution profile.

Therefore, the increased efficiency of the formation of centers in the area of maximum distribution can be explained by two hypotheses:

1. Improvement of the conditions for stabilization of Frenkel anion pairs in the field of maximum efficiency of elastic collisions (for example, due to enhanced aggregation of interstitial defects).
2. Implementation of the Frenkel anion pair generation process additional to the shock mechanism.

Let's discuss these hypotheses. The excess of the experimentally measured intensity of the F^+-band over the thermal intensity has a local, rapidly increasing form (Fig. 3.14, curve 3), which is associated with processes having a threshold character.

The stabilization of defects cannot be attributed to threshold processes, especially since as the proton decelerates; the average energy of displaced atoms decreases and overcoming any barriers near the F^+-centers of stabilization of mobile defects, on the contrary, will be less effective.

Therefore, this hypothesis seems unrealistic. There is a significant increase in ionization losses of proton energy in the proton track in the region of the maximum distribution of F^+-centers.

This is evidenced by the distribution curve of ionization energy losses, normalized to its initial value (Fig. 3.15, curve 2).

Probably, in this case, a critical excitation density of the electronic subsystem of the crystal is achieved, as a result of which the processes of non-elementary generation of anionic Frenkel pairs are initiated.

However, the effect of additional creation of F^+-centers does not matter much, since the number of additionally created F^+-centers and the total number of accumulated F^+-centers are correlated as areas bounded in Fig. 3.14 by curves 1 and 3, respectively. This ratio does not exceed 8%.

It can be seen that if ionization energy losses are used as weighting factors from a comparison of the normalized distributions of elastic and ionization energy losses of protons (Fig. 3.15, curves 1 and 2); the resulting calculated curve of the distribution of F^+-centers will be much worse consistent with the experimental distribution.

Therefore, it can be concluded that the experimentally obtained distribution of F^+-centers is most fully consistent with the distribution of proton energy losses for elastic collisions. On this basis, we conclude that at elevated temperatures of proton irradiation in MgO (I) crystals, the shock mechanism of defect formation in the anionic sublattice of the crystal dominates.

3.5 Summary

1. The predominant type of radiation defects of the anionic sublattice are color centers in proton-irradiated MgO (I) crystals.
2. The dominant mechanism of radiation defect formation in MgO (I) crystals is the shock mechanism of anion displacement at elevated irradiation temperatures.
3. A violation of the linear correlation between the intensity of the F^+-band and proton energy losses due to elastic collisions was noted in the region of the Bregg peak. The reason for the correlation violation may be the non-elementary generation of anionic Frenkel defects at a particularly high intensity of energy losses.
4. The luminescence band excited by UV light with $\lambda = 430$ nm in proton-irradiated crystals indicates the generation of defects in proton tracks similar to defects that occur during deformation of magnesium oxide crystals.
5. Spectral changes in the composition of red photoluminescence indicate the generation of anionic interstitial defects in proton tracks.
6. The developed luminescent technique for registering interstitial defects can be used in highly sensitive methods for monitoring the radiation defectiveness of products made of crystalline magnesium oxide.
7. An experimental curve of the proton energy distribution over the crystal depth is obtained. These data can be used to determine the path of protons in magnesium oxide crystals by their initial energy.

Chapter 4
Stabilization of Frenkel Defects in Crystals of Magnesium Oxide at Impact Displacement of Ions

Contents

The fixation of atoms or ions displaced from the nodes of the crystal lattice is an obligatory stage of accumulation of intrinsic radiation defects of a solid. At this stage, the created and spatially separated elements of Frenkel pairs are transformed into color centers that are stable under experimental conditions.

As a rule, interstitial ions are much more mobile elements of Frenkel pairs in ionic crystals. Therefore, the problem of accumulation of stable color centers is practically reduced to the problem of fixing interstitial ions.

In general, stable interstitial defects can occur during autolocalization of displaced atoms in defect-free areas of the crystal.

However, this process can be realized only at extremely low temperatures (for MgO, apparently, at $T < 27$ K [87]) and, therefore, in most cases it is not relevant.

It is easy to foresee that the most common processes in real crystals are the interaction of displaced particles with the pre-radiation and radiation defects of the crystal.

A. Surzhikov and E. Lysenko, *Creation and Accumulation of Radiation Defects in Single Crystals of Magnesium Oxide*, https://doi.org/10.1007/978-3-031-60207-8_4

The specific type of such interactions and their relative effectiveness are determined by the irradiation conditions, structure and chemical composition of the material.

The shock mechanism of Frenkel pair generation established in Chap. 3 when MgO is irradiated with protons at room temperature is quite trivial.

However, in ionic crystals (possibly in other binary systems), the implementation of the shock mechanism can lead to the appearance of specific processes of formation of interstitial defects associated, in particular, with the exchange of momentum between the sublattices of the crystal, with the presence of a high density of electronic excitations in particle tracks, etc. This aspect of the problem of creating interstitial defects has not been considered in the literature.

The lack of systematic studies of the mechanisms of localization of displaced ions and the crucial importance of this problem for the correct understanding of the basic laws of radiation damage to magnesium oxide crystals served as the basis for consideration in this chapter of the following questions:

1. To establish the most significant processes leading to localization of displaced ions in elastic collisions.
2. To analyze probable models of interstitial defects formed in proton tracks.

It is most expedient to solve these issues by comparing the accumulation and annealing curves of radiation defects in samples of various chemical compositions and by comparing experimental and calculated accumulation curves of color centers.

The solution of the problem formulated above could be obtained only on MgO crystals of increased purity. The content of the main impurities in the unalloyed crystals is presented in Table 2.1. Crystals alloyed with aluminum to a mass concentration of 0.1 and 0.3% were designated respectively as MgO (II): 0.1 Al and MgO (II): 0.3 Al.

The samples were irradiated in air with protons with an energy of 9.3 meV and a particle flux density of $1.75 \cdot 10^{15}$ m^{-1}. The irradiation temperature did not exceed 310 K taking into account the radiation heating of the sample.

The length of proton runs required for calculations according to Chap. 3 was assumed to be 370 μm. The concentration of F^+-color centers was calculated using the Smakula's Equation

$$N_F = 0.87 \times 10^{17} \frac{nU_m}{(n^2+2)^2 f} k_m, \tag{4.1}$$

where n is the refractive index ($n = 1.74$ [1]); U_m is the half-width of the band; k_m is the absorption coefficient at the maximum of the band; f is the oscillator strength (for F^+-centers $f = 0.8$ [29]).

We obtain an expression convenient for calculating the concentration of F^+-centers when substituting the numerical values of the parameters in (4.1). By substituting the numerical values of the parameters in (4.1), we obtain the expression (4.2), convenient for calculating the concentration of F^+-centers:

$$N_F = 5.1 \cdot 10^{15} k_m. \tag{4.2}$$

4.1 Optical Absorption of MgO (II) Crystals

The absorption spectra of unradiated MgO (II) crystals are shown in Fig. 4.1.

Pure single crystals of MgO (II) are characterized by distinct maxima in the region of 5.7 and 4.3 eV, whereas in aluminum-doped samples the curves have no obvious structure.

The spectral composition of the optical absorption induced by radiation is easily established by constructing the difference in the spectra of samples at different radiation doses.

Figures 4.2, 4.3 and 4.4 show the results of subtraction of spectra for pure and doped crystals irradiated sequentially with doses of 3.9×10^7 and 7.3×10^7 Gy.

Thus, the spectra shown in the figures correspond to the absorbed dose of 3.4×10^7 Gy.

A wide asymmetric band with $h_{vm} \sim 5.6$ eV (curves 4) remains in the spectra After subtracting the F^+-bands of absorption with parameters $h_{vm} = 4.92$ eV, $U_m = (0.64 \pm 0.02)$ eV (curves 1), which can be represented as a superposition of bands $h_{vm} =$ 5.7 and 5.32 eV (curves 2–3).

The result of the decomposition of the spectra into Gaussian components is presented in Table 4.1.

It was found that there are no qualitative changes in the spectra by studying the evolution of the spectra with a change in the absorbed dose in the samples Mg (II), Mg (II):0.1Al, MgO (II):0.3 Al.

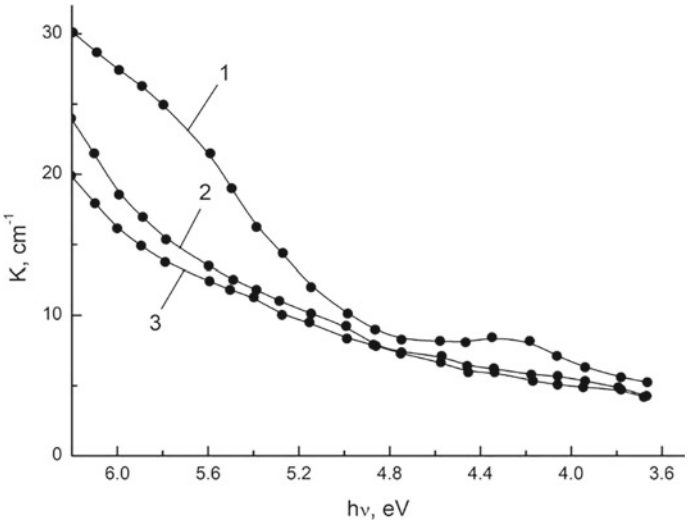

Fig. 4.1 Optical absorption spectra of unradiated crystals MgO (II) (1), MgO (II): 0.1 Al (2), MgO (II): 0.3 Al (3)

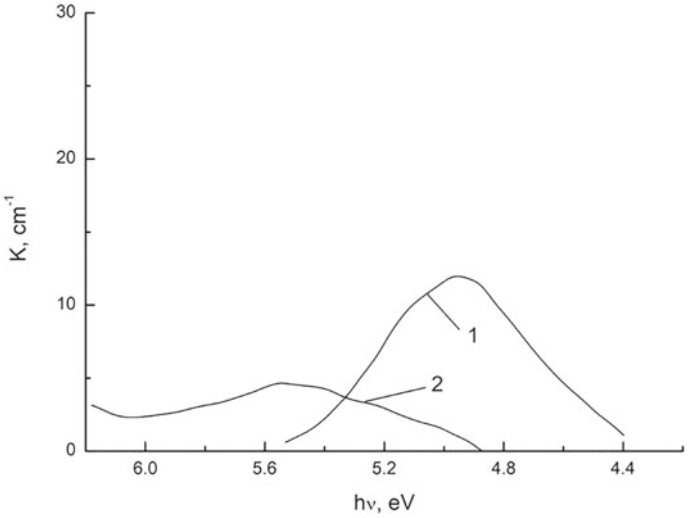

Fig. 4.2 The difference in the optical absorption spectra of an MgO(II) single crystal irradiated with protons with an energy of 9.3 meV at doses of 3.9×10^7 Gy and 7.3×10^7 Gy, where 1, 2 are the components of the spectrum

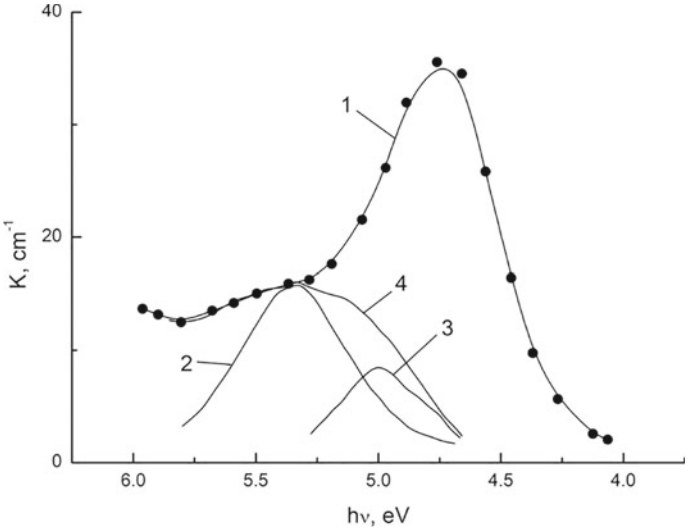

Fig. 4.3 The difference in the optical absorption spectra of a single crystal MgO (II):0.1 Al irradiated with protons with energy of 9.3 meV at doses of 3.9×10^7 Gy and 7.3×10^7 Gy, where 1–3 are the Gaussian components of the spectrum; 4 is the remainder of the spectrum after subtracting the F^+-band

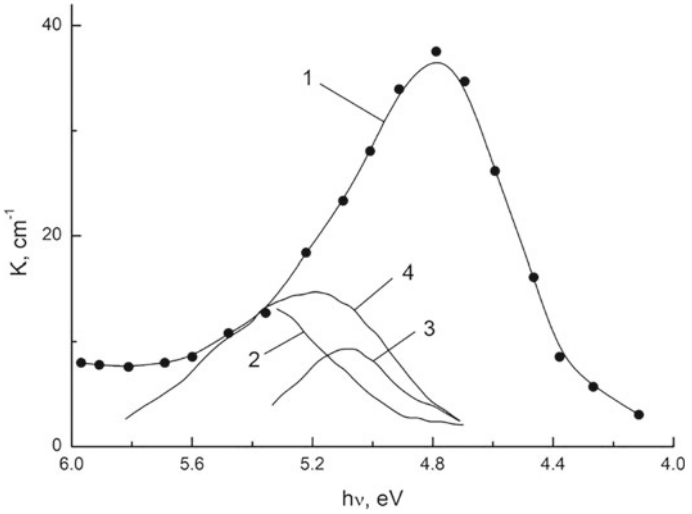

Fig. 4.4 The difference in the optical absorption spectra of a single crystal MgO (II):0.3 Al irradiated with protons with energy of 9.3 meV at doses of 3.9×10^7 Gy and 7.3×10^7 Gy, where 1–3 are the Gaussian components of the spectrum; 4 is the remainder of the spectrum after subtracting the F^+-band

Table 4.1 Gaussian components of the absorption spectra of irradiated crystals of MgO (II) and Mg (II): Al

Absorption band parameter	Curve number according to Figs. 4.2, 4.3 and 4.4			
	1		2	3
h_{vm}, eV	4.92 ± 0.01	5.7 ± 0.02	5.32 ± 0.02	
U_m, eV (half-width)	0.64 ± 0.02	0.66 ± 0.01	0.49 ± 0.02	

4.2 The Role of Trivalent Cations of Substitutive Impurities in the Phenomena of Stabilization of Radiation Defects in Magnesium Oxide

The pre-radiation defectiveness of the crystal lattice has a significant effect on the processes of fixing atoms or ions displaced in the internode.

This factor becomes crucial in the case of ionic crystals with multicharged ions, when the Coulomb interaction between charged fragments of Frenkel pairs causes a particularly high efficiency of reverse recombination processes.

It was previously shown that during proton irradiation of MgO, mainly F^+-color centers are generated.

Therefore, it should be expected that the main part of the oxygen anchored in the internode will have a negative charge. Under these conditions, the stabilizing value

of trivalent cation-substituting impurities with an excess positive charge relative to the crystal lattice should increase.

In this section, we prove the validity of this provision using the example of impurity of Al^{+3} [160,171, 172].

4.2.1 Kinetics of Accumulation of F^+-Centers in Pure and Doped MgO (II) Crystals

Figure 4.5 shows the dose dependences of the accumulation of F^+-centers in MgO (II) crystals (curve 1), MgO (II):0.1 Al (curve 2) and MgO (II):0.3 Al (curve 3) in a wide range of irradiation doses (10^6–2.8×10^8) Gy.

The accumulation curves for small doses are shown in Fig. 4.6.

Comparing the obtained dependences, it can be noted that, regardless of the chemical composition, in the area of low doses of irradiation, the accumulation of F^+-centers, as in MgO (I) crystals, is carried out according to a two-stage law (Fig. 4.6).

The rapid initial stage at doses exceeding 3×10^6 Gy in all samples passes into a slow, close to linear, stage of accumulation of defects. The duration of the first stage coincides with the same value for MgO (I) samples.

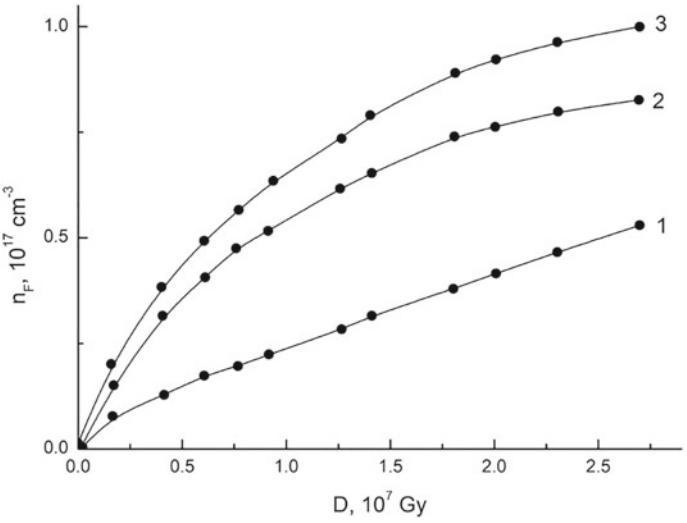

Fig. 4.5 Kinetics of accumulation of F^+-centers at elevated doses of irradiation with protons with an energy of 9.3 meV at 300 K in single crystals MgO (II) (1), MgO (II):0.1A1 (2) and MgO (II):0.3Al (3)

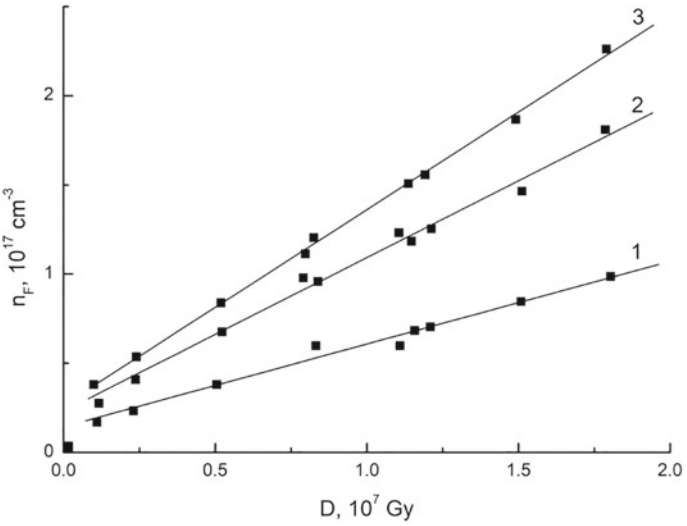

Fig. 4.6 Kinetics of accumulation of F^+-centers in the region of low doses of irradiation with protons with an energy of 9.3 meV in single crystals MgO (II) (1), MgO (II):0.1A1 (2) and MgO (II):0.3Al (3)

The slow linear character of accumulation persists in pure MgO (II) samples in the region of high radiation doses, when nonlinear effects are clearly manifested in doped crystals (Fig. 4.5).

The accumulation curves for all samples run almost parallel to each other at doses exceeding 10^8 Gy.

It can be concluded from this that the dose dependences of the accumulation of centers in doped crystals are not experimental curves and, along with the nonlinear dependence, include a close to linear stage identical to the curve of the accumulation of F^+-centers in pure crystals.

This conclusion is clearly illustrated in Fig. 4.7, where kinetic curves of accumulation of centers in doped crystals are constructed, from which the curve of accumulation of F^+-centers in pure crystals was subtracted.

It is easy to notice that the rate of accumulation of F^+-centers at the slow stage of accumulation correlates significantly with the concentration of impurity ions considering the influence of the $A1^{+3}$ impurity on the character of kinetic curves, namely: the rate of accumulation of defects increases with an increase in the content of $A1^{+3}$ ions in the sample (Figs. 4.5 and 4.6).

Since the efficiency of elastic collisions does not depending on the chemical purity of the crystal, the observed changes in the accumulation rate should be associated with changes in the efficiency of stabilization of interstitial oxygen.

Therefore, it seems legitimate to conclude that the $A1^{+3}$ ions in MgO crystals are effective centers for capturing interstitial oxygen.

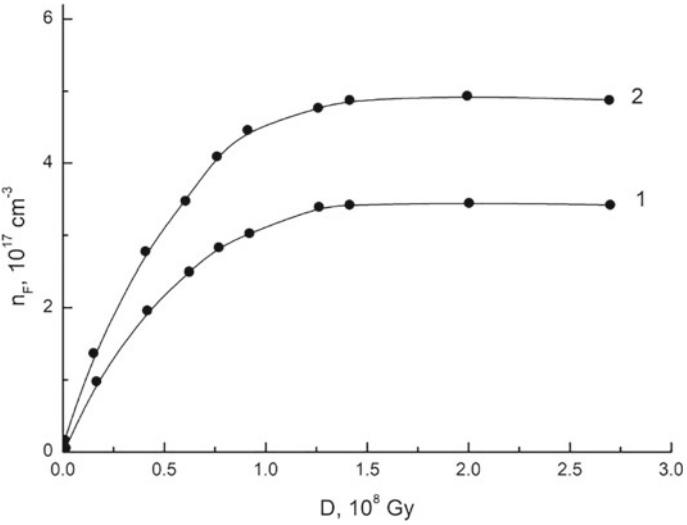

Fig. 4.7 Components of kinetic dependences of accumulation of F^+-centers in crystals MgO (II): 0.1Al (1) and MgO (II): 0.3A1 (2), corresponding to the fixation of interstitial oxygen on $A1^{+3}$ ions

The kinetics of this process, apparently, reflect the dependencies presented in Fig. 4.7.

It should be noted that the curves of Fig. 4.7 are approximated by the equations:

$$\text{For MgO (II) : } 0.1\ \text{Al} \quad n_F = 3.4 \times 10^{17}\{1 - \exp(-0.093t)\}; \tag{4.3}$$

$$\text{For MgO (II) : } 0.3\ \text{Al} \quad n_F = 4.6 \times 10^{17}\{1 - \exp(-0.081t)\}; \tag{4.4}$$

where n_F is in [cm^{-3}]; t is in [h].

The discussion of Eqs. (4.3)–(4.4) will be held in Sect. 4.3.

The accumulation of F^+-centers in pure MgO (II) crystals in a wide dose range obeys an almost linear law unlike doped crystals (Fig. 4.5).

This fact indicates that the mechanism of stabilization of interstitial defects dominates in pure samples, which is not associated with the localization of displaced ions on impurity capture centers.

Otherwise, due to the fact that the chemical purity of MgO (II) crystals is more than three orders of magnitude higher than the purity of doped samples, the accumulation curve of F^+ centers would come to saturation at a much lower level and at much lower doses relative to doped crystals.

Since, as already noted, the efficiency of the generation of primary Frenkel pairs does not depend on the purity of the crystal; the observed linearity of the accumulation of F^+-centers can be explained by the following processes of stabilization of interstitial oxygen (let's call these processes a linear stabilization mechanism):

1. Capture of displaced ions on dislocations, as well as on the external and internal surfaces of the crystal. This process probably has the ability to absorb particles indefinitely.
2. Localization of ions during capture for defects also created by radiation. As shown by Elango, in this case, the accumulation of defects occurs according to a linear law in a wide range of doses [173].

The implementation of the linear stabilization mechanism also fits into the framework of our decomposition of the dose dependences of the accumulation of F^+-center in doped samples into saturating and linear stages of accumulation. Moreover, the linear stage is identical to the kinetics of accumulation of F^+-centers in pure samples.

4.2.2 Kinetics of Band Intensity Change with $h_{vm} = 5.6$ eV

Section 4.1 shows that in the absorption spectra of irradiated crystals, along with the F^+-band, a non-elementary absorption band with $h_{vm} = 5.6$ eV appears.

It is known that in this region of the spectrum, both impurity centers, for example, Fe^{+3} ions [75–77, 101]; defects similar to defects of deformation origin [95, 100] can absorb.

However, the absence of an increment in the absorption band of Fe^{+3} ions with $h_{vm} = 4.3$ eV in proton-irradiated crystals; on the other hand, the intensive growth of the band with $h_{vm} = 5.6$ eV in a wide dose range (Sect. 4.2) suggest that defects similar to defects that occur during crystal deformation are mainly responsible for it MgO. This point of view is also consistent with the results of luminescent studies (Sect. 3.2).

Since the defects responsible for the band with $h_{vm} = 5.6$ eV are created by radiation exposure, it seems useful to analyze the kinetics of changes in the intensity of the band in order to further study the nature of the defects responsible for its appearance.

Figure 4.8 shows the dose dependences of the band intensity with $h_{vm} = 5.6$ eV in MgO (II) crystals (curve 1) and MgO (II): Al crystals (curve 2).

The obtained regularities are characterized by a high degree of linearity of defect accumulation in pure MgO (II) crystals and a slight deviation from linearity in doped samples.

It is noteworthy that a slight change in the mass content of aluminum in the samples from 0.3 to 0.1% does not affect the rate of accumulation of defects responsible for the band with $h_{vm} = 5.6$ eV (the curves for doped samples coincide) and at the same time an increased concentration of Al^{+3} ions in doped crystals leads to a significant increase in the efficiency of accumulation of these defects.

If we plot the dependence of the concentration of accumulated F-centers on the intensity of the band with $h_{vm} = 5.6$ eV in pure crystals, then the obtained straight line indicates the presence of a linear correlation between the creation of F^+-centers and defects absorbing at 5.6 eV (Fig. 4.9).

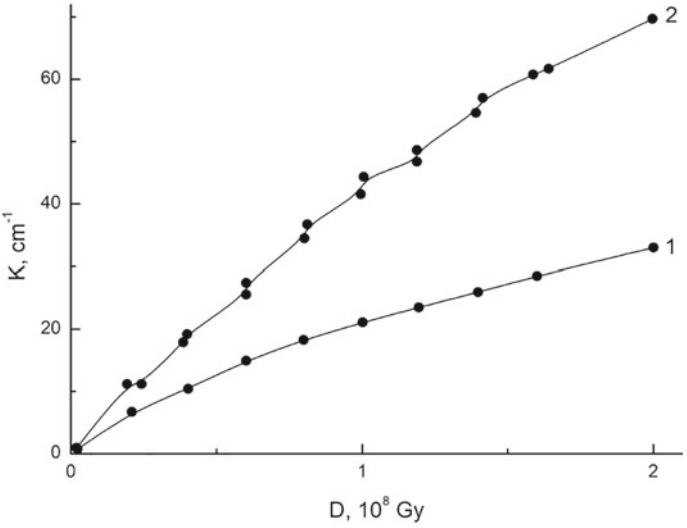

Fig. 4.8 Kinetics of changes in the intensity of the optical absorption band with $h_{vm} = 5.6$ eV for crystals MgO (II) (1) and Mg (II): Al (2) when irradiated with protons with an energy of 9.3 meV at 300 K

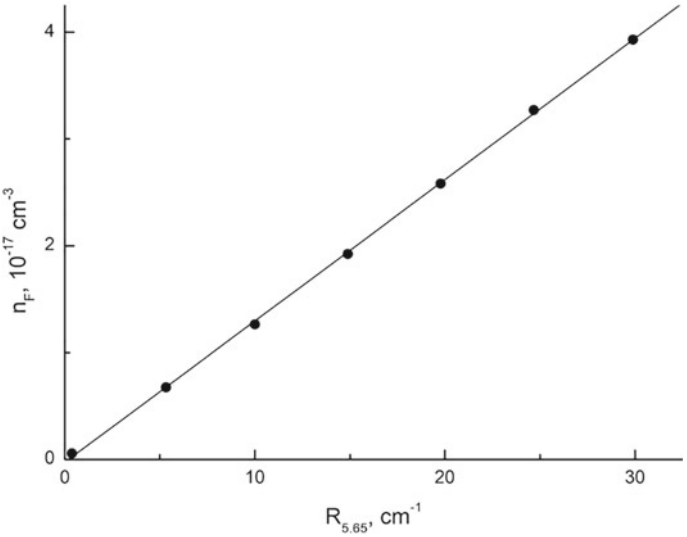

Fig. 4.9 The ratio of the intensity band with $h_{vm} = 5.6$ eV and the concentration of F^+-centers when irradiating MgO (II) crystals with protons with an energy of 9.3 meV at 300 K

This kind of dependence in doped crystals is a power function of the form $n_F \sim k^{2}/3$.

It should be taken into account that the main contribution to its intensity is made by the band with $h_{vm} = 5.73$ eV when interpreting the nature of the defects responsible for the absorption band with $h_{vm} = 5.6$ eV.

It was suggested that bivacansions of oppositely charged ions are responsible for absorption at 5.7 eV when studying the absorption dichroism of deformed crystals [135]. It is even assumed that larger aggregates of vacancies may also be responsible for this band [100, 131].

If we assume that bivacansions are responsible for the band with $h_{vm} = 5.6$ eV in irradiated crystals, the linear dependence of the band intensity on the radiation dose becomes clear.

Indeed, it is possible to distinguish collisions of anions with cationic nodes of the crystal lattice from the whole variety of elastic collisions initiated by a proton. Some part of this kind of collision occurs in the immediate vicinity of the node from which the anion has shifted.

In other words, the part of the anions that received sufficient momentum (from a proton or secondary particle) even at the stage of their displacement, they transfer a fraction of their energy to the neighboring cation, transferring it also to the interstitial position.

A neutral bivacansion and closely spaced interstitial anion and cation are formed as a result of such a correlated collision. The Coulomb interaction between the displaced ions leads to the appearance of a neutral anti-Shottk pair, the fixation of which is largely facilitated by the pre-radiation defect of the crystal (Fig. 4.8, compare curves 1 and 2).

Since the ratio of the energies expended by a proton to form bivacances and F^+-centers is constant on average for one track, then as proton tracks accumulate in the crystal volume, concentrations of bivacances and F^+-centers arise in the same way.

An alternative assumption that bivacansias are born due to strong deformation fields contradicts the effect of chemical purity observed in the experiment on the efficiency of bivacansias accumulation.

Therefore, the above results allow us to conclude that proton bombardment of crystals is accompanied by direct radiation generation of bivacansion, as well as, probably, anti-Shottk pairs.

4.2.3 Annealing of F^+-bands in Irradiated MgO (II) Crystals

The above results of the study of the kinetics of accumulation of centers indicate the existence of several mechanisms for fixing interstitial ions in proton-irradiated MgO crystals. The result of fixing displaced ions should be interstitial defects.

The question arises in this regard: is there connection between the mechanism of fixing the displaced ion and the structure of the interstitial defect formed in this case?

The answer to this question can be obtained by studying the thermal stability of anionic interstitial defects to a certain extent.

Considering that the thermal stability of F-type centers is limited by the stability of interstitial defects in irradiated MgO crystals, the solution to this question is reduced to the study of annealing of F^+-centers in irradiated crystals.

Isochronous annealing of the F^+-band of absorption was performed in pure and doped MgO (II) crystals irradiated with protons at a dose of 1.7×10^7 Gy. Annealing was performed in air for 10 min at each temperature. The samples were placed in resistance furnace on a substrate made of a single crystal MgO plate preheated to a predetermined temperature. The temperature was measured with a chromel–alumel thermocouple.

The measurement results are shown in Figs. 4.10 and 4.11 in the form of curves normalized for the intensity of the F^+-band of the irradiated crystal (after two days of storage in the dark at room temperature).

The Fig. 4.10 shows that the annealing of F^+-centers in unalloyed crystals shows the presence of two stages of annealing. The first stage is observed at temperatures (575–625) K; the second is at temperatures (725–875) K.

The first stage of annealing in doped crystals is significantly suppressed. The second stage, characteristic of pure crystals, does not manifest itself clearly either. If the annealing of F^+-centers in pure samples is completed at temperatures of 895 K, then in aluminum-doped crystals the F^+-centers are completely annealed only at temperatures of 1075 K.

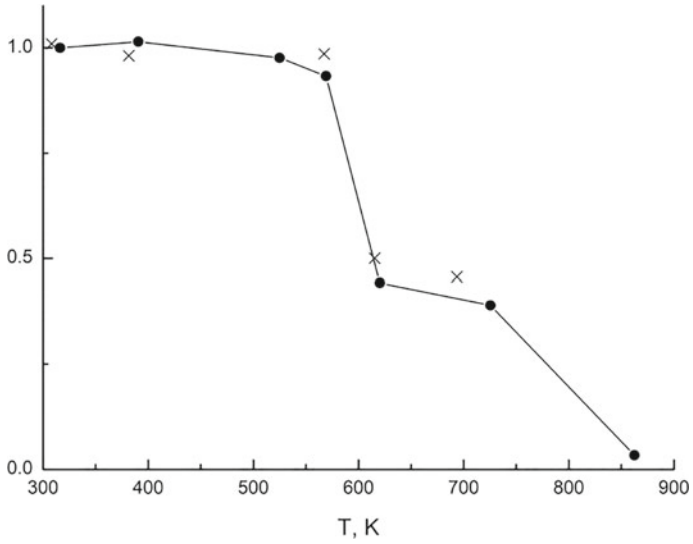

Fig. 4.10 The curve of isochronous annealing of the F^+-band in MgO (II) crystals, normalized to the initial intensity of the F^+-band after irradiation with protons with an energy of 9.3 meV at 300 K with a dose of 8.6×10^6 Gy (x) and 1.72×10^7 Gy (•)

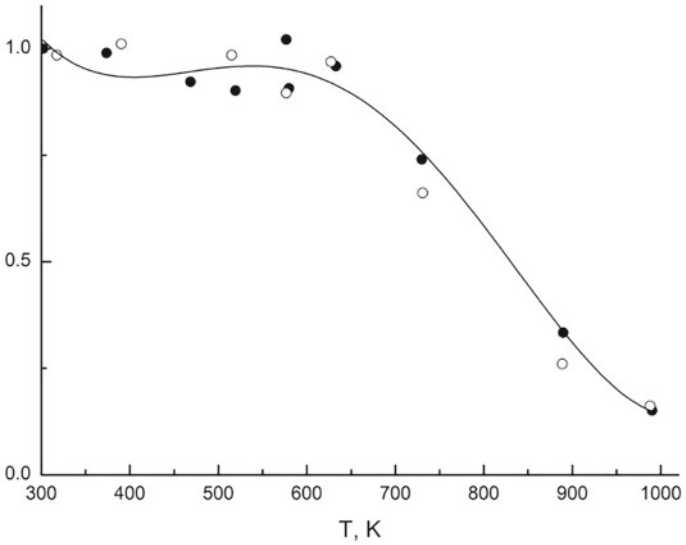

Fig. 4.11 Curve of isochronous annealing of F^+-bands in MgO (II) crystals 0.1 Al (°) and MgO (II):0.3 Al (•), normalized to the initial intensity of the F^+-band after irradiation with protons with an energy of 9.3 meV at 300 K

It was established by the EPR method that molecular oxygen ions O_2^-- arise in neutron-irradiated MgO crystals, occupying one anionic node in close proximity to the cation vacancy in [71].

These defects, called H-centers, are destroyed at temperatures (590–625) K.

The coincidence of the first stage of annealing of F^+-centers in pure crystals with the destruction temperature of the H-centers makes it possible to identify the low-temperature annealing stage with the destruction of the H-centers.

The high-temperature stage is probably associated with the formation of a different, more stable type of interstitial defect. Apparently, this type of defect is the main product of the stabilization mechanism that dominates in pure crystals.

As already noted, the annealing of F^+-centers in doped crystals has a predominantly one-stage character (Fig. 4.11). This stage cannot be identified with any of the stages observed in pure crystals.

It seems reasonable to associate significantly higher stability of F^+-centers in doped crystals with the formation of interstitial defects, which include $A1^{+3}$ ions and interstitial oxygen ions.

We note the following summarizing the results of this section:

1. At least three types of interstitial defects with different thermal stability can occur in proton-irradiated MgO crystals.
2. Defects formed when internode oxygen is captured by A1+3 ions have the highest stability.

3. H-centers have the lowest stability, the generation of which is especially noticeable in pure crystals.
4. Defects with intermediate stability (725–875) K, apparently, are the product of the implementation of the mechanism of stabilization of interstitial ions independent of the chemical purity of crystals.

4.3 Calculation of the Kinetics of Accumulation of Anionic Frenkel Defects in MgO Crystals Under Elastic Proton Scattering

The theoretical description of the kinetic regularities of the accumulation of radiation defects is a useful methodological technique that allows us to give a well-defined physical content to the numerical parameters included in the experimental dependences, which significantly deepens our understanding of the physics of the phenomenon under study.

The main purpose of this section is to select the most adequate theoretical model describing the accumulation of radiation defects in ion crystals under the conditions of the shock mechanism of the birth of primary defects with a qualitative assessment of some characteristics of the mechanism of defect formation during elastic scattering of protons into MgO crystals, further clarifying the mechanisms of fixation of intermediate ions.

The main working expression for calculating the concentration of atoms displaced by elastic collisions is the Eq. (2.1), which is valid for thin targets, within which the particle energy can be considered constant.

Equation (2.1) should be formed to account for the continuous change in the energy of the particle and the transfer of its overwhelming fraction into the electronic subsystem of the crystal in thick inhibitory media.

Let us define by analogy (2.18) the energy expended by a proton on elastic collisions in an anionic sublattice by the integral

$$E_C = \int_{E_0}^{0} \frac{(dE/dx)_C dE}{(dE/dx)_i + (dE/dx)_C}. \tag{4.5}$$

The linear proton energy losses in MgO included in (4.5) are calculated by Eqs. (3.4) and (3.7) at $E > 0.5$ meV. The integrand function in (4.5) was assumed constant and equal to its value in the energy range (0.5–10) MeV at $E = 0.5$ meV, which led to a slight overestimation of the E_C.

It is necessary to emphasize the weak dependence of the EU on the specific value of the limit of applicability (4.4) and (4.5). Thus, the replacement of the limiting energy from 0.5 to 0.2 meV increases the E_C by no more than 9%.

The E_C energy expended by the proton on elastic collisions with the anionic sublattice is released in the crystal volume limited by the particle path value R.

Therefore, the average concentration of displaced anions should be calculated by the Equation

$$N_C = \frac{E_C F t}{2E_d R}, \tag{4.6}$$

where E_d is the threshold energy of displaced anions; F is the particle flux density; t is the irradiation time.

Expression (4.6) can also be obtained directly from the Eq. (2.1) if it is represented as

$$N_C = \frac{1}{2E_d}\left(\frac{dE}{dx}\right)_C Ft, \tag{4.7}$$

and perform the operation of averaging linear energy losses by replacing $\left(\frac{dE}{dx}\right)$ with the relation $\frac{E_C}{R}$.

We find the numerical values of the expressions: $E_c = 1250$ eV; $N_C = 1.74 \cdot 10^{17}$t, where t is given in hours, substituting in (4.5) and (4.6) the parameters corresponding to the experimental conditions. The calculation errors of E_c and N_C can be estimated at 10% and 20%, respectively.

It is necessary to take into account the main factors characterizing the course of radiation processes in MgO crystals at room temperature of irradiation for the correct choice of the calculation model. Let's list them.

1. Vacancies of anions and cations are stationary at temperatures below 1170 K and 700 K, respectively [19–21, 43]. Interstitial ions have high mobility [86].
2. The process of the birth of single-charged Frenkel pairs dominates [129]. A similar situation is observed with neutron irradiation of MgO crystals [136].
3. Interstitial defects are thermally stable at temperatures below 570 K.
4. There is no radiation creation of V-centers (see Sect. 4.2).
5. The accumulation of F^+-centers is provided by two main mechanisms: 1 is effective nonlinear, depending on the content of polyvalent impurity ions; 2 is independent of the chemical purity of the crystal, responsible for the slow linear growth of the F^+-band in a wide range of absorbed doses.

The main provisions of the statistical model developed by Thompson in the study of the accumulation of point defects in metals satisfy the listed requirements to the maximum extent [97].

In general, these provisions are as follows:

1. Vacancies in the crystal are stationary. Interstitial atoms are highly mobile.
2. The crystal contains capture centers of interstitial atoms of a saturating type with an initial concentration of N_{St}, capable of capturing no more than one interstitial atom. Saturation-type traps with a concentration N_{Ut} can capture a non-finite number of interstitial atoms.

3. The atom displaced to the internode either recombines with the vacancy or is trapped. The number of accumulated vacancies is equal to the number of atoms localized on the traps.
4. The vacancy and the trap are surrounded by the same attracting fields.
5. The release of interstitial atoms from traps does not occur.

It is easy to make sure that the impurity ions Al^{+3} are an excellent example of a saturating type of traps, identifying metal vacancies with F^+-centers of MgO and interstitial metal atoms with interstitial oxygen ions O_i^-.

In this case, the Coulomb components of the attracting fields of F^+-centers and Al^{+3} ions will be the same. The thermal stability of the interstitial defects formed in this case is also high (Fig. 4.11).

Dislocations and external and internal surfaces of the crystal can be an example of unsaturated type of traps in MgO.

If we assume that the capture occurs at the dislocation step and considering that the charge of the steps is equal to half the charge of the ions, it should be recognized that in this case, the attracting field of the step will coincide with the field of the F^+-centers.

Another variant of non-saturating capture centers may be defects created by radiation.

According to Thomson's calculations, the accumulation of defects in the presence of only saturating traps is described by the Equation

$$N_V = N_{St}\{1 - \exp(-N_d t/N_{St})\}. \tag{4.8}$$

In the presence of only non-saturating traps

$$N_V = N_{Ut}\left\{\sqrt{1 + 2N_d t/N_{Ut}} - 1\right\}. \tag{4.9}$$

In general

$$N_V = N_1 + N_2; \tag{4.10}$$

$$N_1 = (N_{Ut} + N_{St})\left\{\sqrt{1 + 2N_d N_{Ut} t/(N_{Ut} + N_{St})} - 1\right\}; \tag{4.11}$$

$$N_2 = N_{St}\{1 - \exp(-N_1/N_{Ut})\}. \tag{4.12}$$

N_d is the rate of generation of primary Frenkel defects during elastic scattering of particles, N_{St} and N_{Ut} are the initial concentrations of saturating and non-saturating intercellular ion capture centers, N_V is the concentration of accumulated vacancies identified by us with the concentration of F^+-centers in MgO, t is the irradiation time in Eqs. (4.8)–(4.12).

Equation (4.8) describes a curve saturating at $N_V = N_{St}$. That is, the saturation process depends on the concentration of traps.

It follows from Eq. (4.9) that unsaturated traps cannot lead to saturation, but only give a negative curvature to the graph of the dependence of the concentration of defects on the dose.

In general, the accumulation curve can be decomposed into two components, with one coming to saturation as the saturated traps are filled; the other growing as the square root of the dose according to Eqs. (4.10)–(4.12). Of course, the final saturation is manifested due to the zones of instability of defects at very high doses.

It was previously concluded that there are two mechanisms of accumulation of F^+-centers in MgO crystals when discussing experimental data.

One of them is clearly related to the capture of interstitial oxygen by Al^{+3} ions; the kinetic of this process is expressed by Eqs. (4.3) and (4.4), the analytical form of which coincides with the calculation Eq. (4.8).

The coincidence of Eqs. (4.3) and (4.4) with Eq. (4.8), on the one hand, the role of Al^{+3} impurity ions is confirmed as saturating capture centers. On the other hand, it indicates the correctness of the chosen theoretical description of the defect accumulation process.

Comparison of Eqs. (4.3), (4.4) and (4.8) also makes it possible to estimate the real rate of generation of primary Frenkel anion pairs in the proton track in a form favorable for localization of interstitial oxygen at saturated capture centers.

This speed N_d can be found as the product of the pre-exponential factor N_{St} and the exponent N_d/N_{St}. according to the Eq. (4.8). We find the average value of the N_d generation rate by calculating the product of the corresponding parameters from Eqs. (4.3) and (4.4)

$$N_d = (3.44 \pm 0.23) \times 10^{16}\ \mathrm{cm}^{-3}\ h^{-1}. \tag{4.13}$$

The found value N_d is significantly less than the previously calculated value of the average rate of generation of Frenkel anion pairs

$$\frac{dN_C}{dt} = 1.74 \times 10^{17}\ \mathrm{cm}^{-3}\ \mathrm{h}^{-1}.$$

Experimentally determined values of the threshold energy of displacement E_d were used in calculating N_C [96].

Thus, the annealing of weakly separated Frenkel pairs has already been taken into account when the displaced ion does not leave the instability zone of its vacancy. Therefore, the detected discrepancy between N_d and $\frac{dN_C}{dt}$ should be associated with the following processes:

1. Annealing of Frenkel pairs due to the dynamic ingress of a displaced ion into the instability zone of an alien vacancy.
2. The loss of elastic collision energy to create primary defects in configurations that are inert with respect to capture by Al^{+3} ions.

The last process seems likely, since more complex defects are created along with the F^+-centers, responsible, in particular, for the absorption band with $h_{vm} = 5.6$ eV.

The second mechanism, established experimentally and responsible for the slow linear accumulation of F^+-centers in pure and doped samples with the position of the selected model, should correspond to the capture of displaced oxygen on unsaturated traps.

A high degree of linearity of accumulation in a wide range of doses can be obtained if the condition is met according to Eqs. (4.9)–(4.12)

$$N_d t_{\max}/N_{Ut} \ll 1, \tag{4.14}$$

where t_{max} is the maximum irradiation time corresponding in our experiments to 63 h. Equations (4.9)–(4.12) can be decomposed into a series when condition (4.14) is met; it is easy to establish that $N_V = N_d t$ being limited to the linear term of the decomposition.

It follows from the experimental curve shown in Fig. 4.5 that the linear accumulation stage is described by the expression $N_F = 0.7 \times 10^{16}$. Hence, $N_F = 0.7 \times 10^{16}$ cm^{-3} h^{-1}.

It is easy to estimate the concentration N_{Ut} of unsaturated intercostal oxygen capture centers from condition (4.14) knowing N_d and t_{max}. We get that $N_{Ut} \gg N_d t_{max} = (0.7 \times 10^{16}) \cdot 63 = 4.4 \times 10^{17}$ cm^{-3}.

Thus, in order to ensure the linearity of accumulation in the studied dose range, it is necessary that $N_{Ut} \geq 10^{19}$ cm^{-3}.

Let's now estimate the maximum value of N_{Ut} under the assumption that the dislocations are unsaturated capture centers.

We obtain that there will be 2.5×10^7 anchoring points per 1 cm of the dislocation length assuming that the anchoring points of interstitial ions on the dislocation line are separated by the lattice parameter (4.2 Å).

The concentration of anchoring points turns out to be 2.5×10^{14} cm^{-3} with a real dislocation density of 10^7 cm^{-2}, what is about five orders of magnitude less than it is necessary to preserve the linearity of accumulation.

This fact is clearly illustrated in Fig. 4.12, where the experimental kinetic dependence of the accumulation of F^+-centers in pure samples (curve 1) and the dependence calculated by Eq. (4.9) using the parameters: $N_d = 0.7 \times 10^{16}$ cm^{-3} h^{-1}, $N_{Ut} = 2.5 \times 10^{14}$ cm^{-3} h^{-1} (curve 2) are constructed.

These estimates unambiguously allow excluding dislocations as the dominant channel of cross-border capture of displaced ions.

The condition *Nut* $N_{Ut} \geq 10^{19}$ cm^{-3} is naturally fulfilled if we assume that the potential sites of attachment of intermediate ions are the nodes of the crystal lattice, the concentration of which is 5.4×10^{22} cm^{-3}.

This assumption seems quite real if we take into account that out of a large set of oxygen ions displaced into the internode, some of them, having a certain energy and momentum, can create a stable configuration of the binary defect of the internode localized on the vacancy of the cation when colliding with the cation node.

It is possible to estimate the proportion of such collisions by a value equal to $0.7 \times 10^{16}/3.44 \times 10^{16} = 0.2$ comparing the values of N_d obtained from the Eq. (4.8) (3.44×10^{16} $cm^{-3} \cdot h^{-1}$) and from the Eq. (4.9) (0.7×10^{16} cm^{-3} h^{-1}).

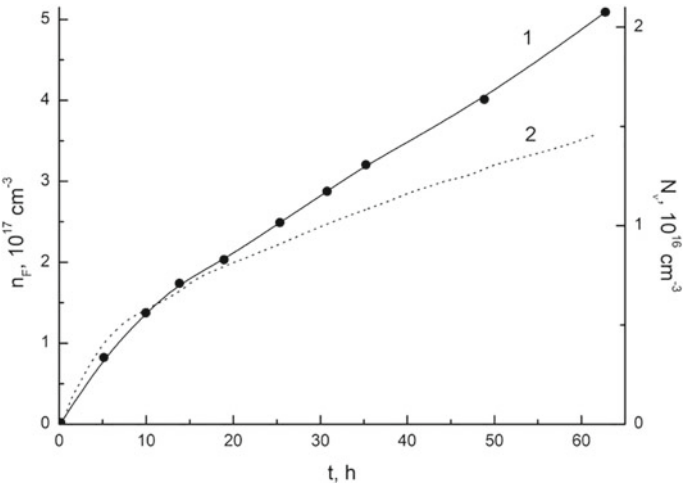

Fig. 4.12 Kinetics of the accumulation of F^+-centers in MgO(II) crystals (1) and the calculated dependence for the accumulation of anionic vacancies according to the model of unsaturated traps [81] (2)

It should be noted that the generation of bivacansion radiation observed in our experiments (the absorption band $h_{vm} = 5.6$ eV) confirms the existence of such a class of collisions.

In addition, the proposed stabilization mechanism explains the absence of radiation formation of cationic vacancies in the composition of the holes of V- and V-centers of staining.

Summarizing the results of this section of the work, we can conclude that:

1. Thompson's statistical model in basic terms correctly reflects the physics of radiation accumulation of point defects under high-energy irradiation of MgO crystals at room temperature.
2. The essential role of Al^{+3} impurity ions as capture centers of interstitial oxygen of the saturating type is confirmed within the framework of this model.
3. Collisions of oppositely charged ions (such as $O_i^- \rightarrow Mg^{+2}$) leading to the formation of binary interstitial defects are observed in the spectrum of collisions of secondary particles. Such collisions between neighboring nodes of the crystal lattice lead to radiation generation of bivacansions.
4. The collisions of interstitial oxygen with the cationic nodes of the crystal lattice with the formation of binary interstitial defects are the most probable process explaining the slow linear stage of accumulation of F^+-centers in pure and doped MgO crystals.

About 20% of the particles From the total number of oxygen which have received energy above the threshold shock displacement from the crystal lattice node really shifts. In turn, about 20% of this number of particles has the energy and momentum necessary for the formation of binary interstitial defects.

4.4 Models of Interstitial Defects in Magnesium Oxide Crystals Irradiated with Protons at Room Temperature

The extremely limited nature of the literature data on the structure and mechanisms of formation of interstitial defects in magnesium oxide crystals was emphasized previously. In general, this limitation is due to the difficulty of direct experimental investigation of interstitial defects and the resulting need for sophisticated analysis of indirect data.

The question of the structure of interstitial defects arising from proton irradiation of MgO is briefly discussed in this section on the base on the above experimental and calculated results on the stabilization of interstitial ions with the involvement of literature data.

We will consistently discuss the most probable models of centers that include and do not include radiation defects of the crystal.

4.4.1 Formation of Interstitial Defects Involving Pre-Radiation Imperfections of the Crystal

The direct correlation between the absorption efficiency of F^+-centers and the concentration of Al^{+3} impurity ions, experimentally and confirmed by calculation, established by us allows to uniquely identify Al^{+3} ions with effective capture centers of interstitial oxygen ions.

Some ambiguity of this conclusion is due to the fact that cationic vacancies are introduced into the crystal simultaneously with the introduction of ions, compensating for the excess charge of the impurity.

Therefore, in general case the stabilization of interstitial oxygen can occur not only when the displaced oxygen at directly captured by the $A1^{+3}$ ion and when at localization of it to the cation vacancy accompanying the Al^{+3} ion.

The fundamental possibility of the latter process in MgO crystals is indicated in work by Henderson and Bowen [136].

It is obvious that the preference of one or another method of fixing interstitial oxygen will be determined by its charge.

Indeed, it is difficult to imagine the capture of a negatively charged ion onto a negatively charged cationic vacancy, whereas its interaction with an excess positive impurity charge relative to the lattice will lead to a decrease in the crystal energy. And, conversely, the localization of oxygen to the vacancy will be preferable as a result of the interaction of the elastic fields of the neutral oxygen atom and the cationic vacancy having opposite signs.

Let's consider from the point of view of displacement physics what charge the oxygen ions leaving the nodes have. The separation of an electron from a displaced ion is most effective when the orbital velocity of the electron is comparable to the velocity of the ion nucleus [126], that is, when the kinetic energy of the nucleus E_{nuc}

and the ionization potential of the ion *Eioi* are related by the ratio $E_{nuc} = (M/t)\ Eioi$, where M and m are the masses of the nucleus and the electron.

The ionization potential of the free negative oxygen ion is 1.47 eV [137]. Focusing on this value, we get that only at the energies of the nuclei exceeding 40 keV, oxygen will shift in the neutral state.

We find that the probability of anion acquiring energy exceeding 40 keV is 0.13% by calculations.

Therefore, only 0.13% of the displaced ions will be in the neutral state. Our data on photoluminescence of irradiated crystals are consistent with this conclusion, indicating the predominant formation of F^+-centers, and, consequently, that interstitial oxygen has a negative charge [129].

It can be concluded taking into account the negative charge of interstitial oxygen, that the dominant type of impurity interstitial defect in the samples of MgO (II): Al is an associate of the oxygen ion located in the internode and the $A1^{+3}$ ion, i.e. the O_i^-- Al^{+3}complex.

4.4.2 Interstitial Defects in Defect-Free Areas of MgO Crystals

The experimental studies performed indicate the existence of a mechanism for stabilizing displaced oxygen in irradiated magnesium oxide crystals that does not depend on the chemical purity of the crystal.

The analysis of the learned results (Sect. 4.3) proves that this mechanism cannot be associated with the dislocation structure of the crystal (which also practically does not depend on the chemical purity of the sample).

It is concluded that the formation of stable interstitial configurations during the interaction of displaced oxygen with the cationic nodes of the crystal lattice is most likely.

It is necessary to take into account some well-known results of exposure to high doses of electron and neutron irradiation on MgO crystals to correctly describe the structure of such a configuration [10, 110, 136]:

1. Direct observations using electron microscopes have established the formation of clusters of interstitial ions containing approximately the same amounts of anions and cations. Clusters are transformed into dislocation loops of the interstitial type with a further increase in the radiation dose [10, 49].
2. No radiation creation of V^- and V-centers was observed regardless of the type of high-energy particles [56, 99, 111]. At the same time, clusters and dislocation loops of the vacancy type are formed at elevated doses [10].

It is obvious that the structural unit of the interstitial cluster is a pair of closely spaced interstitial anions and cations, which can be called an anti-Schottky pair. That is, the formation of interstitial clusters is preceded by the formation of stable anti-Schottky pairs in the early stages of high-energy irradiation.

The reality of anti-Schottky pairs as primary products of radiation defect formation is confirmed by the radiation generation of bivacansions, which we observed by the appearance and growth of the absorption band with $h_{vm} = 5.6$ eV.

Bivacansias are as if the "imprint" of the anti-Shottky pair born, since the statistical, uncorrelated creation of closely spaced vacancies is an unlikely process.

It should be noted that the correlated distribution of vacancies of anions and cations in neutron-irradiated MgO crystals was also observed in the work of Henderson and Bowen [49], who found that the formation of color centers (bivacansion with a localized electron) after high-temperature annealing of irradiated crystals occurs with an activation energy half the activation energy of migration of cationic vacancies. The activation energy of the formation of F_C^+-centers is compared with the activation energy of the migration of free cationic vacancies only at the late stages of annealing.

The absence of the creation of V^- and V°- centers and at the same time cationic vacancies to concentrations sufficient for the formation of vacancy clusters at later stages of irradiation indicates that the cationic vacancies created by radiation are in a state that prevents the formation of V^- and V°-centers.

In other words, there must be a defect with an effective positive charge near the cationic vacancy. An anionic vacancy or a positively charged aggregate interstitial defect can be such charge-compensating defect. In particular, a defect that is born in correlated collisions and it is called a binary interstitial defect in the previous section.

Let's clarify our understanding of correlated collisions in binary ionic crystals.

As is known, collisions are realized in the cascades of collisions that develop during the passage of a fast particle, along with collisions that lead to the ejection of atoms or ions from the nodes of the crystal lattice, when the incoming particle, knocking out the atom from the node, itself takes its place. These are so-called collisions with substitution [99]. This type of collisions is typical for particles having energy close to the threshold energy of displacement E_d.

If the dislodged oxygen ion has energy close to the threshold energy of displacement of the magnesium ion, then it can dislodge the cation and occupy its node when it collides with the cation node. The dislodged cation, having minimal energy, thermalizes in the vicinity of its node.

However, the presence of a negative oxygen ion in the cation node is unstable; it is displaced into the interstitial space by thermal vibrations of the lattice. Naturally, the displacement of the oxygen ion will occur mainly in the direction of the cation when the electric field of the interstitial cation is applied. The anion and the cation form in close proximity in the internode an anti-Schottky pair, having a single positive charge and therefore captured by the cation vacancy created in the same process.

The nature of the potential barrier preventing the restoration of the cation node remains unclear; it is probably provided by sufficient binding forces in the anti-Schottky pair, which as a whole cannot annihilate with the cationic vacancy and the different symmetry of the relaxation of the crystal lattice around the cubically symmetric vacancy and the axially symmetric anti-Schottky pair.

The need for a barrier disappears if we imagine another version of this process, when not the anion itself is displaced from the cation node, but only its excess electron, which is captured by the interstitial magnesium ion. This is all the more

likely because the wave functions of the anion and cation overlap at the collision stage. A cationic node with a neutral oxygen atom in it has an effective negative charge and therefore attracts a once-charged internode cation.

In fact, even in this case we have an anti-Schottky pair localized on a cationic vacancy with a slightly different distribution of the electron density in it (shifted to magnesium) and a different geometry of the defect (the anionic fragment of the pair is located in the cation node).

Thus, the proposed model of a binary interstitial defect as an anti-Schottky pair localized on a cationic vacancy and the scheme of its formation, consistent with our experimental results, explain the above data on the occurrence of interstitial clusters and the apparent absence of generation of cationic vacancies in a natural way.

We deliberately did not take into account the possibility of a mirror-symmetric process, when a collision with a substitution initiates an initially displaced cation, since it is difficult to imagine that a cation with low energy could leave the instability zone of its vacancy. The interaction of the F^{+}–O_i^{-} pair is weaker by 4 times than the interaction of the pair in the Coulomb approximation.

4.5 Summary

1. It is proved that the stabilization of anionic Frenkel defects is carried out by structure-sensitive and fundamental mechanisms of fixation of interstitial ions under the high-temperature action of high-energy proton fluxes on magnesium oxide crystals,
2. It has been established that the impurities of trivalent metals are effective capture centers of interstitial oxygen. On this basis, a method is proposed to increase the radiation resistance of magnesium oxide products, which consists in preliminary purification of raw materials from impurities of trivalent metals.
3. The model of the fundamental mechanism of stabilization of Frenkel defects in the form of the process of formation of anti-Schottky defects localized on radiation-created cationic vacancies is substantiated.
4. An unlimited increase in the intensity of the absorption band at 5.6 eV indicates radiation generation in the proton tracks of color centers identical to defects of deformation origin. The most probable model of such defects is anion-cationic bivacansions.
5. The applicability of Thompson's phenomenological theory to describe the nonlinear component of the accumulation of radiation defects in magnesium oxide crystals irradiated by protons is substantiated.
6. The generation rates of separated Frenkel anion pairs in magnesium oxide crystals under elastic proton scattering are established. The rate of displacement of anions captured on impurity centers is 3.444×10^{16} cm^{-3} h^{-1}. The displacement rate of autolocalizing anions is 0.7×10^{16} cm^{-3} h^{-1}.

Chapter 5
Creation of F^+-Centers in Proton Tracks at Low Irradiation Temperatures

Contents

The experimental results presented in Chap. 3 did not reveal the dominant contribution of non-elementary mechanisms of radiation defect formation during irradiation of magnesium oxide crystals with protons.

This conclusion relates to the area of room temperature irradiation and cannot be mechanically extended to other temperature ranges.

In order to study the relative (relative to the shock mechanism) efficiency of the non-shock creation of anionic Frenkel defects in proton tracks in magnesium oxide crystals in an extended range of irradiation temperatures, this chapter discusses the results of a study of the temperature dependence of the efficiency of accumulation of F^+-centers, isochronous annealing of defects and thermostimulated conductivity in the temperature range (80 ÷ 300) K.

The combination of these methods allows to establish the functional form of the dependence of the anion displacement rate on temperatures.

In turn, it is possible to judge the predominant mechanism of the displacement of ions into interstitial positions by the nature of the functional dependence.

A methodological technique is used based on the analysis of kinetic patterns of accumulation of F^+ and V-color centers with variations in the irradiation temperature in the range (80 ÷ 300) K to study the processes of defect formation in this chapter.

A. Surzhikov and E. Lysenko, *Creation and Accumulation of Radiation Defects in Single Crystals of Magnesium Oxide*, https://doi.org/10.1007/978-3-031-60207-8_5

The concentration of P^+-type centers was determined from optical measurements as previously in this work.

An indirect, but significantly more sensitive method of measuring thermally stimulated conduction currents was used to register V-type centers with low optical activity. This method was justified and used in Mallard's works to register hole centers in magnesium oxide [138, 139].

The applicability of the method is based on the purely electron–hole type of electrical conductivity of magnesium oxide crystals in a wide temperature range.

The essence of the method is the radiation creation of defects at a temperature when they are stable, the subsequent heating of the crystal in an electric field until the defects are destroyed and the measurement of the resulting electric current.

It is necessary to know the cross sections of electron and hole capture by traps in the crystal, energy levels and concentrations of all types of traps and recombination centers to determine the absolute concentration of collapsed defects from the curves of thermostimulated conductivity currents.

This task is not feasible for real crystals; therefore this method is used mainly to determine the relative concentrations of defects.

The main objects of the study were single crystals of MgO (I) having the chemical composition given in Table 2.1. The choice of less pure single crystals of MgO (I) is due to the fact that the stabilization of mobile fragments of Frenkel pairs is significantly facilitated in crystals with a developed defect.

Therefore, they should be expected to have a more effective, experimentally detectable contribution of the processes of non-elementary creation of stable Frenkel defects.

Low-temperature irradiation of samples and measurement of optical absorption spectra were carried out on the installation, which is an articulation of the SF-4A spectrophotometer, an optical cryostat and a cyclotron ion conduit [140].

The energy and current density of the proton beam were 6.8 meV and 1.24×10^{15} m^{-2} s^{-1}, respectively, in these experiments.

5.1 Effect of Temperature on the Efficiency of Accumulation of F^+-Centers in MgO During Proton Irradiation

The accumulation of radiation defects is a complex process in which three main stages can be distinguished. At the first stage, there is a direct or indirect transfer of momentum to the displaced target atom.

The next stage consists in the spatial separation of the components of the resulting Frenkel pair. The stabilization of the separated pair elements in the crystal lattice completes the process.

The overlap of several stages significantly complicates the description of the mechanism of generation of primary defects, based on the established patterns of accumulation.

However, the nature of the displacement mechanism can be established by analyzing the nature of changes in the curves of accumulation of point defects with a change in the irradiation temperature. This analysis is based on the following.

During shock defect formation, the displacement of ions and their separation occurs without heat exchange with the crystal lattice. Therefore, the temperature dependence of the efficiency of defect accumulation is determined in this case by the temperature dependence of the process of fixing the separated fragments of the Frenkel pair.

The crystal temperature has a significant effect on the act of displacement itself (due to the dependence on the temperature of many parameters of electronic excitations) and on the subsequent stages of the formation of stable defects in the case of the displacement of ions in a non-elementary way.

The effect of temperature on the fixation of displaced atoms can be revealed by studying the isochronous annealing of accumulated defects.

Significant consistency should be expected during the curve of the temperature dependence of the efficiency of defect accumulation and the curve of isochronous annealing at the shock method of ion displacement according to the above. The absence of such a correlation will indicate a significant contribution of non-elementary processes to the radiation defect formation of the crystal.

5.1.1 Optical Absorption of MgO (I) Crystals Irradiated at Low Temperatures

A decrease in the irradiation temperature does not significantly affect the spectral composition of the additional optical absorption of crystals in the studied spectral wavelength range.

The additional absorption spectra of isodose irradiated MgO (I) crystals measured at the irradiation temperature are shown in Fig. 5.1 for the temperature range (80 ÷ 300) K.

It is easy to see that, the intensity of optical absorption increases with a decrease in the irradiation temperature; this effect is especially noticeable in the short-wavelength region of the spectrum.

The decomposition into Gaussian components of the spectra obtained for temperatures (88 ÷ 300) K, according to the decomposition procedure described earlier, indicates the predominance of absorption bands with maxima at 4.92 eV, 4.3 eV and h_{vm} ~ (5.4 ÷ 5.6) eV in the spectra.

The position of the band with h_{vm} ~ 4.92 eV and its half-width within the measurement errors correspond to the parameters of the F^+-band in MgO at liquid nitrogen

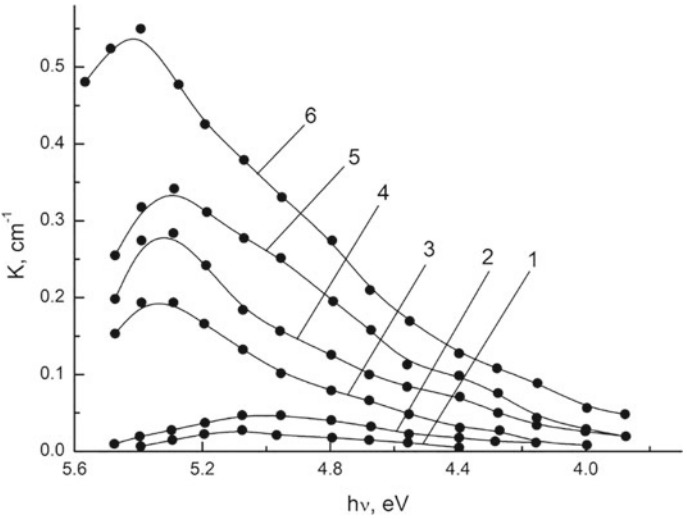

Fig. 5.1 The spectra of additional optical absorption of MgO (I) crystals irradiated by protons at a dose of 6×10^6 Gy, measured at different irradiation temperatures, where 1 is 300 K; 2 is 236 K; 3 is 191 K; 4 is 165 K; 5 is 124 K; 6 is 88 K

temperature [42]. The absorption with $h_{vm} \sim 4.3$ eV weakly depends on the crystal temperature and is identified by us with optical transitions in Fe^{+3} ions [74–77].

It is characteristic that, the absorption band of Fe^{+3} ions in MgO (I) crystals in the studied dose range is not saturated at low temperatures unlike samples irradiated at room temperature.

Apparently, this fact is due to the significantly higher efficiency of iron oxidation in MgO (I) crystals at low temperatures.

The non-elementary absorption band with h_{vm} at $(5.4 \div 5.6)$ eV from the available data cannot be identified with a specific model of any color center. This band is also present in MgO (II), MgO (II): Al crystals irradiated with protons at room temperature and in crystals irradiated with neutrons [78].

A complex dependence of the intensity of the band with an h_{vm} of ~ 5.4 eV on the temperature of irradiation and annealing of crystals is noted in the following sections of the work, but, its nature is not discussed in this work due to the lack of sufficient data.

The induced optical absorption does not change qualitatively with an increase in the absorbed dose, what indicates the constancy of the absorption spectral composition. Probably, changes in the concentration of accumulated defects do not lead to the emergence of new types of optically active centers in the studied range of absorbed doses.

The results presented in this section indicate that, in general, there are no differences in the composition of optically active defects created by radiation in relation to the irradiation of crystals at room temperature at low-temperature irradiation of MgO (I) crystals in the studied range of absorbed doses mainly.

5.1.2 *Accumulation of Radiation Defects at Low Irradiation Temperatures*

The intensities of the selective bands of additional optical absorption naturally depend on the absorbed dose and the irradiation temperature.

Figure 5.2 shows the dose dependences of the concentration of accumulated F^+-centers for irradiation temperatures in the range (88 ÷ 300) K.

It is easy to see that, the accumulation curves of F^+-centers represent a superposition of two stages: a fast initial and a slow linear one in the studied range of doses and temperatures.

The fast initial stage becomes especially evident at temperatures above 190 K, when the efficiency of the slow linear stage is significantly reduced.

This character of the accumulation curves of F^+-centers is identical to the similar dependencies described in previous chapters and can also be explained by the effective capture of electrons on the pre-radiation vacancies of anions at the initial stage of irradiation and the slower process of radiation creation of F^+-centers at the linear stage.

This interpretation is in agreement with the fact that the saturation level of the fast stage coincides in order of magnitude with the content of monovalent cation-substituting impurities in MgO (I) crystals, which serve as a measure of the number of pre-radiation vacancies of anions.

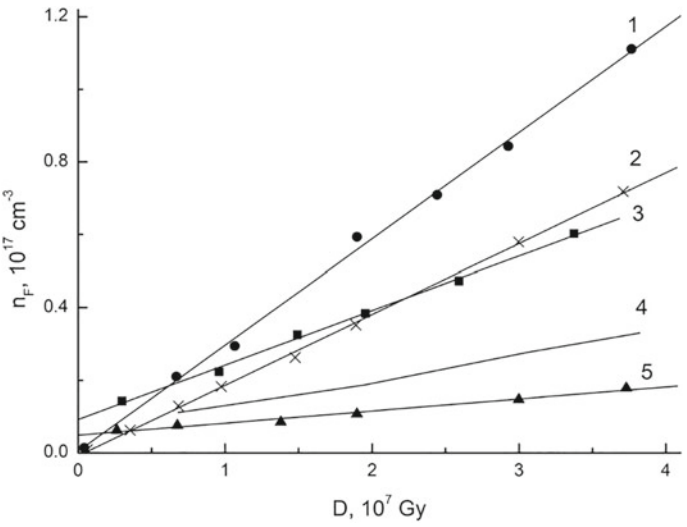

Fig. 5.2 Kinetics of accumulation of F^+- centers in MgO (I) crystals under irradiation by protons with energy of 6.8 meV at temperatures, where 1 is 88 K; 2 is 165 K; 3 is 191 K; 4 is 235 K; 5 is 300 K

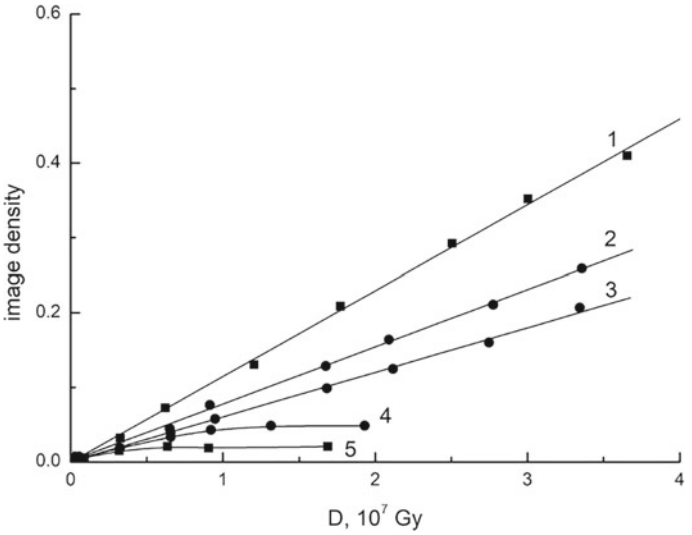

Fig. 5.3 Kinetics of changes in the intensity of optical absorption of F^{+3} accumulation ions in MgO (I) crystals irradiated by protons with energy of 6.8 meV at temperatures, where 1 is 88 K; 2 is 165 K; 3 is 191 K; 4 is 235 K; 5 is 300 K

On the other hand, the linearity of accumulation up to concentrations of ~ 1018 cm'^3 indicates an extremely large capacity of the source of anionic vacancies responsible for the accumulation of centers at a slow stage. Probably, this source is the anionic nodes of the crystal lattice.

The influence of temperature on the nature of the dependence of the absorption band of Fe^{+3} ions (h_{vm} ~ 4.3 eV) on the radiation dose is more significant (Fig. 5.3).

The intensity of the band with h_{vm} ~ 4.3 eV increases almost linearly at temperatures below 190 K (Fig. 5.3, dependencies 1 ÷ 3), whereas this process is rapidly saturated at a relatively low level at higher temperatures (Fig. 5.3, dependencies 4 ÷ 5).

It can be judged that the oxidative effect of proton irradiation on Fe^{+3} ions decreases sharply in the temperature range (190 ÷ 230) K from these data.

The complex band with $h_{vm} = (5.4 \div 5.6)$ eV did not decompose into components. Therefore, the kinetic curves of changes in the optical density shown in Fig. 5.4 at $h_{vm} = 5.4$ eV only approximate the actual changes in the intensity of the absorption bands in the short-wavelength region of the spectrum.

Nevertheless, it can be seen that the intensity of short-wave absorption depends on the irradiation temperature from the data presented in Fig. 5.4.

Indeed, an increase in the irradiation temperature from 88 to 124 K leads to a significant decrease in the rate of absorption growth at $h_{vm} = 5.4$ eV (Fig. 5.4, dependences 1 and 2). The accumulation rate at temperatures (165 ÷ 190) K increases so that the accumulation curve for temperature 165 K coincides with the curve for

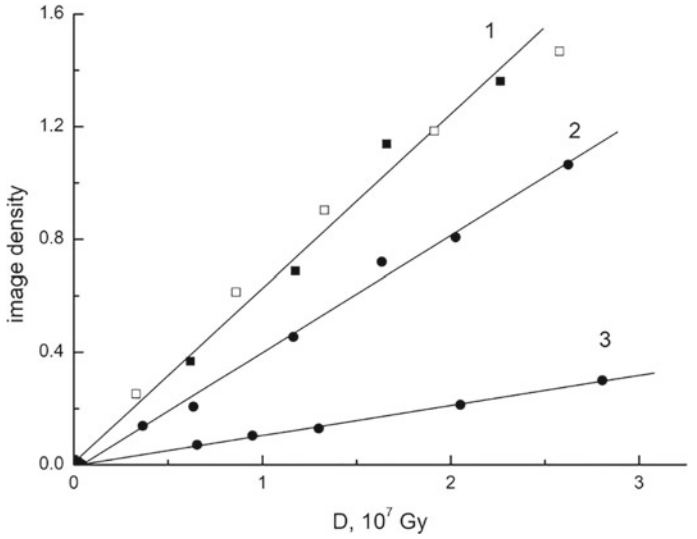

Fig. 5.4 Kinetics of changes in the intensity of optical absorption at 5.4 eV in MgO (I) crystals irradiated by protons at energy of 6.8 meV at temperatures, where 1 is 88 K (■) and 165 K (□); 2 is 124 K; 3 is 235 K

T = 88 K. The rate of absorption growth at 5.4 eV decreases again with increasing temperature at temperatures above 190 K (Fig. 5.4, Dependence 3).

Thus, the results presented in Fig. 5.4 indicate the existence of an optimal temperature for the accumulation of defects responsible for absorption in the region of h_{vm} = (5.4 ÷ 5.6) eV.

The presence of an optimal temperature indicates the thermally stimulated processes of birth and annealing of defects responsible for the short-wave absorption of MgO (I) crystals.

5.1.3 Effect of Temperature on Accumulation and Annealing of Centers in MgO (I) Crystals

It follows that at the linear stage, the rate of accumulation of F^+-centers in crystals significantly depends on the crystal temperature from the data presented in Fig. 5.2.

The specific type of this dependence obtained from the dose curves is shown in Fig. 5.5.

It can be seen that the rate of accumulation of F^+-centers η (T) in the interval (88 ÷ 300) K is a decreasing function of temperature. This dependence is approximated by an analytical expression with an accuracy of at least 10%:

$$\eta(T) = \left[1 + 194\exp(-0.085/kT)\right], \tag{5.1}$$

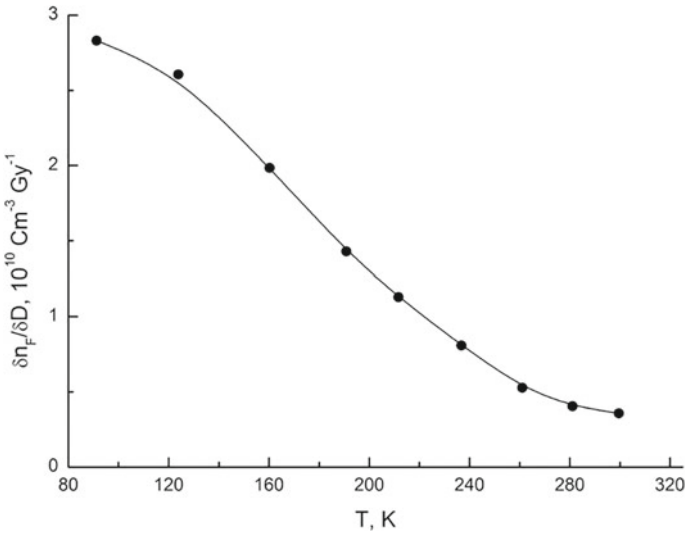

Fig. 5.5 Temperature dependence of the efficiency of accumulation of F^+-centers in MgO (I) crystals under irradiation by protons with energy of 6.8 meV

where $\eta(T)$.

Consider the nature of the decline in the rate of accumulation of F^+-centers.

It is known that the probability P_o of the formation of a defect stable under experimental conditions can be represented as a superposition of elementary probabilities [141] $P_0 = P_1 P_2 P_3$, where P_1 is the probability of creating a Frenkel pair, P_2 is the probability of separation of its fragments, P_3 is the probability of stabilization of the separated fragments of the Frenkel pair.

In general, each of the elementary probabilities depends on temperature, and thus the temperature dependence of the accumulation rate will be expressed in terms of the temperature dependence of the probability P_o

$$\eta(T) \sim P_0(T) = P_1(T) \cdot P_2(T) \cdot P_3(T). \tag{5.2}$$

The scattering cross-section, the collision energy and the cascade function practically do not depend on the crystal temperature at the shock mechanism of generating Frenkel pairs. So, it is not a function of temperature in this case.

A wide range of energies is transmitted in the process of elastic scattering of particles to ions displaced from the nodes of the crystal lattice from the maximum T_m to the threshold value of the displacement energy E_d. Ions that have received sufficient energy are separated from the vacancy dynamically; so, the probability of separation P_2 does not depend on the temperature of the crystal for a part of the ions. Low-energy ions that lose their pulse within the interaction sphere can be separated from vacancies either by channeling and focusing or by thermally activated migration.

The probability of separation of P_2 will be a decreasing function of temperature in the case of channeling and focusing. The probability of P_2 increases with increasing temperature with thermally activated separation [114, 142].

Modern studies of the mechanisms of separation of F-H-pairs in silk-halide crystals have shown that the most likely mechanism of separation is thermally activated hopping diffusion of H-centers, whereas the mechanism of focused collisions is irrelevant.

Probably, the channeling mechanism is also irrelevant; since machine modeling detects only one channeled particle out of 10^4 at statistical scattering of particles.

Thus, the probability of separation of P_2 is an increasing function of temperature. If we take into account the possibility of channeling and focusing some part of the separating fragments of Frenkel pairs, this will only lead to some weakening of the increasing nature of the temperature dependence P_2.

We conclude that the probability of separation of the components of Frenkel pairs P_2 is a non-decreasing function of temperature from the above.

The probability of fixing the separated components of Frenkel pairs P_3 is determined by the ratio of concentrations and capture cross-sections between the stabilization centers of interstitial ions and vacant nodes of the crystal lattice.

The temperature dependence of P_3 can be estimated in the temperature range, when the thermal release of trapped internode ions can be neglected as follows.

Let N_1 and S_1 be the concentration and cross-section of internode ion capture by stabilization centers, N_2 and S_2 be the concentration and cross-section of internode ion capture by vacant nodes of the crystal lattice. The probability P_3 can be represented as

$$P_3 = N_1 S_1 (N_1 S_1 + N_2 S_2)^{-1} = (1 + N_2 S_2 / N_1 S_1)^{-1}. \tag{5.3}$$

We obtain the following expression for the radius of the capture sphere, assuming that the capture of an interstitial ion occurs at a distance when the potential energy of interaction of an ion with the capture center is equal to its kinetic energy of thermal motion kT (considered that internode ions are thermalized) or more generally μkT and taking the interaction potential as

$$U(r) = \frac{-\alpha}{r^m}$$

$$\frac{-\alpha}{r^m} = \mu kT, \quad r = (-\alpha/\mu kT)^{1/m}$$

So the capture section is

$$S = \pi(-\alpha/\mu kT)^{2/m} = CT^{-2/m}, \tag{5.4}$$

where $C = (-\alpha/\mu T)^{2/m} = const.$

We get, substituting Eq. (5.4) into Eq. (5.3),

$$P_3(T) = \left[1 + N_2C_2T^{-2/m_2}/N_1C_1T^{-2/m_1}\right] = \left[1 + BT^n\right]^{-1}, \qquad (5.5)$$

where $B = N_2C_2/N_1C_1 = const;$. $n = \frac{2}{m_1} - \frac{2}{m_2}$.

The exponent of the degree of n can be negative, equal to zero or a positive number depending on the ratio of the "stiffness" of potentials m_1 and m_2.

Accordingly, $P_3(T)$ will be an increasing temperature-independent or decreasing function of temperature according to Eq. (5.5).

It was established that with sufficient accuracy the parameter m varies within (2 ÷ 3) for the interaction of neutral defects and is equal to 1 for charged centers when studying the spatial separation of F-H-centers in silk-halide crystals.

The most probable charge state of an anionic Frenkel pair is the state $O_i^- - F^+$-center [129]. The centers of stabilization of interstitial anions can serve as alternating ions of Me^{+3} or atoms of transition elements of the Fe^{+2} and Cr^{+2} type neutral with respect to the crystal lattice.

It is obvious that the interaction of charged $O_i^- - F^+$-pairs will be described by a potential with m = 1, interactions of the $O_i^- - Me^{+2}$ type with m_1=(2 ÷ 3), interactions of the type $O_i^- - Me^{+3}$ with $m_1 = 1$. It can be seen from this consideration that in the general case $m_1 = (1 \div 3)$ and $m_2 = 1$.

Then n and the probability $P_3(T)$ turns out to be a non-decreasing function of temperature.

The release of trapped oxygen ions will compete with the capture process at a temperature when the oxygen localized on the traps is not stable; $P_3(T)$ may turn out to be a decreasing function of temperature in this case.

Therefore, it is important to determine the range of temperature stability of the localization of interstitial oxygen, within which $P_3(T)$ does not decrease with increasing temperature.

We performed experiments on isochronous annealing of MgO (I) single crystals irradiated at a temperature of 88 K for this goal.

Isochronous annealing of MgO (I) crystals irradiated at 88 K with a dose of 2×10^7 Gy was studied. The annealing duration at a fixed temperature was 10 min. The samples were cooled to the initial temperature (88 K) after annealing; the absorption spectra were measured.

Figure 5.6 shows the absorption spectra of the irradiated and annealed single crystal MgO (I) at consistently increasing temperatures, from which the absorption spectrum of the irradiated crystal was subtracted. So, the spectra shown in the figure demonstrate changes in the optical absorption of the irradiated sample after annealing.

It can be seen that there are no significant changes in absorption in the F^+-band region in the studied annealing temperature range (88 ÷ 290), except for an increase in the optical density after annealing at (175 ÷ 180) K, probably due to a long-wave decay of the intense band with $h_{vm} = 5.4$ eV.

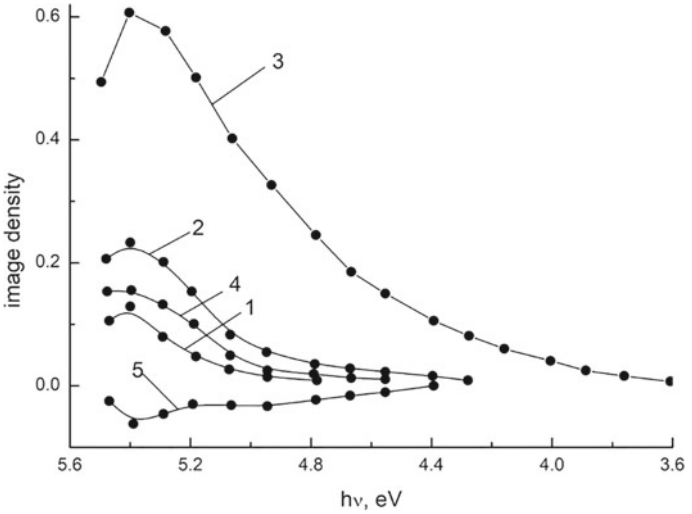

Fig. 5.6 Absorption spectra of MgO (I) crystals irradiated at 88 K by protons at a dose of $2 \cdot O^7$ Gy and annealed at temperatures, where 1 is 115 K; 2 is 140 K; 3 is 175 K; 4 is 255 K; 5 is 275 K. The absorption spectrum of the irradiated crystal was subtracted from the absorption spectra of annealed crystals

The obtained dependence indicates the absence of annealing of F^+-centers in the temperature range (88 ÷ 260) K. Consequently, there are no internode oxygen traps unstable in this temperature range.

The dependence on the temperature of the optical absorption intensity at 5.4 eV turned out to be not trivial (Fig. 5.6).

The curve of the isochronous annealing of the F^+-band, normalized to its initial intensity, is shown in Fig. 5.7.

The absorption intensity at 5.4 eV increases with increasing the annealing temperature, reaching a maximum at (170 ÷ 190) K and then decreases.

The intensity of this band becomes lower than its initial value in the irradiated sample at annealing temperatures above 275 K. It should be noted that tendency to decrease the intensity of the F^+-band at $T > 275$ K appears (Fig. 5.7).

The conclusion about the thermal stability of interstitial oxygen at temperatures (88 ÷ 260) K leads to the conclusion that in this temperature range the probability of stabilization of displaced oxygen ions is $P_3(T)$ in crystals, MgO (I) is a non-decreasing function of temperature.

The analysis of temperature measurements of elementary probabilities P_2 and P_3 presented above proves their non-decreasing nature with an increase in the irradiation temperature in the range (88 ÷ 260) K.

Consequently, the observed decrease in the rate of accumulation of F^+-centers at these temperatures (Fig. 5.5) is caused by a pronounced temperature-stimulated decrease in the probability of creating anionic Frenkel defects P_1, so, by a decrease in the generation rate of primary Frenkel pairs.

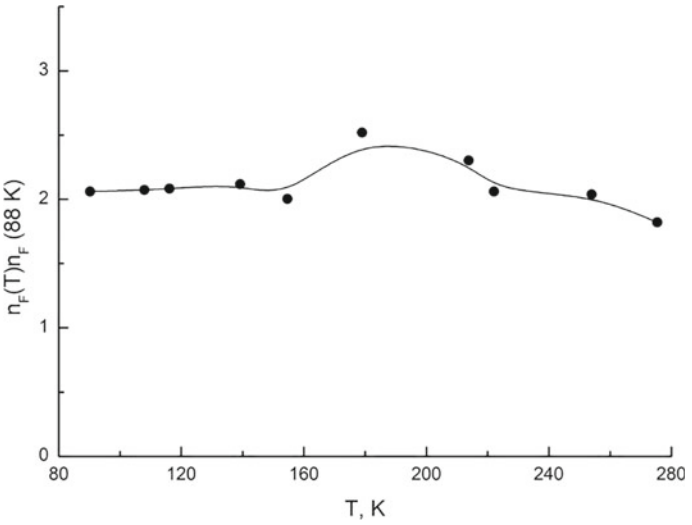

Fig. 5.7 Curve of isochronous 10-min annealing of the F^+—band of absorption in an MgO (I) crystal irradiated at 88 K with protons (dose 24×10^7 Gy). The dependence is normalized for the intensity of the band after irradiation of the crystal

This fact contradicts the concept of the shock mechanism and is obviously a consequence of the relationship of electronic processes with the low-temperature mechanism of defect formation in MgO (I) crystals.

In this regard, the coincidence of the activation energy of the decay of the accumulation rate of F^+-centers in Eq. (5.1) with the binding energy of G-excitons in MgO, equal to 0.08 eV, does not seem to be accidental [5].

It can be assumed that stable states of G-excitons are required for the realization of shock generation of anionic Frenkel pairs.

Then an increase of temperature will lead to an increase in the thermal instability of excitons with a corresponding decrease in the rate of accumulation of F^+-centers.

It is necessary to establish the boundary of the thermal stability of excitons in MgO, which is real under the conditions of our experiment to verify this assumption. The experiments carried out by us in this direction are described in the next section of the work.

5.2 Thermally Stimulated Conductivity of Irradiated MgO(I) Crystals

The experiments aimed at determining the temperature of thermal dissociation of excitons in MgO were based on the following concepts [15].

The dynamic equilibrium arising during irradiation between the processes of generation and recombination of electronic excitations leads to the establishment of a quasi-stationary gas concentration of electron–hole pairs and excitons.

The ratio of exciton concentrations and electron–hole pairs is a temperature-dependent value due to the thermal instability of excitons.

Earlier, a low efficiency of radiative recombination through local levels at low (~90 K) temperatures was noted in the study of MgO cathodoluminescence; this fact is associated with the predominant creation of excitons at these temperatures.

The equilibrium in the electron excitation gas shifts towards electron–hole pairs at temperatures when excitons are thermally unstable; it leads to a significant increase in recombination impurity luminescence and greater efficiency of the formation of color centers on pre-radiation vacancies.

Ignition of recombination impurity glow in MgO at temperatures (220 ÷ 280) K was observed in [12]. The effectiveness of the formation of V-type hole centers recorded using the thermally stimulated conductivity (TSC) method was monitored under the conditions of our experiment.

A typical TSP current curve of a sample irradiated at 140 K is shown in Fig. 5.8.

The irradiation was carried out with protons with energy of 10 meV, so that the proton path approximately corresponded to the thickness of the samples selected for the experiment. The curve shows weak peaks at 190 K, 230 K, 290 K and two orders of magnitude more intense peak at (370 ÷ 380) K.

The identification of the observed peaks is based on the identity of the TSC curve obtained by us with the curves of thermally stimulated luminescence (TSL) of X-ray MgO crystals [128].

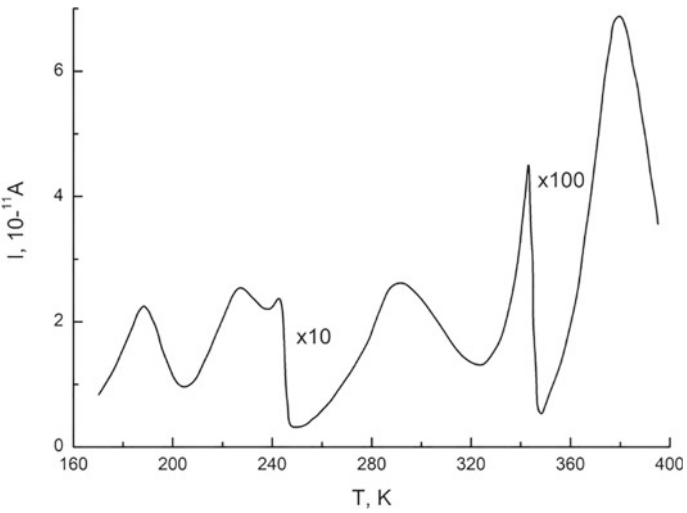

Fig. 5.8 Dependence of the TSC current on temperature for an MgO (I) crystal irradiated at 140 K by protons with energy of 10 meV and a dose of 2×10^6 Gy

TSL peaks were associated with the destruction of the electron Cr^+-center and hole V_{Na} (190 K)-, V_{Li} (230 K)- and V_{Al} (370 K)-centers by parallel measurements of TSC and EPR [73].

Since the decay of these centers leads to the release of electrons or holes, the correspondence of the TSC and TSL curves is uniform.

The validity of comparing the peaks of TSC and TSL is confirmed by the following data:

1. The intensity of all TSP peaks reaches saturation after short-term irradiation, which is clearly illustrated by the dependence of the intensity of the TSC peak at 370 K on the irradiation time shown in Fig. 5.9. This fact indicates that centers formed on pre-radiation defects are responsible for the peaks of TSC.
2. The activation energy of the fracture of the defect responsible for the TSC peak at 370 K, calculated from the initial slope of the low-temperature branch of the peak, is equal to (1.0 ± 0.1) eV and coincides with the energy of destruction of V_{Al}-centers.
3. The ratio of the intensity of the TSC peak at 370 K to the peak intensities at 190 K and 230 K approximately corresponds to the ratio of the concentration of Al ions to the concentration of Cr, Na and Li ions in the sample.

Thus, the predominant type of hole center in irradiated MgO (I) crystals are V_{Al}-centers formed when holes are captured by pre-radiation complexes "impurity V^{+3}-vacancy cation" as follows from Fig. 5.8. Such complexes can be designated as V_{Al} centers.

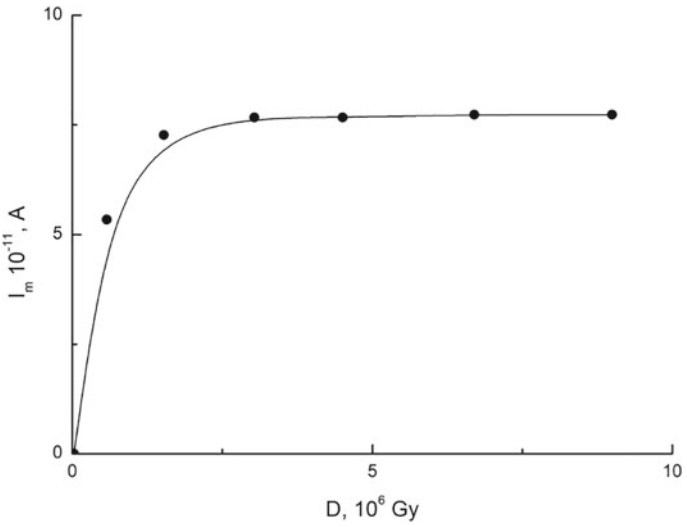

Fig. 5.9 The dependence of the current at the maximum of the TSC peak at 370 K on the radiation dose of protons with energy of 10 meV

The speed of accumulation of V_{Al}-centers is proportional to the product of the concentration of V_{Al}^{-}-centers by the quasi-stationary concentration of free holes, according to the gas-kinetic theory of chemical reactions.

Since the concentration of V_{Al}^{-}–centers is constant, a change in the efficiency of accumulation of V_{Al}-centers can occur only when the density of free holes changes.

Thus, it is possible to monitor the change in the quasi-stationary concentration of holes in the valence band by controlling the efficiency of creating V_{Al}-centers.

The temperature dependence of the efficiency of the accumulation of V_{Al}-centers was obtained by us under isodose irradiation of samples (t = 120 min) for different temperature values with following the measuring the intensity of the TSP peak at 370 K.

The measurement results are shown in Fig. 5.10.

The accumulation efficiency varies slightly in the temperature range (140 ÷ 200) K as can be seen from the figure and increases sharply at temperatures above 200 K. A sharp increase in the efficiency of the accumulation of V_{Al}-centers indicates a significant increase in the concentration of holes in the valence band.

Since, the irradiation conditions remained unchanged with the exception of temperature and the redistribution of charge from unstable Cr^{+}-, V_{Na}- and V_{Li}-centers due to the incommensurability of their concentration with the concentration of V_{Al}^{-}-centers cannot provide a noticeable increase in the efficiency of accumulation of V_{Al}-centers, the source of additional holes should be considered thermally unstable excitons at T > 200 K.

This conclusion is confirmed by the ignition of impurities of recombination luminescence observed in [12] at temperatures above 200 K.

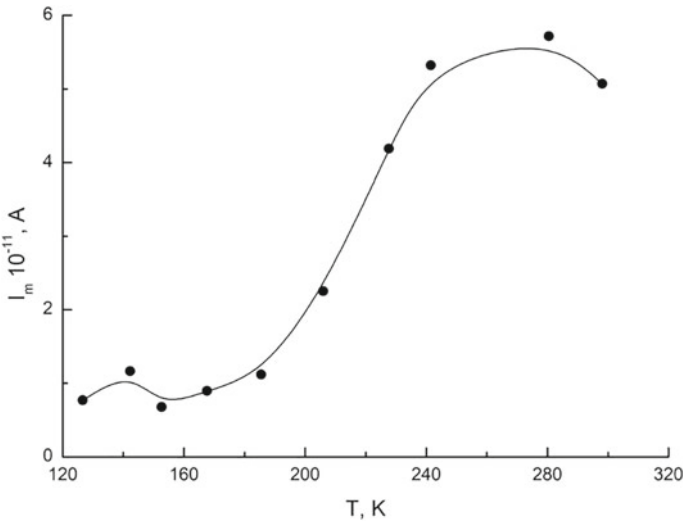

Fig. 5.10 The dependence of the current at the maximum of the TSC peak at 370 K on the temperature of isodose irradiation by protons with energy of 10 meV and a dose 8×10^6 Gy

The temperatures of increasing the efficiency of the accumulation of V_{Al}-centers and the ignition of recombination luminescence coincide despite the differences in the chemical compositions of the MgO (I) samples and the samples used in [12] and other experimental conditions.

This fact testifies to the unified, fundamental nature of the process that caused these phenomena. It is obvious that the thermionization of excitons satisfies this criterion.

Thus, based on the above, we conclude that excitons in MgO crystals are thermally unstable and dissociate into electron–hole pairs at temperatures above 200 K.

5.3 Nature of Low-Temperature Efficiency Change Accumulations of F^+-centers

The probable models of processes causing the thermostimulated phenomena observed in the experiment are considered on the basis of the above experimental results and their preliminary analysis in this section.

The main results on low-temperature accumulation of centers, discussed in the previous sections, are as follows:

1. There is a significant decrease in the rate of accumulation of F^+-centers with an increase in temperature, due to a decrease in the probability of generation of primary Frenkel pairs as shown earlier. This phenomenon is explained by the temperature-dependent non-elementary generation of anionic Frenkel defects ignoring the effects of channeling and focusing.
2. It is established that excitons in MgO are thermally unstable at temperatures above 200 K; the relaxation of excitations of the electronic subsystem occurs mainly through recombination of electron–hole pairs at local levels under these conditions.
3. It is shown that kinetics of the increase in the intensity of the absorption band at 4.3 eV are symmetrical to the accumulation curves of F^+-centers throughout the studied dose range in the temperature range (88 ÷ 190) K. However, there is no change in the intensity of the band with $h_{vm} = 4.3$ eV at temperatures above 190 K.

The results, listed above, in aggregate fully satisfy the hypothesis of the non-shock generation of anionic Frenkel defects under low-temperature proton irradiation, when the displacement of anions occurs during the decay of complex electronic excitations formed from excitons [109, 143].

Indeed, an extremely high gas density of excitons and electron–hole pairs is formed at the initial moment of time in the proton track, sufficient to achieve a significant probability of statistical creation of excitons within the sphere of their pair interaction.

Interacting excitons with characteristic time τ_1 form bound states capable of disintegrating into a Frenkel pair.

Temporary degradation of the track occurs at the same time, due to the high mobility of unreliaxed electronic excitations, as a result of which the initial excitation density decreases rapidly.

The density of recombinationally generated excitons for this reason (which probably takes time $\tau_2 >> \tau_1$) turns out to be sufficient for the effective creation of binary excitations.

The efficiency of direct formation of bound states at temperatures of thermal instability of excitons due to their thermal dislocation decreases sharply with an activation energy close to the binding energy of excitons for the same reason.

Therefore, the contribution of non-elementary creation of defects in proton tracks is insignificant at room temperature.

The oxygen ions displaced in the non-shock process seem to have increased activity with respect to the capture of Fe^{+2} ions with its recharge to the Fe^{+3} state, so, they are effective oxidizers of transition element ions.

Therefore, the speed of recharge of iron ions also decreases with an increase in temperature when the speed of non-shock generation of interstitial oxygen decreases.

Therefore, the coincidence of the temperature of a sharp decrease in the speed of iron recharge to 0 and the temperature of the thermal dislocation of excitons is not accidental.

The need to involve binary excitons rather than single excitons to explain the non-binary generation follows from the following.

Firstly, experimentally non-shock generation of defects is observed only under the condition of intense excitation of the electronic subsystem of crystals.

Secondly, the calculated value of the energy of the formation of the anionic Frenkel pair in MgO is approximately twice the energy of excitons.

Thirdly, the ability to form a covalent bond between the hole components of excitons O^- is significantly higher due to the lack of electrons on the loosening σ*-orbital of the O_2^{2-} molecule,. Relaxation of the nuclei of the biexiton excites local oscillations, which creates favorable conditions for the transition of one of the nuclei of the biexiton to the internode.

The degree of fundamentality of the proposed mechanism of non-elementary generation of anionic defects remains unclear. It cannot be excluded from the available data that the decay of binary excitation occurs in defective areas of the crystal, for example, in the vicinity of impurity ions of transition metals (Fe^{+2}, Cr^{+2}, etc.).

5.4 Summary

We can conclude that based on the results of this chapter:

1. An effective mechanism of non-shock generation of anionic Frenkel defects is carried out during low-temperature irradiation of magnesium oxide crystals by protons.

2. The temperature (190 ÷ 200) K can be taken as the upper temperature limit of the non-shock mechanism.
3. The stability of excitons in magnesium oxide crystals is limited to a temperature of less than 190 K with respect to ionization.
4. The dose and temperature correlation between the concentration of accumulated Fe^+-centers and the intensity of absorption of Fe^{+3} ions indicates the essential role of iron ions as stabilizers of anions displaced in the non-shock process.
5. The radiation resistance of magnesium oxide products operating at low irradiation temperatures can be significantly increased by cleaning raw materials from impurities of transition elements.

Chapter 6
Accumulation of F-Type Color Centers in Crystals of Magnesium Oxide at High Excitation Densities Accelerated Electrons of Subthreshold Energy

Contents

The objective of this chapter is to investigate the possibility of non-shock generation of anionic vacancies in magnesium oxide crystals at high radiation exposure.

The objective of this chapter is to investigate the possibility of non-shock generation of anionic vacancies in magnesium oxide crystals at high radiation exposure.

The most promising for solving this problem is the use of high-current beams of accelerated electrons with an energy less than the threshold value of the elastic displacement of the oxygen ion from the regular node of the crystal lattice to the internode (> 0.33 meV) as a source of high excitation densities.

It is known that the capture by the anionic vacancy field of one or two electrons in magnesium oxide crystals leads to the formation of F^+ and F-color centers, respectively, for which the position of the maxima of the absorption and luminescence bands, the value of their half-width, the strength of the oscillators and the temperature range of stability are reliably established.

Therefore, information about the presence of anionic vacancies in crystals can be obtained from absorption and luminescence measurements.

The separation of pre-radiation and anionic vacancies created under the action of a high-current electron beam is supposed to be carried out by means of a comparative analysis of kinetic curves of accumulation of F-type color centers with an increase in the absorbed radiation energy of a high-current electron beam, high-energy protons and X-rays.

A. Surzhikov and E. Lysenko, *Creation and Accumulation of Radiation Defects in Single Crystals of Magnesium Oxide*, https://doi.org/10.1007/978-3-031-60207-8_6

The study of X-ray crystals will allow identifying the processes associated with the pre-radiation defectiveness of the crystal and crystals irradiated with protons allow identifying the processes associated with newly generated defects of the crystal lattice.

The dependence of the efficiency of accumulation of F-type color centers on the electron beam current density should serve as proof of responsibility for the non-elementary generation of anionic vacancies in magnesium oxide crystals of high densities of radiation exposure.

MgO (I) crystals were used as objects of research in solving this problem (Table 2.1).

Irradiation and all measurements were carried out at a sample temperature of 298 K.

6.1 Accumulation of F^+-Centers in Magnesium Oxide Crystals at High Excitation Densities by Accelerated Electrons

The task of this section is to establish the nature of the origin of anionic vacancies on which color centers are formed when magnesium oxide crystals are irradiated with a high-current electron beam—on pre-radiation or created during irradiation.

The problem methodically was solved by comparing the kinetic curves of accumulation of F + -color centers in magnesium oxide crystals with an increase in the absorbed radiation energy of a high-current electron beam, high-energy protons and X-rays [186–189].

The choice of methodological approach to solving the problem is due to the following considerations:

1. The curves of the increase in the number of F-centers created in KCl and MgO crystals by ultraviolet radiation are given in [104] (Fig. 6.1).

The process of accumulation of F-centers for KCl is divided into two stages.

Defects that existed in the crystal before irradiation are involved in the first stage, which quickly tends to saturation, according to the author; only their own radiation defects in the second stage appear, the number of which increases linearly over a wide range with the time of irradiation.

The accumulation of F-centers for MgO is carried out in one rapidly saturating stage, associated by the author with the presence of pre-radiation defects.

The presence of a linear stage in the kinetic curve of accumulation of F-centers with an increase in the absorbed radiation energy is proposed to be used as a criterion for the generation of Frenkel anion pairs in magnesium oxide crystals from a comparison of the kinetic curves of accumulation of F-centers in KCl and MgO under the action of ultraviolet radiation, as well as from the appearance of a linear stage in the kinetic curve of accumulation of F-centers in MgO only under the action of accelerated particles whose energy is above the threshold.

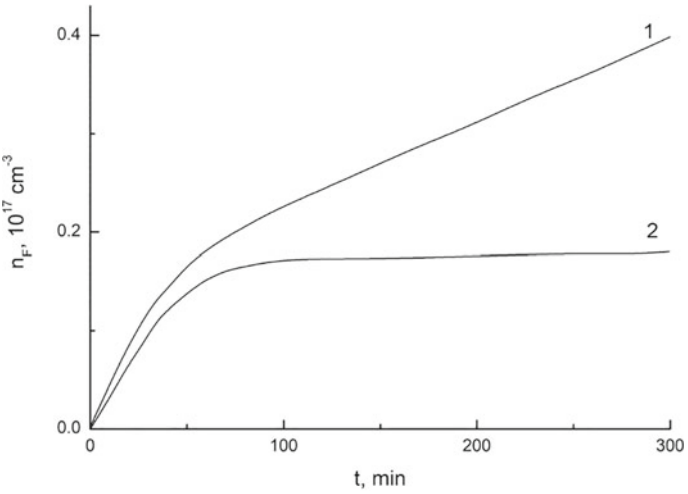

Fig. 6.1 Kinetic accumulation of F^+-centers in crystals of KCl (**1**) and MgO (**2**) under irradiation with VUV radiation [123]

2. Magnesium oxide crystals obtained by melting the charge in an electric arc contain a significant amount of impurity ions with an effective charge other than two electron charges. The appearance of this type of impurities in the process of crystal growth should be accompanied by Schottky disorder: one vacancy will be formed for every two such impurity ions. The concentration of impurities of the Me^+ type in the studied MgO (I) crystals (Table 2.1) is of the order of 10^{16} cm^{-3}. Therefore, the concentration of pre-radiation anionic vacancies can be estimated by this value.

The following happens in this case.

Since X-rays are not capable of creating new anionic vacancies in magnesium oxide crystals [95, 96] and the formation of F-centers is carried out when electrons are localized on pre-radiation anionic vacancies [10], the accumulation of F^+-centers in this case should be described by a one-stage rapidly saturating kinetic curve [104].

Moreover, the maximum possible concentration of F^+-centers should not exceed the concentration of pre-radiation anionic vacancies, i.e. be at the level of 10^{16} cm^{-3}.

Irradiation of magnesium oxide crystals with high-energy particles leads to the creation of anionic vacancies [99].

Therefore, the kinetic of the accumulation of F^+-centers in MgO with an increase in the absorbed radiation energy of accelerated protons should be a two-stage curve at least.

The first stage is caused by the formation of F^+-centers on pre-radiation anion vacancies; the second is caused by the generation of Frenkel anion pairs during irradiation. Moreover, the concentration of F^+-centers at the end of the first stage of the kinetic curve should also be at the level of 10^{16} cm^{-3} as in the case of X-ray irradiation.

The accumulation of F^+-color centers at the second stage of the kinetic accumulation curve under irradiation with high-energy protons should occur linearly in a wide range of values of the absorbed radiation energy.

Thus, a comparison of the kinetic curves of accumulation of F^+-centers in magnesium oxide crystals when irradiated with a high-current electron beam with the kinematic curves of accumulation of F^+-centers when irradiated with X-rays and high-energy protons will make it possible to separate the radiation-stimulated effects associated with pre-radiation anionic vacancies and those generated during irradiation.

We will consider the results on the accumulation of F^+-centers in magnesium oxide crystals with an increase in the absorbed energy of radiation from a high-current electron beam, X-rays and high-energy protons in the light of the above arguments.

The values of the concentration of F^+-centers given in the infusion in their work, they were calculated according to the Smakula's formula

$$n_{F^+} = 0.87 \cdot 10^{17} n(n^2 + 2)^{-2} f^{-1} W \alpha_{F^+}, \tag{6.1}$$

where $\alpha_{F^+} n$ is the refractive index; f is the strength of the oscillator; W is the width of the absorption band of the F^+ -centers at half the height ; α^{F+} is the absorption coefficient at the maximum of the F^+-band.

The Equation taking into account values of W = 0.62 eV; n = 1.74; f = 0.8 at sample temperature of 300 K from [33] is below

$$n_{F^+} = 5.05 \cdot 10^{15} \alpha_{F^+} \quad \left[\text{cm}^{-3}\right] \tag{6.2}$$

It should be noted that the value of the absorption coefficient (α_{F^+}) at the maximum of the F^+ absorption band was always determined only after the decomposition of the additional optical absorption spectrum into elementary components in this work.

Figure 6.2 shows the dependence of the concentration of F^+-color centers in magnesium oxide crystals with an increase in the absorbed energy of X-ray radiation.

The accumulation of F^+-centers is described by a one-stage rapidly occurring kinetic curve.

The maximum concentration of F^+-centers is 6×10^6 cm^{-3}, which corresponds to the concentration of pre-radiation anionic vacancies, according to our estimates.

The kinetic of the accumulation of F^+-centers with an increase in the absorbed radiation energy of high-energy protons is shown in Fig. 6.3.

Two stages are distinguished in the kinetic curve of the accumulation of F^+-centers: 1 is a sharp increase in the concentration of F^+-centers and 2 is a slow increase in their number.

The presence of two stages in the kinetic curve indicates the presence of two sources of anionic vacancies in the crystals [104].

The first stage is caused by the formation of F^+-centers on pre-radiation anion vacancies; the second stage is caused by the generation of Frenkel anion pairs during proton irradiation [104].

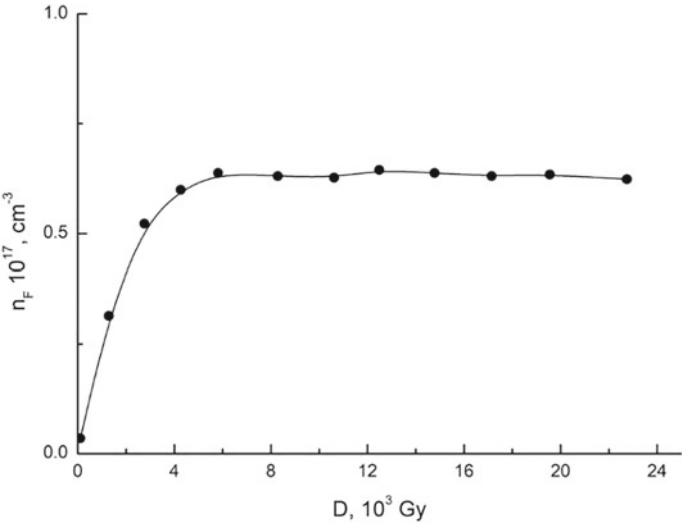

Fig. 6.2 Kinetic accumulation of F^+-centers in MgO (I) crystal at irradiating by X-rays

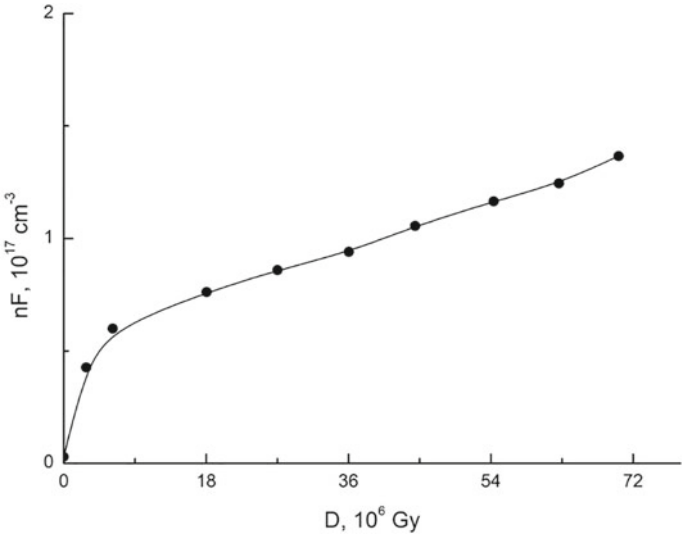

Fig. 6.3 Kinetic accumulation of F^+- centers in MgO (I) crystal at irradiating by high—energy protons

Indeed, the comparability of the concentration of F^+-centers at the end of the first stage of the kinetic accumulation curve with an increase in the absorbed proton energy (6×10^6 cm^{-3}) with the maximum concentration of F^+-centers in X-ray crystals, as well as the high efficiency of the accumulation of F^+-centers in this section of the

kinetic curve give reason to attribute responsibility for the first stage in the kinetic curve of accumulation of F^+-centers in magnesium oxide crystals when irradiated with protons of pre-radiation anionic vacancies.

The linearity of the change in the number of F + -centers in a wide range of absorbed proton radiation energy, as well as the significant excess of the concentration of F^+-color centers at the second stage of the kinetic accumulation curve over the estimated concentration of pre-radiation anion vacancies, serve as an indicator of the generation of Frenkel anion pairs in magnesium oxide crystals when irradiated with high-energy protons.

Figure 6.4 shows the kinetics of accumulation of F + -color centers in magnesium oxide crystals with an increase in the absorbed radiation energy of a high-current electron beam.

It is typical for it:

1. two-stage;
2. high efficiency of accumulation of F^+-centers in the first stage;
3. the coincidence of the values of the concentration of F^+-centers at the end of the first stage with the maximum concentration of F^+-centers in X-ray crystals;
4. the linear nature of the change in the number of F^+-centers at the second stage in a wide range of absorbed radiation energy;
5. the concentration of F^+-centers at the second stage exceeds the concentration of pre-radiation anionic vacancies.

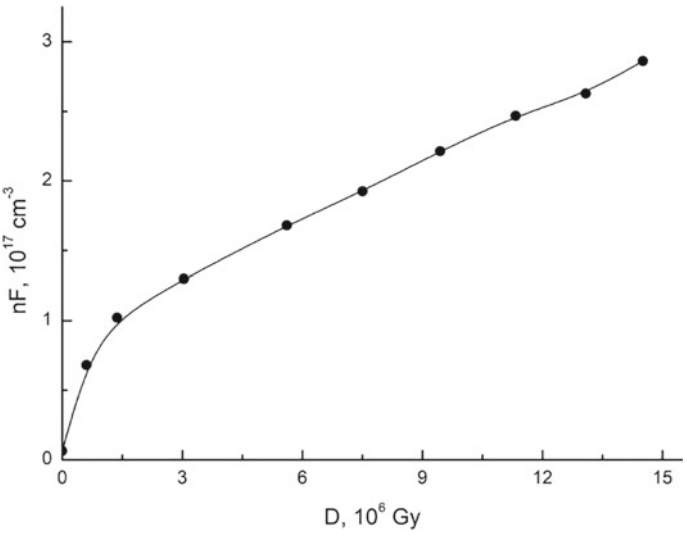

Fig. 6.4 Kinetic accumulation of F^+- centers MgO (I) crystal at irradiating by a high-current electron beam (j = 1000 A • cm^{-2})

Such a coincidence of kinetic curves of accumulation of F^+-centers with an increase in the absorbed radiation energy of a high-current electron beam and high-energy protons makes it possible to extend the interpretation of two stages in the kinetics of accumulation of F^+-centers during proton irradiation and in the case of electron irradiation.

Then, the first stage in the kinetic curve of the accumulation of F^+-centers in magnesium oxide crystals when irradiated with a high-current electron beam is due to the formation of color centers on pre-radiation anion vacancies, the second is due to the generation of Frenkel anion pairs during irradiation.

Since the energy of accelerated electrons in the beam (0.135 meV) is significantly lower than the threshold electron energy (0.33 meV) required to create Frenkel anion pairs in magnesium oxide crystals by elastic collisions, the results obtained indicate the possibility of non-shock generation of F^+-centers (anion vacancies) in MgO (I) when irradiated with a high-current beam electrons.

6.2 Effect of the Current Density of the Accelerated Electron Beam on the Accumulation of F^+-Centers in Magnesium Oxide Crystals

It is known that irradiation with X-rays and low-intensity flow of electrons of subthreshold energy does not lead to the accumulation of Frenkel anion pairs in magnesium oxide crystals [10, 104].

Therefore, the results given in Sect. 6.1 on the non-shock generation of anionic vacancies in MgO (I) when irradiated with a high-current electron beam can be explained by a specific feature of high radiation exposure powers.

In this case, a certain threshold value in the power of the absorbed radiation energy should be observed in the implementation of the non-elementary mechanism of Frenkel anion pairs in magnesium oxide crystals; it should manifest itself in the absence of a second (linear) stage in the kinetic curve of accumulation of F^+-centers in MgO (I) when irradiated with a high-current electron beam, the subthreshold energy with a current density less than this threshold value.

If the specific feature of high excitation densities in a non-elementary defect formation is the possibility of the decay of collective electronic excitations into structural defects, then the efficiency of the mechanism of non-elementary generation of Frenkel anion pairs in magnesium oxide crystals should increase with increasing radiation exposure power, since the number of elementary excitations per unit volume increases and the probability of their meeting increases.

This phenomenon can manifest itself with an increase in the efficiency of accumulation of F^+-centers at the second stage of the kinetic accumulation curve with an increase in the beam current density when irradiated with a high-current electron beam in an MgO (I) crystal.

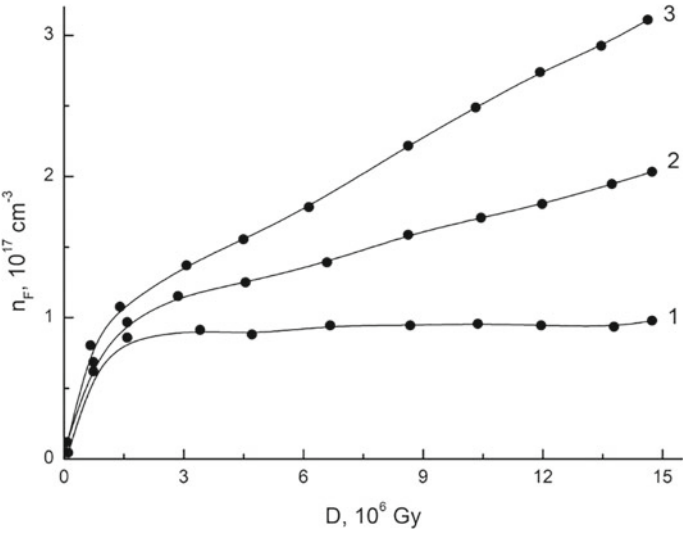

Fig. 6.5 Kinetics of accumulation of F^+-centers in a magnesium oxide crystal at irradiating by electron beam of various densities, where 1 is 80 A • cm^{-2}; 2 is 500 A • cm^{-2}; 3 is 1000 A • cm^{-2}

A study of kinetic curves of accumulation of F^+-centers in MgO (I) crystals under irradiation with a high-current electron beam was carried out different current densities based on the above in order to test the hypothesis of responsibility for the non-elementary generation of radiation defects in the anionic sublattice of magnesium oxide of the mechanism of decay of collective electronic excitations and to establish a threshold value of the power of absorbed radiation energy sufficient for its realization,

The results of the experiments are shown in Fig. 6.5.

The concentration of F^+-centers at the end of the first section of the kinetic curve is the same for different excitation densities (Fig. 6.5).

There are differences in the change in the concentration of F^+-centers at the second stage of kinetic dependence: the accumulation efficiency increases with an increase in the electron beam current density as expected.

The dependence of the energy costs for the accumulation of one stable F^+-center on the current density of the electron beam in the pulse is shown in Fig. 6.6.

The ratio of the interval of the radiation energy absorbed by the sample to the concentration of the F^+-centers created at the same time (at the second stage of the kinetic curve) is taken as a measure of energy costs.

It should be noted that there is no second stage in the kinetic curve of accumulation of F^+-centers when the electron beam current density is less than ~ 100 A·cm^{-2} (4.7×10^{11} Gy s^{-1}), due to the formation of color centers on anionic vacancies created during irradiation (Fig. 6.5).

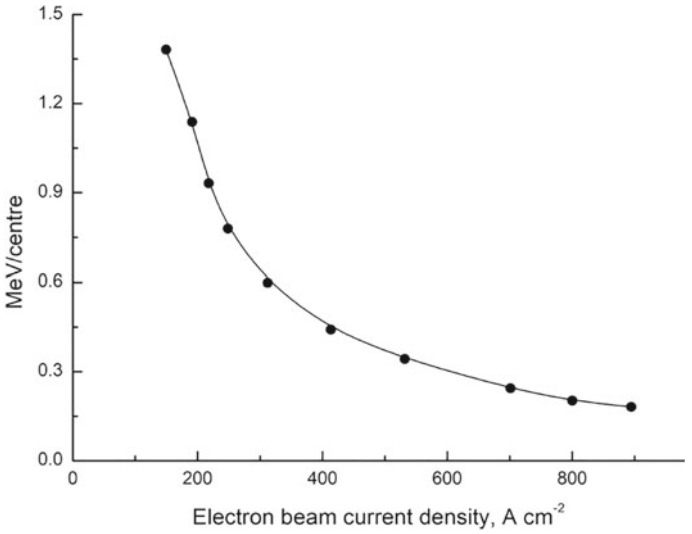

Fig. 6.6 Dependence of energy costs for the accumulation of one F^+-center in magnesium oxide crystals on the electron beam current density

Therefore, the power value of the absorbed radiation energy of a high-current electron beam of ~ 4.7×10^{11} Gy s^{-1} should be considered as the minimum necessary for the implementation of the mechanism of non-shock generation of stable Frenkel anion pairs in magnesium oxide crystals.

6.3 Summary

The following conclusions can be drawn based on the results of this chapter.

1. The possibility of non-shock generation of anionic vacancies in magnesium oxide crystals at high radiation exposure is shown.
2. The dependence of the efficiency of accumulation of vacancy components of Frenkel anionic pairs in MgO (I) crystals on the power of the absorbed radiation energy of a high-current electron beam of subthreshold energy is found.
3. A threshold value of the power of the absorbed radiation energy of a high-current electron beam of ~ 4.7×10^{11} Gy s^{-1} has been established in the implementation of a non-elementary mechanism of radiation defect formation in an anionic sublattice of magnesium oxide.

Chapter 7
Stabilization of Interstitial Oxygen Ions Formed Under the Action of a High-Current Electron Beam in the Crystal Lattice of Magnesium Oxide

Contents

The process of accumulation of radiation defects in solids depends to a certain extent on the efficiency of fixing displaced atoms or ions in the crystal lattice. Therefore, data on the behavior of interstitial defects are particularly important when analyzing radiation phenomena.

The most complete information in this regard is available regarding alkali-halide crystals. Work in this direction is in the initial stage of development and there is practically no data on the behavior of interstitial defects for oxides of alkaline earth metals.

We put forward an assumption about the stabilization of interstitial oxygen ions displaced by a high-current beam of electrons of subthreshold energy near impurity ions with an excessive positive charge based on the analysis of the general state of the problem.

Single crystals of magnesium oxide with different content of impurity ions MgO (I) and MgO (II) were used as objects of research in accordance with this (Table 2.1).

A. Surzhikov and E. Lysenko, *Creation and Accumulation of Radiation Defects in Single Crystals of Magnesium Oxide*, https://doi.org/10.1007/978-3-031-60207-8_7

A comparative analysis of the effects of accumulation of radiation defects in these materials is one of the methodological methods for solving the problem of the sites of fixation of interstitial oxygen ions.

The processes of formation of radiation defects in crystals of various impurity composition under the action of a high-current electron beam and their lifetime in a nanosecond time interval after the end of the irradiation pulse, were compared to separate the fundamental effects of radiation defect formation in magnesium oxide crystals from structure-sensitive ones.

7.1 About Possible Locations of Interstitial Oxygen Ions in the Crystal Lattice of Magnesium Oxide

In general, three channels of stabilization of interstitial ions in ionic crystals are possible:

1. Autolocalization of ions in the internodes of the crystal lattice.
2. Mutual stabilization of internode components of anionic and cationic Frenkel pairs.
3. Stabilization of interstitial ions near various imperfections of the crystal lattice.

The location of an ideal magnesium oxide lattice of an oxygen ion in the interstitial space is difficult; since its extremely high mobility has been established even at extremely low temperatures [85].

We do not exclude the possibility of stabilization of interstitial oxygen ions by interstitial magnesium ions in the case of irradiation of magnesium oxide crystals with high-energy particles that create interstitial magnesium ions through elastic collisions with Mg^{2+} ion nuclei.

The creation of Antishottk pairs in our case of irradiation with a high-current electron beam with an energy of $(0.1 \div 0.2)$ MeV, is unlikely, since the creation of interstitial magnesium ions by the ionization mechanism of radiation defect formation is unlikely.

Imperfections of the crystal lattice, which can be pre-radiation cationic vacancies, dislocations and impurity ions, are the most likely places of stabilization of interstitial oxygen ions in magnesium oxide crystals, as it seems to us.

Cationic vacant nodes of the crystal lattice of magnesium oxide can serve as a place for stabilization of the interstitial oxygen atom. Since the electron color centers are observed by us, as shown earlier, only in the form of F^+-centers and since double ionization of an oxygen ion is unlikely, it is most likely that oxygen is displaced in the charged state in the form of O- from a regular node of the crystal lattice under the action of a high-current beam of accelerated electrons. In this case, cationic vacancies cannot serve as a place of stabilization of interstitial oxygen ions.

Dislocations, as places of runoff of interstitial oxygen ions, are also unable to provide the concentrations of stable F^+-centers observed by us of 6.3×10^{17} cm^{-3}.

Indeed, the maximum possible concentration of internode ion fixation sites on the dislocations of the crystal lattice is determined by [144] due to the electrostatic interaction

$$C = n_s n_d, \tag{7.1}$$

where n_S is the maximum possible number of steps on the dislocation; n_d is the dislocation density.

The value of n_S for screw dislocations can be estimated using the Burgers vector (b) [145]

$$n_{s(w)} = \frac{1}{b}. \tag{7.2}$$

Equation for sliding planes {110} typical of a NaCl-type crystal lattice [146] is

$$b = \frac{a}{\sqrt{2}}. \tag{7.3}$$

The value of n_S for edge dislocations is estimated using the lattice parameter (a) [145]

$$n_{s(k)} = \frac{1}{a}. \tag{7.4}$$

There is in specially undeformed crystals [194]

$$n_d \approx 10^6 \div 10^7 \text{cm}^{-2}. \tag{7.5}$$

Therefore, we obtain $C_{(w)} = 3 \times 10^{14}$ cm^{-3}, $C_{(k)} = 2 \times 10^{14}$ cm^{-3} taking the value of the dislocation density n_d in magnesium oxide crystals 10^7 cm^{-2} and the value of the lattice parameter $a = 4.2 \times 10^{-8}$ cm [147] by Eq. (7.1).

Elastic interaction of interstitial ions can be carried out only with edge dislocations, since screw dislocations do not create compression regions. In this case, interstitial ions are located along the dislocation core, whose diameter for ionic crystals usually does not exceed $5b$ [148].

Therefore, the maximum possible concentration of the sites of attachment of interstitial oxygen ions in magnesium oxide crystals will not exceed 2×10^{14} cm^{-3} due to the elastic interaction of interstitial ions with dislocations.

Secondly, the energy of elastic interaction of point defects with dislocation lines is small and amounts to $(0.2 \div 0.3)$ eV. Therefore, the fixation of interstitial oxygen ions on dislocations will not be effective at temperatures close to room temperature.

Since the F^+-color centers in magnesium oxide crystals are stable to higher temperatures (more than 500 K) [43], the discussed mechanism of stabilization of interstitial oxygen ions in MgO is especially not realized.

It remains to be assumed that the stabilization of negatively charged oxygen ions displaced from the regular nodes of the magnesium oxide crystal lattice under the action of irradiation with a high-current electron beam is carried out mainly near impurity ions having an excessive positive charge relative to the crystal lattice.

This point of view is confirmed by the following results:

1. It is shown that the presence of an impurity increases the rate of accumulation of F-type color centers when studying the dependence of the absorption coefficient in the F-band on the absorbed radiation energy of neutrons and high-energy electrons in crystals with different content of impurity iron ions ($5 \times 10^{-2} \div 6 \times 10^{-3}$) % [93].
2. We have studied the optical absorption spectra of MgO (I) and MgO (II) crystals after irradiation with a high-current electron beam. It has been found that there is no accumulation of F^+-color centers in MgO (II) with a significantly lower content of impurity cation-substituting ions unlike MgO (I) crystals.
3. Chapter 6 shows that the second stage of the kinetic curve of accumulation of F^+-centers in MgO (I) crystals under the action of a high-current beam of accelerated electrons, due to the formation of F^+-centers on the anion vacancies created by irradiation, has a linear character.

The linearity of accumulation, in turn, indicates that the capacity of the flow of interstitial oxygen ions significantly exceeds the maximum concentration of F^+-centers (6.3×10^{17} cm^{-3}).

We estimate the concentration of the capture centers of interstitial oxygen ions of the order of 10^{19} cm^{-3} from these considerations.

It is noteworthy that the content of impurity cation-substituting ions with an excessive positive charge in the studied MgO(I) crystals is of the same order.

Thus, it can be assumed as a working hypothesis that impurity cation-substituting ions with an excessive positive charge relative to the lattice can be effective fixing points for oxygen ions displaced from regular nodes of the crystal lattice under the action of a high-current electron beam in crystals of magnesium oxide of technical purity.

Moreover, it is necessary to highlight the ions that acquire an excessive positive charge during irradiation (Fe^{2+}, Ni^{2+}, Pb^{2+}) [10] from impurity cation-substituting ions as the most effective centers of stabilization of interstitial oxygen ions, since the excess charge of impurity ions Al^{3+}, Si^{4+} must be compensated by cation vacancies created during crystal growth.

The following sections of the paper present the results of studies aimed at verifying the hypothesis expressed.

7.2 Investigation of the Generation of F^+-Color Centers in Single Crystals of Magnesium Oxide Under the Action of a High-Current Beam of Accelerated Electrons of Nanosecond Duration

We analyzed the role of impurity ions in radiation defect formation in magnesium oxide crystals from the point of view of stabilization of interstitial oxygen ions in Sect. 7.1.

The differences in the accumulation of F^+-color centers under the action of a high-current electron beam in crystals of various degrees of purity are satisfactorily explained from these positions.

However, it is necessary to establish the degree of influence of impurity ions on the primary process of the non-elementary creation of Frenkel anion pairs in magnesium oxide crystals at high excitation densities in order to further develop the proposed assumption about the fixation of interstitial oxygen ions by impurity ions with an excessive positive charge.

The optical absorption spectra and luminescence spectra of MgO (II) crystals in the nanosecond time interval when irradiated with subthreshold energy electron pulses and the lifetime of F-type electronic color centers after the end of the irradiation pulse in MgO (I) and MgO (II) crystals were studied for this goal.

The choice of objects and methods of research is due to the following considerations.

Stable electron color centers have not been registered in MgO (II) crystals after irradiation with a high-current electron beam.

Therefore, the creation of F-type color centers should not occur in the case of the influence of impurity ions on the process of non-shock generation of Frenkel anion pairs in magnesium oxide in these crystals during irradiation with a high-current electron beam of subthreshold energy.

Information on the registration of electronic color centers in MgO (II) crystals during irradiation will indicate the fundamental nature of the mechanism of non-shock generation of Frenkel anion pairs in magnesium oxide.

Figure 7.1 shows examples of waveforms characterizing the change in time of optical transmission (a) and luminescence (b) of a sample under the action of a radiation pulse.

The optical density $D(t)$ at time t_i after the start of the irradiation pulse can be determined from the waveform (a) as

$$D(t) = \lg \frac{l_0}{l_i}. \tag{7.6}$$

Here l_0 and l_i are proportional to the intensity of the probing light transmitted through the sample before and after the start of the irradiation pulse, respectively.

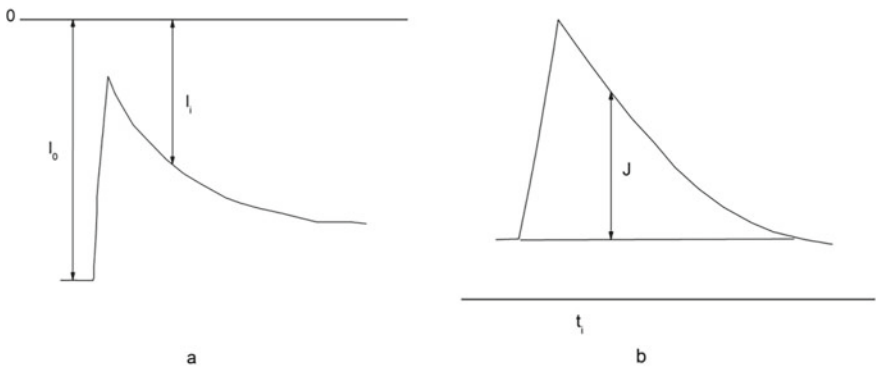

Fig. 7.1 Examples of changes in the waveforms of changes in time of optical transmission (**a**) and luminescence (**b**) of a magnesium oxide crystal under the influence of a radiation pulse

The full spectrum of optical absorption of a sample at a certain moment after the start of the irradiation pulse can be constructed from the results of optical density measurements at different wavelengths of probing light emitted by a monochromator.

The luminescence spectrum is constructed based on the readings of the luminescence intensity l_i at certain wavelengths.

Curve 1 characterizes the optical absorption spectrum of the MgO (II) crystal, which changes at 300 K 200 ns after the start of the irradiation pulse (Fig. 7.2).

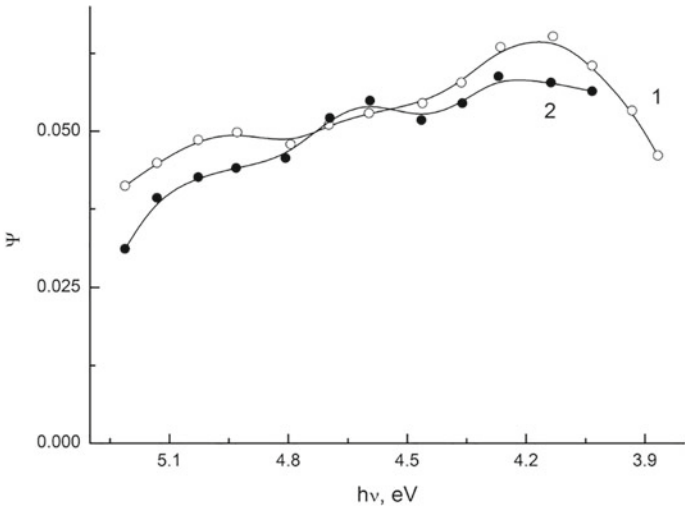

Fig. 7.2 Optical absorption spectra of the MgO (II) crystal after 200 ns of the start of the radiation pulse (j = 1000 A cm^{-2}), where 1 is 300 K; 2 is 80 K

There is an increase in the value of the optical density in the absorption band of the F-type color centers (~ 4.92 eV) in the spectrum of additional optical absorption as follows from the figure.

The change in the optical absorption spectra at a sample temperature of 80 K did not reveal any significant changes in the intensity of this absorption band (Fig. 7.2, curve 2).

Since there is no accumulation of F^+-centers in MgO (II) crystals when irradiated with X-rays, it can be concluded that there is an extremely insignificant content of pre-radiation anionic vacancies in the crystals.

However, in order to be sure that the observed optical absorption is not associated with pre-radiation anionic vacancies, the studied crystals were irradiated with fifteen irradiation pulses before measurement, which, in our opinion, should lead to the filling of all pre-radiation anionic vacancies.

The luminescence spectra of MgO (II) crystals under the action of a radiation pulse were studied to confirm the generation of electronic color centers in magnesium oxide crystals under the action of a high-current electron beam of subthreshold energy and to establish their structure (F^+ or F).

Figure 7.3 shows the luminescence spectrum of a magnesium oxide crystal measured at a sample temperature of 300 K after 10 ns after the start of the high-current electron beam irradiation pulse.

There is a band of luminescence with a maximum at 3.2 eV (the glow of F^+-centers) in the luminescence spectrum. The glow of the F-centers (2.4 eV) is not observed.

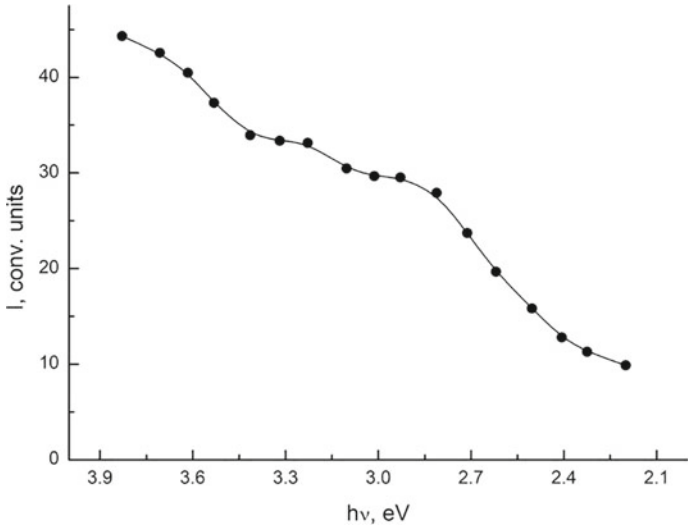

Fig. 7.3 The luminescence spectrum of the MgO (II) crystal at 300 K irradiation after 10 ns of the start of the electron flux irradiation pulse with a beam current density of 1000 A cm^{-2}

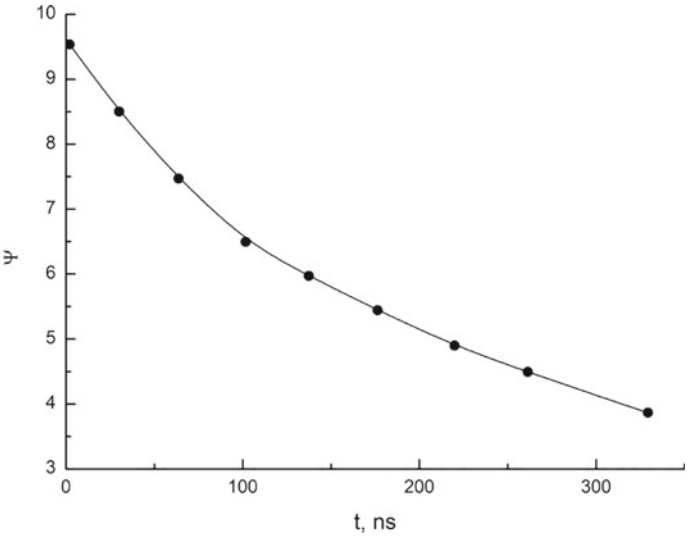

Fig. 7.4 The change in the optical density at the maximum of the F^+-band of absorption of the MgO (II) crystal after the irradiation pulse (j = 1000 A cm^{-2}; T = 300 K)

Processing of the luminescence attenuation data allowed establishing that the relaxation time constant of the glow of the F^+-centers is 27 ns.

We conducted a study of the relaxation of optical absorption in MgO (II) crystals with time after the end of the irradiation pulse in order to study the stability of the color centers responsible for the absorption band in the region of 4.92 eV.

It is established that the defects responsible for optical absorption in the absorption band region of the F-type color centers are unstable (Fig. 7.4).

Two time constants are observed: $\tau_i \approx 1\ 00$ ns, $t_i > 10$ microseconds in the relaxation of the optical density. Moreover, the number of color centers decreases three times in relation to their concentration immediately after the end of the irradiation pulse after 300 ns after the irradiation pulse.

Relaxation of optical absorption of F^+-color centers in impurity crystals of magnesium oxide MgO (I) after exposure to a high-current pulse of accelerated electrons has also been studied.

It is established that there is no short component in the relaxation of the optical absorption of F^+-centers and relaxation is carried out with a time constant greater than 10 microseconds for crystals of this series (Fig. 7.5).

Thus, F^+-electronic color centers are created in MgO (II) crystals with a low content of impurity ions under the action of a high-current beam of accelerated electrons of subthreshold energy. This indicates the fundamental nature of the mechanism of non-shock generation of radiation defects in the anionic sublattice of magnesium oxide crystals at high excitation densities.

The presence of a short component in the relaxation of the optical density in the absorption region of F^+-color centers for MgO (II) crystals and the absence of

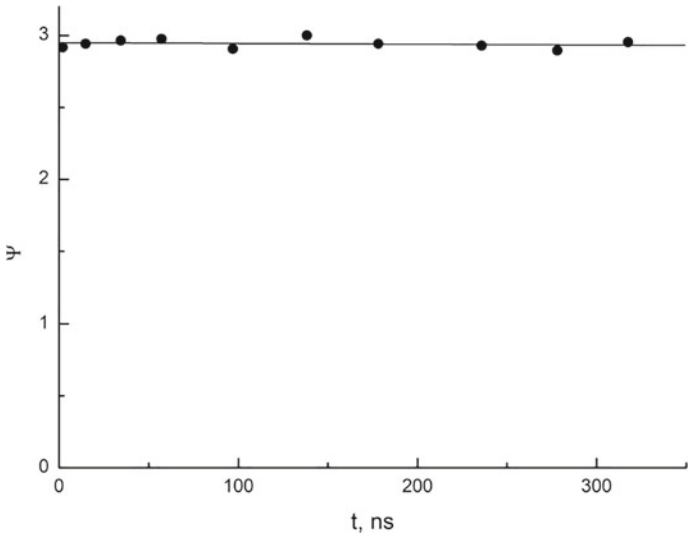

Fig. 7.5 The change in the optical density at the maximum of the F^+-band of absorption of the MgO (I) crystal after the irradiation pulse (j = 1000 A cm^{-2}; T = 300 K)

this component for MgO (II) crystals is probably due to the insignificant number of effective sites of fixation of interstitial oxygen ions in MgO (II).

Since the difference between MgO (I) and MgO (II) crystals lies in the different concentrations of impurity ions in them, the obtained results confirm our assumption about the effective role of impurity ions as centers of stabilization of interstitial oxygen ions.

7.3 Correlation in the Accumulation of F^+-Color Centers and Changes in the Charge State of Impurity Iron Ions in Single Crystals of Magnesium Oxide under Irradiation with a High-Current Electron Beam

The most promising study is the nature of changes in the concentration of F^+-color centers under the action of a high-current electron beam from the content of such impurity ions in crystals To test the assumption about the localization of interstitial oxygen ions in magnesium oxide crystals near impurity ions with an excessive positive charge.

However, growing a large batch of magnesium oxide crystals with specified concentrations of impurities is associated with great difficulties.

Therefore, we have used a different methodological technique. It is based on well-known fact of recharging impurity ions of transition metals under the action of

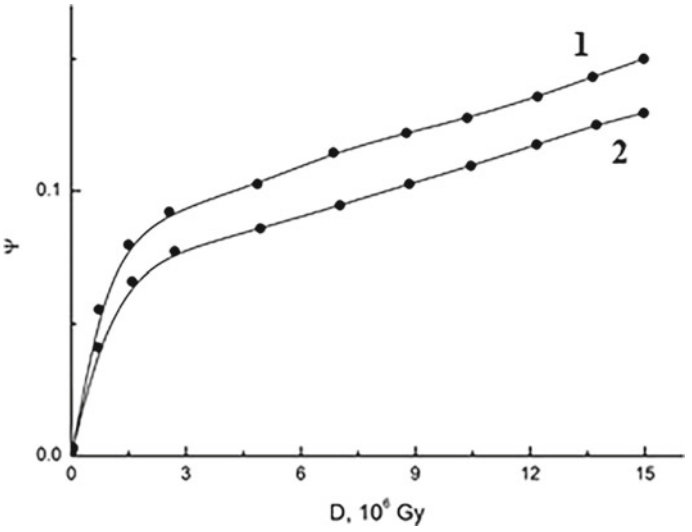

Fig. 7.6 The change in optical density in the maxima of the absorption bands of F + -band of absorption (1) and Fe^{+3} (2) with an increase in the absorbed radiation energy of accelerated electrons in MgO (I) ($j = 200$ A cm^{-2})

irradiation [10] and consists in comparing the kinetics of accumulation of F^+-centers in MgO (I) crystals and the process of transition of impurity ions Fe^{2+} to the Fe^{3+} state with an increase in the absorbed radiation energy of a high-current electron beam.

A thorough study of the optical absorption spectra of MgO (I) crystals has established that the change in the optical density in the maximum absorption bands of F^+-centers (4.92 eV) and Fe^{3+} (4.3 eV) occurs according to the same law with an increase in the absorbed radiation energy of accelerated electrons (Fig. 7.6).

As in the case of accumulation of F^+-centers the change in the charge state of impurity iron ions is carried out in two stages.

This type of kinetic curve of accumulation of F^+-centers in magnesium oxide crystals under the action of a high-current beam of accelerated electrons is due to the presence of two different sources of anionic vacancies in the crystals. F^+-centers are formed on pre-radiation vacancies at the first stage; they are formed on those created during irradiation at the second stage.

Let's take a closer look at the first section of the kinetic curve. Figure 7.7 shows the kinetics of changes in the optical density in magnesium oxide crystals in the absorption bands of F^+-centers and Fe^{3+} when irradiated with X-rays for this purpose.

A rapid increase in optical density and simultaneous achievement of stationary values are observed at the same course of kinetic curves.

X-rays do not create new anionic vacancies in magnesium oxide crystals and the formation of F^+-centers occurs on pre-radiation anionic vacancies. Further X-ray

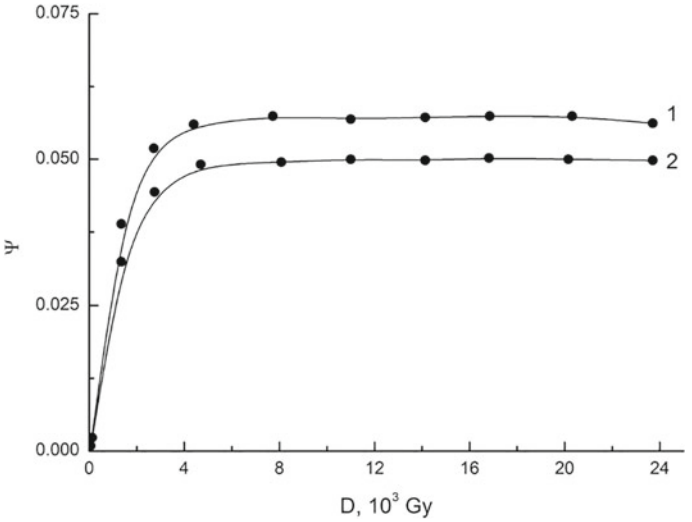

Fig. 7.7 Change in the optical density in the maxima of the absorption bands of F^+-centers (**1**) and Fe^{+3} (**2**) with increase in the absorbed energy of X-ray radiation in MgO (I)

irradiation of magnesium oxide crystals no longer leads to an increase in the optical density in the absorption band of F^+-centers at a steady level of occupancy of anionic pre-radiation vacancies.

Then, such a correlated behavior of changes in optical density in the absorption bands of F^+-centers and Fe^{3+} (exactly the same type of kinetic curves, simultaneous establishment of stationary values) with the time of X-ray irradiation allows to conclude that the transfer of impurity iron ions to the highest valence state during X-ray irradiation is limited by the presence of pre-radiation anionic vacancies in magnesium oxide crystals.

This relationship between the change in the concentrations of Fe^{3+} ions and pre-radiation anionic vacancies can be explained by the capture of the components of electron–hole pairs formed during irradiation on pre-radiation vacancies and Fe^{2+} ions with the formation of F^{+-}centers and Fe^{3+} ions, respectively. So, the first stage of the kinetic curve of the accumulation of F^+-centers in magnesium oxide crystals under the action of a high-current beam of accelerated electrons and the accumulation of F^+-centers during X-ray irradiation will be described by the scheme:

$$\begin{aligned} &\text{Irradiation} \rightarrow \overline{e} + p; \\ &V_a + \overline{e} \rightarrow F^{+*} \rightarrow F^+ + hv; \\ &\mathrm{Fe}^{2+} + p \rightarrow \mathrm{Fe}^{3+*} \rightarrow \mathrm{Fe}^{3+} + hv. \end{aligned} \tag{7.7}$$

Unused electron–hole pairs are annihilated and no accumulation of F^+-centers and Fe^{3+} is observed during further irradiation at a certain steady-state level of electron filling of pre-radiation anionic vacancies.

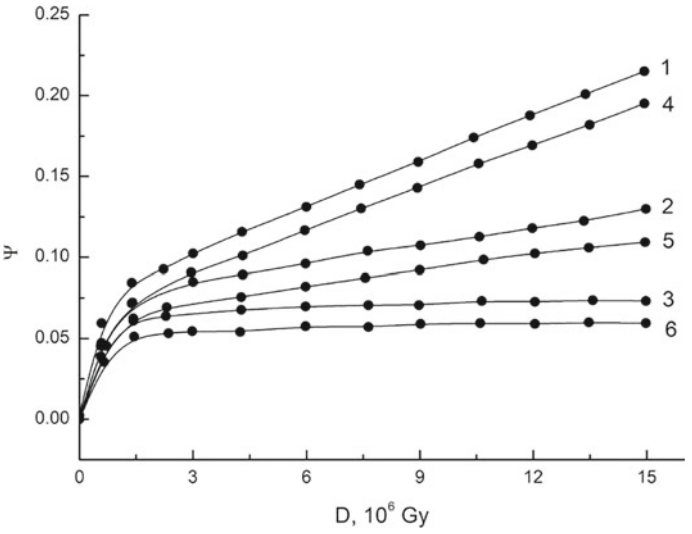

Fig. 7.8 The change in the optical density in the maxima of the absorption bands of the F^+-centers (1 ÷ 3) and Fe^{+3} (4 ÷ 6) in MgO (I) at different current densities of the accelerated electron beam, where 1 and 4 are 800 A cm^{-2}; 2 and 5 are 200 A cm^{-2}; 3 and 6 are 80 A cm^{-2}

We conducted study of the kinetics of changes in the optical density in the maxima of the absorption bands of F^+ centers and Fe^{3+} at different electron beam current densities (Fig. 7.8) to study the second stages in the kinetic curves of changes in the concentration of F^+-centers and Fe^{3+} with an increase in the absorbed energy of electron radiation.

It is established that an increase in the beam current density leads not only to an increase in the efficiency of the accumulation of F^+-centers and also causes a more efficient flow of the process of transition of impurity iron ions to the Fe^{3+} state.

The qualitatively identical type of kinetic curves is drawn to attention.

However, the second stage of the kinetic curve of the accumulation of F^+-centers is due to the formation of defects in the anion vacancies created during irradiation with a high-current electron beam. Probably, in this case, the efficiency of the $Fe^{2+} \rightarrow Fe^{3+}$ transition is determined by the concentration of Frenkel anion pairs created during irradiation.

Therefore, it seems feasible to explain the correlated behavior of the optical density in the maxima of the optical absorption bands of the F^+-color centers and Fe^{3+} at this stage of the kinetic curves according to the scheme:

1. Creation of a Frenkel anion pair in the form of F^+—O under the action of a high-current beam of accelerated electrons.
2. Migration of interstitial ions to impurity ions of transition metals Fe^{2+}.
3. Oxidation of impurity ions Fe^{2+} by interstitial oxygen ions to form a stable complex: Fe^{3+}- interstitial oxygen ion O^{2-}.

$$Fe^{2+} + O^{-} \rightarrow Fe^{3+}O^{2-} \tag{7.8}$$

A similar situation should be realized for other impurity ions of transition metals of the donor type in our opinion; we were able to establish this only for iron ions only, because only the parameters of the absorption band of Fe ions were reliably established.

7.4 Influence of the Calcination Temperature of Magnesium Oxide Crystals on the Accumulation of Radiation Defects of Them

We have studied the optical absorption spectra of MgO (I) crystals after calcining them in air for (20 ÷ 200) minutes at temperatures (300 ÷ 1750) K and rapid cooling on a massive copper substrate and after irradiation of crystals hardened by X-rays and in the same way by a high-current beam of accelerated electrons in order to verify the proposed explanation of the correlated change concentrations of Fe^{3+} and F^{+}-center ions with increase in the absorbed radiation energy of a high-current electron beam (Sect. 7.3).

We proceeded from the following considerations when setting up these experiments.

Molecular oxygen from the gas phase on the crystal surface dissociates into atoms and diffuses into the crystal volume at certain temperatures. The diffusion of oxygen through the crystal lattice will most likely be carried out in atomic form, since it is easier to realize it in such a neutral state. The oxygen atom diffuses through the lattice, occupies an anionic vacancy, while "healing" of pre-radiation anionic vacancies should be observed.

Impurity cation-substituting transition metal ions acquire an excessive positive charge during the "healing" of anionic vacancies. In particular, Fe^{2+} ions transition to the Fe^{3+} state. The subsequent increase in the temperature of the magnesium oxide crystal will lead to further oxidation of impurity ions of this type by interstitial oxygen atoms and the formation of a complex "Fe^{3+}-oxygen ion in the interstitial".

There are no pre-radiation interstitial oxygen ions in magnesium oxide crystals; pre-radiation anionic vacancies were created during the growth of single crystals due to the entry of corresponding inovalent impurity ions into the crystal lattice and the removal of part of the oxygen ions from regular lattice sites to the surface to preserve the electroneutrality of the crystal volume.

Therefore, a decrease in the concentration of pre-radiation anionic vacancies in magnesium oxide crystals during high-temperature air calcination will indicate the diffusion of oxygen from the gas phase into the crystal volume.

Let us consider the mechanism of accumulation of F^{+}-color centers on pre-radiation anionic vacancies and the transfer of impurity ions of Fe^{2+} to the Fe^{3+} state from these positions.

There should be fewer and fewer anionic pre-radiation vacancies for the formation of F^+-color centers on them due to the diffusion of oxygen from the gas phase; consequently, fewer and fewer unpaired hole components of electron–hole pairs are for the implementation of the $Fe^{2+} + p \rightarrow Fe^{3+}$ transition by irradiation* $\rightarrow Fe^{3+} +$ hv.

Therefore, an increase in the calcination temperature of magnesium oxide crystals, starting from a certain value, will lead to a decrease in the concentration of F^+-centers of the oxide and radiation-generated Fe^{3+} ions during subsequent X-ray irradiation. Subsequent X-ray irradiation should not lead to the formation of F^+-centers and to the transfer of Fe^{2+} ions to the Fe^{3+} state at temperatures corresponding to the filling of most of the pre-radiation anionic vacancies.

As our research has shown calcination of magnesium oxide crystals at temperatures (400 ÷ 1100) K does not change the optical absorption spectrum of the initial crystal (Fig. 7.9, curve 1).

The optical absorption spectra of crystals irradiated with X-rays after treatment in the specified temperature range coincide with the optical absorption spectrum of the X-ray-irradiated initial crystal (Fig. 7.9, curve 2).

A further increase in the crystal calcination temperature leads to an increase in the optical density in the absorption band of Fe^{3+} ions (4.3 eV) (Fig. 7.10).

Irradiation with X-rays of crystals calcined at (1200 ÷ 1300) K makes it possible to detect a decrease in additional optical absorption in the absorption bands of F^+-centers (4.92 eV) and Fe^{3+} ions (4.3 eV) with an increase in the calcination temperature (Fig. 7.11).

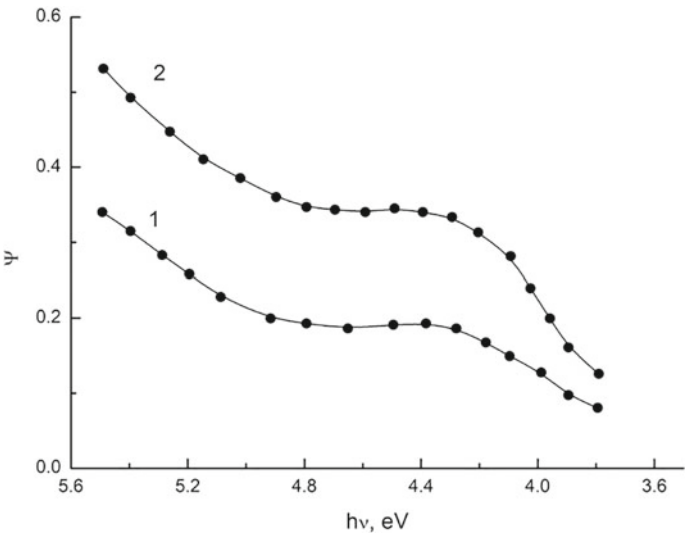

Fig. 7.9 Optical absorption spectra of an MgO (I) crystal with a thickness of 250 microns, where 1 is initial; 2 is irradiated with X-ray rays up to 5×10^4 Gy at 300 K

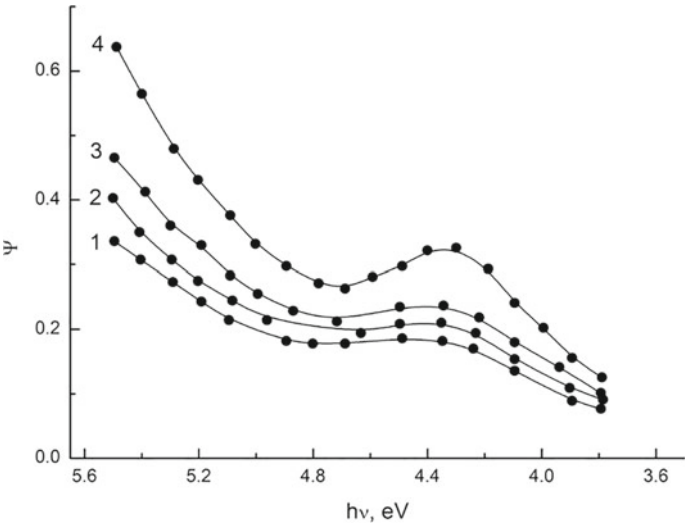

Fig. 7.10 Optical absorption spectra of an MgO (I) crystal with a thickness of 250 microns, where 1 is initial; 2, 3 and 4 are calcined for 20 min in the air at 1200 K; 1300 K and 1400 K, respectively

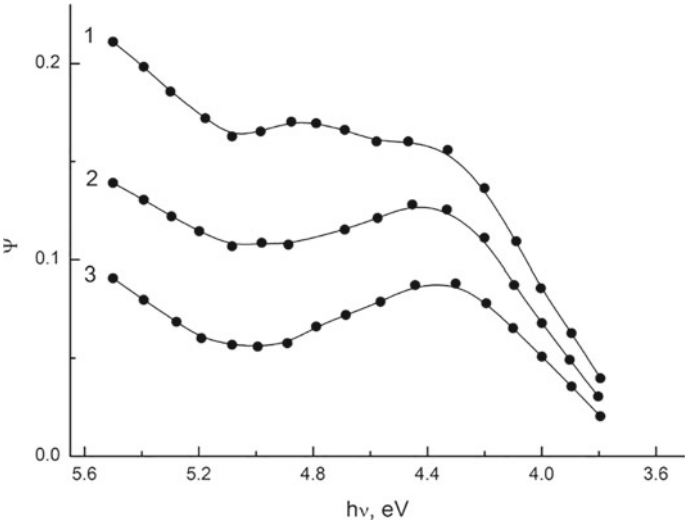

Fig. 7.11 Spectra of additional optical absorption of an MgO (I) crystal irradiated with X-rays up to 5×10^4 Gy, where 1 is initial; 2 and 3 are calcined for 20 min in air at 1200 K and 1300 K, respectively

Exposure of magnesium oxide crystals for 30 min at 1400 K under X–ray irradiation does not change the obtained optical absorption spectrum in the studied region (3.8 ÷ 5) eV, i.e., there are no processes of creating F^+-color centers and the $Fe^{2+} \rightarrow Fe^{3+}$ transition in such crystals, under the action of X-rays.

If, in fact an increase in the temperature of magnesium oxide crystals leads to a decrease in the number of pre-radiation anionic vacancies, then the sample is heated in air at 1400 K for 30 min (after which there is no accumulation of F^+-centers in magnesium oxide crystals under the action of X-rays) in the kinetic curve of accumulation of F^+-centers when irradiated with a high-current beam accelerated electrons will be missing the first stage, due to the filling of pre-radiation vacancies.

The results of the experiment are shown in Fig. 7.12.

The accumulation of F^+-color centers is described by a one-stage kinetic curve with an increase in the absorbed radiation energy of accelerated electrons after holding the magnesium oxide crystal at 1400 K for 30 min.

Thus, these results confirm our proposed scheme of accumulation of F^+-centers on pre-radiation anionic vacancies of magnesium oxide crystals.

If the scheme of accumulation of Frenkel pairs in magnesium oxide crystals under the action of a high-current electron beam is correct, then, there should be no accumulation of F^+-color centers and the transfer of impurity Fe^{2+} ions to the Fe^{3+} state when irradiated with a high-current electron beam in crystals hardened from temperatures above 1400 K. The overwhelming number of impurity iron ions will

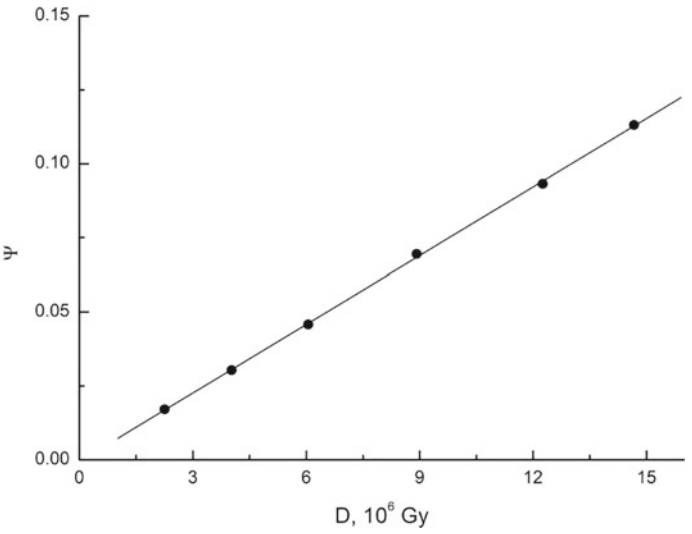

Fig. 7.12 The change in the optical density at the maximum of the F^+-band of absorption of the MgO (I) crystal when irradiated with a high-current electron beam (j = 600 A cm^{-2}) after pre-calcination in air for 30 min at 400 K

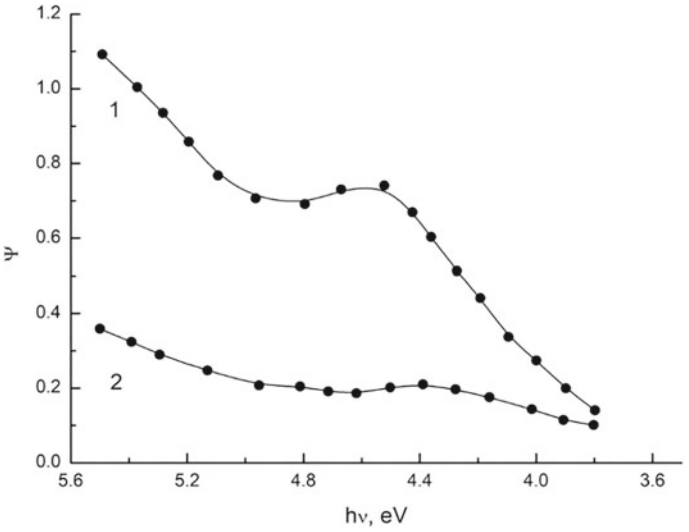

Fig. 7.13 Optical absorption spectra of MgO (I) crystals with a thickness of 200 microns, where 1 is initial; 2 is calcined in air for 50 min at 1500 K

be transferred to the Fe^{3+} state and blocked by interstitial oxygen ions from the gas phase; there will be no free iron ions to stabilize the interstitial oxygen ions created by irradiation in this case.

Indeed, the optical absorption spectrum of crystals calcined at 1750 K in air for 50 min does not change in the studied region (5.5 ÷ 3.8) eV when irradiated with a high-current electron beam as our experiments have shown (Fig. 7.13).

The creation of F^+-centers in MgO (I) when irradiated with a high-current electron beam at the concentrations given in Sect. 7.2 in non-calcined crystals should lead to noticeable changes in the optical absorption spectrum, since it equals 0.2 at $n_{F^+} = 3 \times 10 \times {}^{17}\ \mathrm{cm}^{-3}$ by Eq. (7.1).

The appearance of a new absorption band of ~ 4.6 eV in the optical absorption spectrum of a magnesium oxide crystal calcined at 1750 K is probably due to a shift in the short-wavelength region of the spectrum of the maximum absorption band of the impurity ion Fe^{3+} and due to perturbation of its environment by an interstitial oxygen ion from the gas phase.

7.5 Summary

The following conclusions can be drawn based on the results of this chapter.

1. The process of non-shock generation of anionic vacancies in magnesium oxide crystals at high radiation exposure is fundamental.

2. Impurity ions of transition metals, in particular, iron, which acquire an excessive positive charge during irradiation, serve as the most effective places for fixing interstitial oxygen ions created in MgO when irradiated with a high-current beam of accelerated electrons of subthreshold energy.
3. The detected new absorption band with a maximum of about 4.3 eV in the optical absorption spectrum of magnesium oxide crystals subjected to high-temperature calcination in air is probably due to the complex: impurity ion Fe3+-interstitial oxygen ion.

Chapter 8
Experimental Study of Interstitial Oxygen Ions in Magnesium Oxide Crystals

Contents

As is known, the processes of radiation accumulation of Frenkel anionic pairs in ionic crystals are experimentally studied by registering defects created with the participation of vacancies and interstitial ions.

Radiation disturbances of the anionic sublattice in silk-haloid crystals are reliably manifested by optical and EPR measurements, which was the key to their in-depth and comprehensive study.

A less favorable situation develops when studying radiation defect formation in MgO. Currently, defects with a vacancy nature (F^+ and F-centers) are reliably recorded. The works of previous years indicate that the methods of absorption and EPR spectroscopy are not very effective for detecting interstitial oxygen ions in MgO.

In this regard, the search and use of new methods for the registration of interstitial components of Frenkel anionic pairs in magnesium oxide crystals are extremely important for the radiation physics of alkali-earth metal oxides in general and in particular for solving infusion problems.

We came to the conclusion that photoluminescence and positron annihilation methods could be promising in this regard based on the analysis of the literature data.

This chapter presents the results of studies aimed at applying the above methods to identify interstitial oxygen ions in MgO crystals irradiated with a high-current beam of electrons of subthreshold energy.

Methodical task is supposed to be solved by compiling optical absorption spectra, photoluminescence spectra and correlation curves of annihilation radiation

A. Surzhikov and E. Lysenko, *Creation and Accumulation of Radiation Defects in Single Crystals of Magnesium Oxide*, https://doi.org/10.1007/978-3-031-60207-8_8

of positrons for magnesium oxide crystals irradiated with a high-current beam of electrons of subthreshold energy, and for crystals irradiated with X-rays and high-energy protons.

Single crystals of MgO (I) were used as objects of research (Table 2.1), since the accumulation of F^+-color centers does not occur in MgO (II) under the action of a high-current electron beam of subthreshold energy as was shown above.

8.1 Investigation of Photoluminescence in Magnesium Oxide Crystals Irradiated by a High-Current Electron Beam

In 1977, the authors discovered a change in the spectral composition of the cathodoluminescence of magnesium oxide crystals during the implantation of Mg^{2+} and O^{2-} ions alternately [130]. It was found that the introduction of O^{2-} ions into the MgO lattice enhances the glow in the long-wavelength region of the spectrum (~ 1.7 eV), while the introduction of magnesium ions leads to the appearance of an additional component of luminescence in the short-wavelength part of the spectrum (~2.8 eV).

Since the efficiency induced in the crystal during ion implantation does not significantly depend on the type of ion being implanted, it can be assumed that the detected changes in the luminescence spectra are associated with defects that include interstitial ions of acid and magnesium.

It seems useful to study the luminescent characteristics and single crystals of magnesium oxide exposed to irradiation assuming, as a working hypothesis that defects consisting of interstitial oxygen ions are responsible for the glow in the red region of the spectrum.

We have conducted a study of the spectral composition of the photoluminescence of MgO (I) crystals irradiated by a high-current electron beam and X-rays. Luminescence was excited by light from the F-band absorption region at a sample temperature of 300 K.

The results of the experiment are shown in Fig. 8.1.

Photoluminescence spectra were obtained on the same magnesium oxide crystal. Initially, the sample was exposed to X-rays; photoluminescence was studied. Then the same sample was additionally irradiated with a high-current beam of accelerated electrons; the photoluminescence spectrum was re-measured after it. Such procedure allows to identify the effects associated with the impact of a high-current beam of accelerated electrons, in our opinion.

It is known that radioactive transitions in Cr^{3+} ions make a significant contribution to the red luminescence of magnesium oxide crystals.

Luminescence in this region of the spectrum is observed in crystals exposed to X-rays due to it, probably (Fig. 8.1a). The maximum glow is at 1.7 eV; the width at half the height is 0.30 eV.

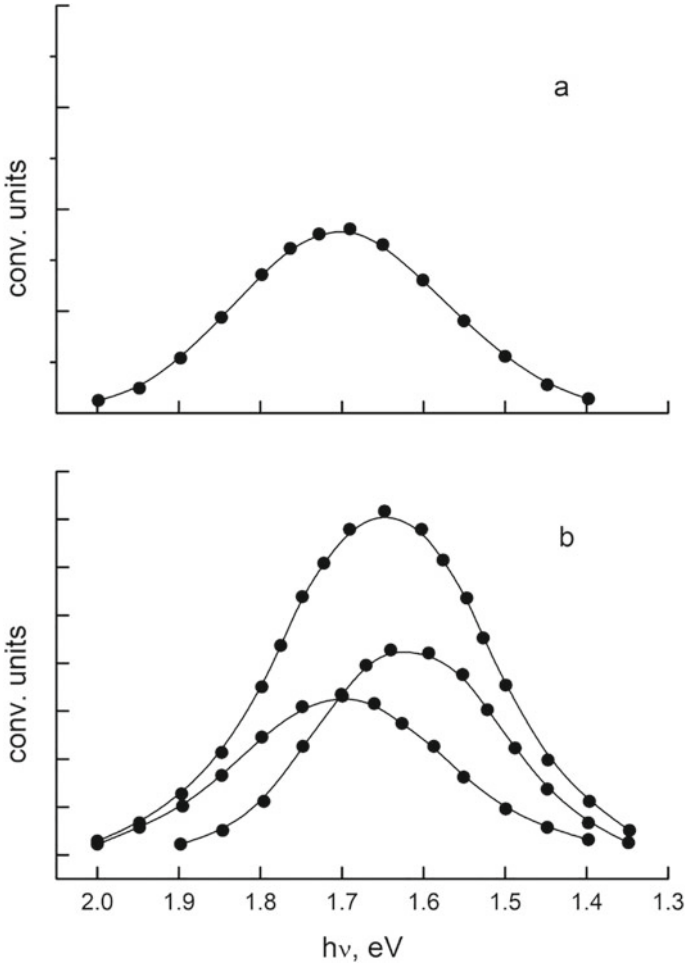

Fig. 8.1 Photoluminescence spectra of the MgO (I) crystal, where a is irradiated with X-rays up to 5×10^4 Gy; b is irradiated with a high-current electron beam ($j = 1000$ A • cm^{-2}) up to 15×10^6 Gy (curve 1) and the result of decomposition into Gaussian components (curves 2 and 3)

The maximum of the luminescence band shifts to a longer wavelength region of the spectrum in comparison with X-ray samples in magnesium oxide crystals irradiated with a high-current beam of accelerated electrons (Fig. 8.1b). The glow strip has a non-elementary appearance. Decomposition of it into Gaussian components (curves 2 and 3) showed the presence of a new luminescence band, compared with the photoluminescence spectrum of X-ray crystals. The maximum of this glow band is located at 1.62 eV; the width at half the height is 0.26 eV. The parameters of the other band coincide with those observed in X-ray crystals.

The detected difference between the photoluminescence spectra of MgO irradiated by a high-current beam of accelerated electrons and X-rays can be explained by the creation of new intrinsic radiation defects in the anionic sublattice of crystals, magnesium oxide under powerful excitation.

Therefore, the luminescence band with a maximum at 1.62 eV, appearing in the photoluminescence spectrum of magnesium oxide crystals irradiated with a high-current electron beam and absent in the spectra of X-ray samples, it should include to intrinsic defects of the crystal lattice of radiation origin.

This assumption is confirmed by the dependence of the luminescence intensity in the red region of the photoluminescence spectrum of magnesium oxide crystals on the absorbed radiation energy of X-rays and a high-current beam of accelerated electrons.

The intensity of the glow in the band with a maximum at 1.7 eV reaches saturation a few minutes after the start of irradiation of magnesium oxide crystals with X-rays, which confirms the responsibility for this glow of pre-radiation defects.

The luminescence intensity in the band with a maximum at 1.62 eV increases with an increase in the absorbed radiation energy of a high-current electron beam (Fig. 8.2).

A linear correlation with an increase in the absorbed radiation energy of a high-current electron beam should be observed in the case of responsibility for this band in the photoluminescence spectrum of magnesium oxide crystals of radiation defects,

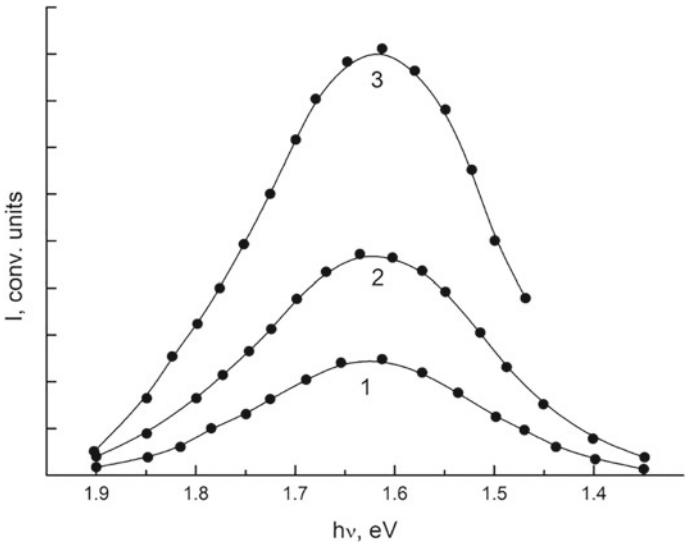

Fig. 8.2 The change in the luminescence intensity at 1.62 eV in MgO (I) with an increase in the absorbed radiation energy of a high-precision electron beam (j = 1000 A • cm^{-2}), where 1 is 2 × 10^6 Gy; 2 is 6 × 10^6 Gy; 3 is 13 × 10^6 Gy

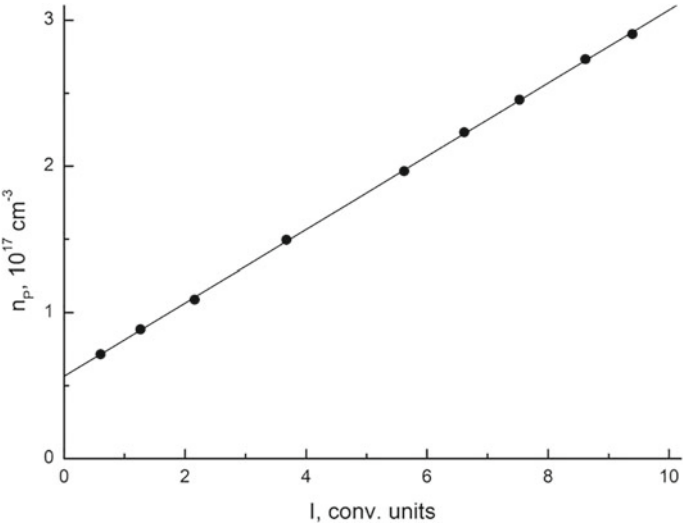

Fig. 8.3 The change in the concentration of F^+-centers and the intensity of luminescence at 1.62 eV in MgO (I) with an increase in the absorbed energy of electron radiation (j = 1000 A •cm^{-2})

which include an interstitial oxygen ion, between changes in the concentrations of F^+-centers (complementary to interstitial oxygen ions) and these defects.

Figure 8.3 shows the dependence of the change in the concentration of F^+-centers and the intensity of the glow in the band with a maximum at 1.62 eV with an increase in the absorbed radiation energy of a high-current electron beam.

There is a proportionality between the change in the concentration of F^+ centers and the intensity of the luminescence band with a maximum at 1.62 eV as follows from this figure.

The fact that the line on the graph does not pass through the origin is explained by the formation of F^+-centers on pre-radiation anionic vacancies at low values of the absorbed radiation energy. A certain number of F^+-centers are already present in the crystals of magnesium oxide; there are no interstitial oxygen ions yet at the same time.

Heating of magnesium oxide crystals irradiated by a high-current electron beam to 700 K anneals the F^+-centers and leads to the disappearance of luminescence in the band with a maximum at 1.62 eV. Subsequent X-ray irradiation does not restore it.

The correlated change in the concentration of F^+-centers and the intensity of the glow in the band with a maximum at 1.62 eV gives reason to believe that defects are responsible for the glow band with a maximum at 1.62 eV in the MgO photoluminescence spectrum, which include interstitial oxygen ions with an increase in the absorbed radiation energy of a high-current electron beam and the temperature of subsequent annealing.

This point of view is confirmed by experiments in [200], in which, similar results were obtained and a similar conclusion was made when studying the spectral composition of photoluminescence of magnesium oxide crystals irradiated with high-energy protons and X-rays.

Thus, we associate with the realization of a non-elementary process of formation of intrinsic interstitial radiation defects of the crystal lattice (oxygen ions) at high excitation densities the anomalies detected in the photoluminescence spectra of magnesium oxide crystals irradiated with a high-current electron beam of subthreshold energy, compared with the photoluminescence spectra of X-ray crystals.

8.2 Study of Positron Annihilation in Single Crystals of Magnesium Oxide

The most likely centers of positron capture in solids are negatively charged defects.

Since the appearance of new positron annihilation centers in the material should lead to changes in the shape of the annihilation photon angular distribution curve (ADAPh), it seems possible for us to obtain information about the radiation generation of interstitial oxygen ions in magnesium oxide crystals by analyzing the shape of ADAPh curves in irradiated and non-irradiated samples.

ADAPh curves were studied in the initial MgO (I) crystals irradiated with high-energy protons, X-rays, a high-current beam of electrons of subthreshold energy and after high-temperature annealing of crystals in air to verify the proposed assumption.

It is known that Frenkel anion pairs in magnesium oxide crystals are generated when irradiated with high-energy particles and are not created when excited by X-rays [10, 95, 99].

Chapter 7 shows the possibility of creating oxygen ions in the interstitial crystal lattice MgO due to the diffusion of the latter from the gas phase into the crystal volume during high-temperature calcination of samples in air.

Therefore, it is possible to distinguish the changes inherent in interstitial oxygen ions in the angular distribution of the annihilation radiation of positrons by comparing the ADAPh curves for magnesium oxide crystals irradiated with high-energy protons, X-rays and calcined in air.

The presence of changes caused by interstitial oxygen ions in the ADAPh curve for magnesium oxide crystals irradiated with a high-current electron beam of subthreshold energy will indicate the non-simultaneous generation of interstitial oxygen ions in MgO at high excitation densities.

Figure 8.4 shows the ADAPh curves normalized by one area for the initial MgO (I) crystal and subjected to the above influences.

The parameters of the curves (width at half the height W and the relative change in the counting rate at the maximum of the curves) are given in Table 8.1.

ADAPh was converted into difference curves of the pulse distribution of electron–positron pairs according to the method proposed in [149, 150] and based on the model

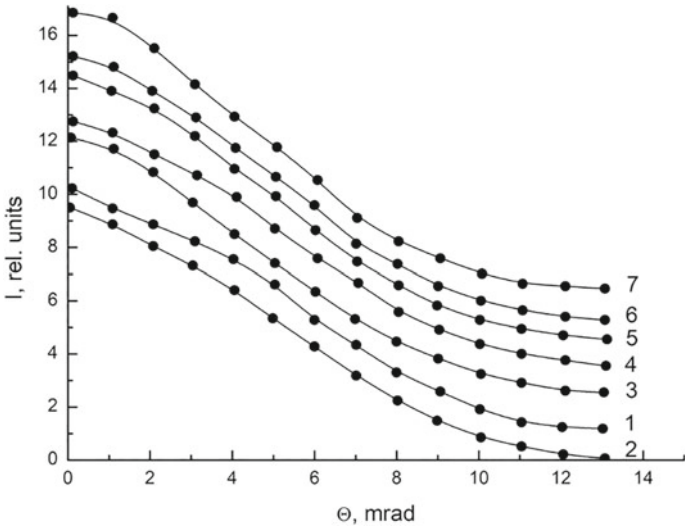

Fig. 8.4 Normalized per area ADAPh curves in MgO (I), where 1 is initial; 2 is irradiated with X-rays up to 4.2×10^4 Gy; 3 and 4 are irradiated with protons up to 7.2×10^7 Gy and 2×10^7 Gy; 5 is calcined in air at 1750 K for 35 min; 6 and 7 are irradiated with a high-current electron beam up to 2.2×10^6 G and 15×10^6 G

Table 8.1 Parameters of the angular distribution curves of annihilation photons normalized by one area in magnesium oxide crystals subjected to various influences

Impact	W	1%
The initial crystal	12.2	0
After irradiation with high-energy protons at a sample temperature of 300 K (E = 10 meV; j = 0.04 μA · cm^{-2})		
(a) 2×10^7 Gy;	11.8	2.2
(b) 7.2×10^7 Gy	10.8	5.4
After irradiation with a high-current beam of accelerated electrons (E = 0.135 meV; j = 1000 A · cm^{-2})		
(a) 2.2×10^6 Gy;	2.2	6.5
(b) 15×10^6 Gy	10.0	9.9
After 35 min of warming up and rapid cooling on a copper substrate at 1750 K	10.6	9.8
After X-ray irradiation		
(a) 1.4×10^3 Gy;	12.0	2.8
(b) 4.2×10^4 Gy	12.0	2.8

of positron annihilation in quasi-free collisions with ion electrons matrices of matter for the analysis of experimental curves.

Processing the angular distribution curves of annihilation gamma quanta for defective substances gives

$$\tilde{n}(\xi) = n(\xi) + n_D(\xi) \tag{8.1}$$

where $\tilde{n}(\xi)$ is the pulse density of electrons in the matrix of matter, which is restored according to experimental data for the initial crystal; $n_D(\xi)$ is the pulse distribution of electron–positron pairs of positron and positronium states localized in the region of defects.

Thus, $n_D(\xi)$ can be determined comparing $n(\xi)$ and $\tilde{n}(\xi)$.

Figure 8.5 shows the difference pulse distribution of electron–positron pairs in the defect region for magnesium oxide crystals irradiated with X-rays; Fig. 8.6 shows it for a crystal irradiated with high-energy protons.

A comparison of the data presented in the figures shows that there are differences in the difference pulse distribution of electron–positron pairs for these two crystals.

There is an additional band with a maximum = 5.0 in the pulse distribution for a magnesium oxide crystal irradiated with high-energy protons (Fig. 8.6) in comparison with an X-ray crystal (Fig. 8.5).

Irradiation of magnesium oxide crystals with high-energy protons, unlike X-rays, leads to the accumulation of their own radiation defects of the crystal lattice [10, 104]. Therefore, an additional band with a maximum at = 5.0 in the pulsed distribution

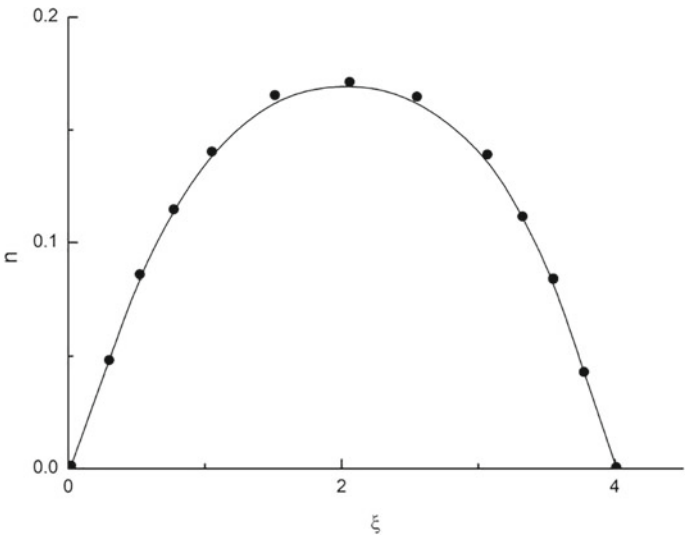

Fig. 8.5 Difference pulse distribution of electron–positron pairs in an MgO (I) crystal irradiated with X-rays up to 4.2×10^4 Gy

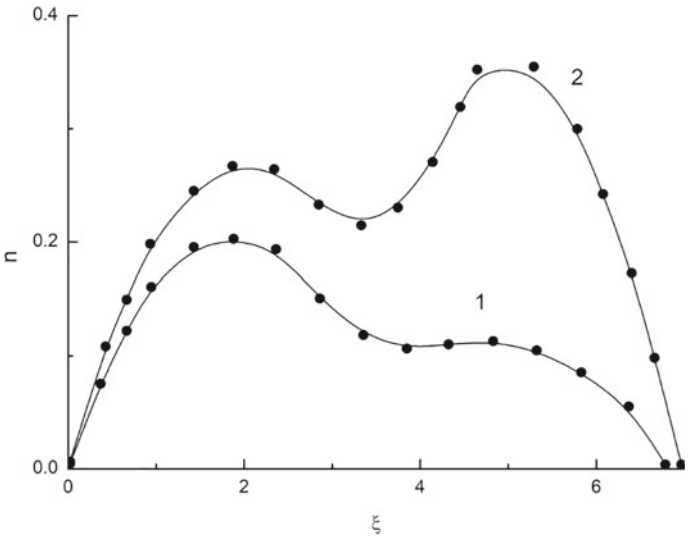

Fig. 8.6 Difference pulse distribution of electron–positron pairs in MgO (I) crystal irradiated with protons, where 1 is 2×10^4 Gy; 2 is 12×10^7 Gy

of electron–positron pairs in proton-irradiated crystals (Fig. 8.6), compared with X-ray-irradiated crystals (Fig. 8.5), is due to its own radiation defects.

There is an additional band with a maximum $\xi = 5.0$ in the pulse distribution for a magnesium oxide crystal irradiated with high-energy protons (Fig. 8.6) in comparison with an X-ray crystal (Fig. 8.5).

Irradiation of magnesium oxide crystals with high-energy protons, unlike X-rays, leads to the accumulation of their own radiation defects of the crystal lattice [10, 104]. Therefore, an additional band with a maximum at $\xi = 5.0$ in the pulsed distribution of electron–positron pairs in proton-irradiated crystals (Fig. 8.6), compared with X-ray-irradiated crystals (Fig. 8.5), is due to its own radiation defects.

Frenkel cationic and anionic pairs, of which cationic vacancies and interstitial oxygen ions can act as centers of annihilation of positively charged positrons, are the most likely intrinsic radiation defects in magnesium oxide crystals formed under the action of a stream of high-energy protons.

If cationic vacancies are responsible for the appearance in the pulse distribution of electron–positron pairs of a band with a maximum at $\xi = 5.0$, then the intensity in this band $n_D(\xi)$ should not increase with increase in the temperature of calcination of magnesium oxide crystals in air, since it has been established that such treatment does not lead to the creation of cationic vacancies [46, 111, 138].

The experimental results (Fig. 8.7) indicate the opposite; increase in the calcination temperature of magnesium oxide crystals in air leads to increase in the intensity of the band with a maximum at $\xi = 5.0$ in the pulsed distribution of electron–positron pairs in these crystals.

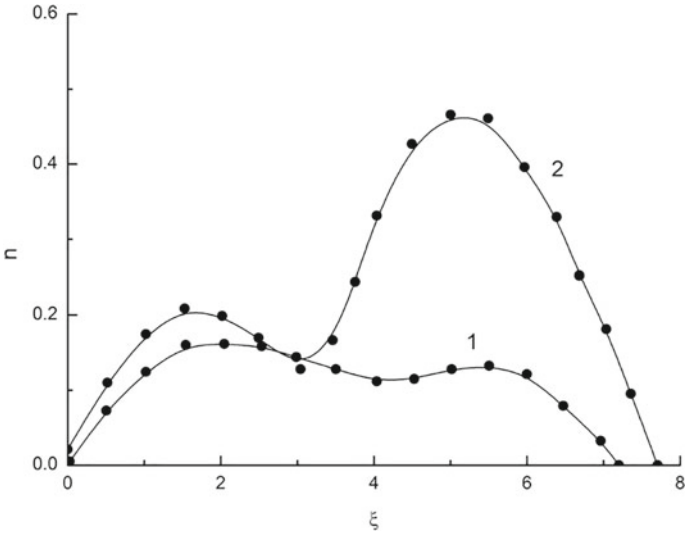

Fig. 8.7 Difference pulse distribution of electron–positron pairs in MgO (I) crystal calcined at 1400 K (**1**) and 1750 K (**2**) for 35 min in air

Thus, the appearance in the pulse distribution of electron–positron pairs of a band with a maximum at $\xi = 5.0$ in magnesium oxide crystals is not associated with cationic vacancies, but probably with interstitial oxygen ions.

The optical absorption spectra of MgO (I) crystals under irradiation with high-energy protons were studied to verify this assumption in parallel with the study of URAF curves.

A correlation has been established between the change in the band with a maximum at $\xi = 5.0$ (Fig. 8.6) and the optical density in the absorption band of F^+-centers (Fig. 6.3) with an increase in the absorbed energy of proton radiation.

The appearance of a band with a maximum at $\xi = 5.0$ is not registered in the pulse distribution of electron–positron pairs at low values of the absorbed radiation energy, when F^+-centers are formed on pre-radiation anionic vacancies and the concentration of Frenkel anionic pairs is extremely small. The pulse distribution in this case is similar to that shown in Fig. 8.5 for an X-ray crystal of magnesium oxide.

Heating of magnesium oxide crystals in air for 15 min at a temperature of 700 K completely anneals the F^+-centers after irradiation with high-energy protons. At the same time, a band with a maximum at $\xi = 5.0$ disappears in the pulse distribution of electron–positron pairs. Subsequent irradiation of the crystal with X-rays does not lead to its restoration.

Since the F^+-color centers are complementary to interstitial oxygen ions, it is possible to make an assumption about the responsibility for the band with a maximum at $\xi = 5.0$ in the pulsed distribution of electron–positron pairs of intrinsic radiation defects, which include interstitial oxygen ions.

The appearance of band with a maximum at $\xi = 5.0$ and increase of its intensity with an increase in the calcination temperature should be observed, since such treatment leads to the creation of an excessive amount of interstitial oxygen ions in the crystal lattice (Chap. 7) in case of correct conclusion in the pulsed distribution of electron–positron pairs for a magnesium oxide crystal calcined in air at high temperature.

The results of the experiment are shown in Fig. 8.7.

The appearance in the pulse distribution of electron–positron pairs of a band with a maximum at $\xi = 5.0$ (curve 1) and an increase in the intensity of this band with an increase in the calcination temperature to 1750 K (curve 2) were found for magnesium oxide crystals after calcination in air at 1400 K.

It can be concluded that the band with a maximum at $\xi = 5.0$ the pulse distribution of electron–positron pairs of magnesium oxide crystals is caused by a defect, which includes an interstitial oxygen ion based on the above.

A comparison of the pulse distributions of electron–positron pairs in magnesium oxide crystals irradiated with protons (Fig. 8.6) and a high-current electron beam (Fig. 8.8) allows to establish their qualitative similarity. The pulse distribution of electron–positron pairs is similar to the one shown in Fig. 4.5 for X-ray crystals at low values of absorbed energy, when the formation of F^+-centers is carried out on pre-radiation vacancies; a band appears in the pulsed distribution of electron–positron pairs at $\xi = 5.0$, the intensity of which increases with a further increase in the absorbed radiation energy at large values of the absorbed radiation energy (Fig. 8.8).

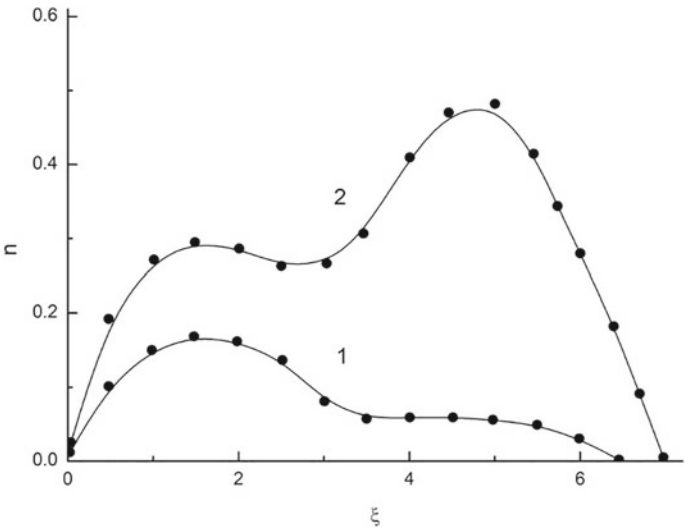

Fig. 8.8 Difference pulse distribution of electron–positron pairs in an MgO (I) crystal irradiated with electrons (j = 1000 A cm^{-2}), where 1 is 2.2 × 10^4 Gy; 2 is 15 × 10^6 Gy

A correlation has been established in the variation with an increase in the absorbed radiation energy, the absorption coefficient in the F^+-band (Fig. 6.4) and the intensity of the band with a maximum at = 5.0 in the pulsed distribution of electron–positron pairs both for magnesium oxide crystals irradiated with high-energy protons and for crystals irradiated with a high-current electron beam.

Moreover, a correlation is found in the rate of increase in the values of these two quantities with an increase in the current density of the accelerated electron beam. The appearance of a band with a maximum at $\xi = 5.0$ was not registered in the pulse distribution of electron–positron pairs at beam densities less than ~ 100 A cm^{-2}, at which there is no accumulation of Frenkel anionic pairs in magnesium oxide crystals (Chap. 6).

Heating magnesium oxide crystals in air for 15 min at a temperature of 700 K after irradiation with a high-current electron beam, completely anneals the F^+-centers. At the same time, the band with a maximum at $\xi = 5.0$ disappears in the pulse distribution of electron–positron pairs. Subsequent X-ray irradiation of the crystal does not lead to its restoration.

Thus, the appearance of a band with a maximum at $\xi = 5.0$ in the pulsed distribution of electron–positron pairs for magnesium oxide crystals is due to defects that include interstitial oxygen ions. The presence of this band in the pulsed distribution of electron–positron pairs for crystals irradiated with a high-current beam of electrons of subthreshold energy indicates the non-elementary generation of interstitial oxygen ions in magnesium oxide crystals at high excitation densities.

8.3 Summary

The following conclusions can be drawn based on the results of this chapter.

The defects, which include interstitial oxygen ions, are responsible for the glow in the band with a maximum at 1.62 eV in the MgO photoluminescence spectrum and for the band with a maximum at = 5.0 in the pulsed distribution of electron–positron pairs.

The appearance of these effects in magnesium oxide crystals irradiated with a high-current beam of electrons of subthreshold energy indicates a non-elementary mechanism of generation of interstitial anions in MgO at high densities of radiation exposure.

Appendix

We would especially like to note that the fundamental results on the characteristics of radiation defect formation in radiation-resistant materials at high densities of radiation exposure, presented in this publication, were effectively the basis for a large amount of applied research in radiation materials science.

The use of the aforementioned high densities of radiation exposure in combination with high temperature fields made it possible to establish and study a number of fundamentally new applications, which we have identified as a separate class—radiation-thermal effects and processes in inorganic materials.

This includes high-temperature radiation-stimulated diffusion, acceleration of processes of stimulation and unusual transformation of the phase composition of materials and their structural parameters, and much more [150–176].

A. Surzhikov and E. Lysenko, *Creation and Accumulation of Radiation Defects in Single Crystals of Magnesium Oxide*, https://doi.org/10.1007/978-3-031-60207-8

References

1. Whited, R.C., Walker, W.C.: Exciton spectrum of CaO and MgO. Phys. Rev. Lett. **22**(26), 1428–1430 (1969)
2. Levin, A.A., Syrkin, Y.A.K., Dyatkina, M.E.: The problem of monoatomic multiply charged ions and the nature of chemical bonds in inorganic crystals. Adv. Chem. **XXXVIII**(2), 193–221 (1969)
3. Sibley, W.A., Chen, V.: Radiation damage in MgO. Phys. Rev. **160**(3), 712–716 (1967)
4. Marfuyain, A.C.: Introduction to Mineral Physics. Nedra, Moscow (1974)
5. Roessler, D.M., Walker, W.C.: Electronic spectrum and ultraviolet optical properties of crystalline MgO. Phys. Rev. **159**(3), 733–738 (1967)
6. Ermoshkin, A.L., Lovchikov, B.A.: Proceedings of the third all-union meeting on radiation physics and chemistry of ionic crystals, Latvia, Riga 119–120 (1975)
7. Pantelides, S.T., Mickich, D.J., Kunz, AB: Electronic structure and properties of MgO. Phys. Rev. **10**(12), 5203–5212 (1974)
8. Fomichev, V.A., Zinkina, T.M., Zhukova, I.I.: Study of the energy structure of TgO using ultrasoft X-ray spectroscopy. Russ. Phys. J. **10**(10), 3073–3081 (1968)
9. Chen, Y., Williams, R.T., Sibley, W.A.: Defect luminescence of the irradiated MgO. J. Lumin. **1–2**, 633–640 (1970)
10. Henderson, B, Wertz, J.E.: Defects in the alkaline earth oxides. Adv. Phys. **17**(70), 749–855 (1968)
11. Kalder, K.L., Kyarner, T.N., Lushchik, Ch.B., Malysheva, A.V.: Short-wave luminescence of MgO crystals. J. Appl. Spectrosc. **25**(4), 639–644 (1976)
12. Valbis, Y.A., Rachko, Z.A., Springis, M.E.: Edge luminescence of single MgO crystals. Sci. Notes Latvian State Univ. **245**(4), 122–128 (1975)
13. Kuusman, I.L., Fel'dbah, E.H.: Edge cathodoluminescence of crystals in the VUF region of the spectrum. Russ. Phys. J. **23**(2), 461–466 (1981)
14. Rachko, Z.A.: Short-wave luminescence of magnesium oxide. The thesis, Latvia, Riga (1980)
15. Annenkov, Yu.M., Pritulov, A.M.: Thermally stimulated conductivity of MgO crystals irradiated with protons. Russ. Phys. J. **9**, 132–134 (1981)
16. Harding, BC, Price, D.M., Mortlok, AL.: Cation self-diffusion in single crystal MgO. Phil. Mag. **23**(182), 399–408 (1971)
17. Harding, B.C., Price, D.M.: Cation self-diffusion in MgO up to 2350 °C. Phil. Mag. **26**(1), 253–260 (1972)
18. Harding, B.C.: The energy of formation of a Schottky defect in MgO. Phys. Lett. A **40**(3), 227–228 (1972)

A. Surzhikov and E. Lysenko, *Creation and Accumulation of Radiation Defects in Single Crystals of Magnesium Oxide*, https://doi.org/10.1007/978-3-031-60207-8

19. Hughes, A.E., Henderson, B.: Colour Center in Simple Oxides. In: Point Defects in Solid. Springer US (1972)
20. Fench, A.J., Duck, M.J.: Radiation damage in oxides. I. Defect formation in MgO. J. Phys. C Solid State Phys. **6**(7), 1134–1147 (1973)
21. Glass, A.M.: Reactions between vacancies and impurities in MgO. I. Cr^{+3}—ion impurities. J. Chem. Phys. **469**(6), 2080–2091 (1967)
22. Lushchik, Ch.B., Vitol, I.K., Elango, M.A.: Decay of electronic excitations into radiation defects in ionic crystals. Usp. Fizicheskih Nauk **122**(2), 223–251 (1977)
23. Lushchik, C.B.: Intrinsic Electronic Excitations and Defects of Ionic Crystals. Academy of Sciences of the Estonian SSR, Institute of Physics, Estonia, Tartu (1978)
24. Bete, G.A., Ashkin, Yu.: Passage of Radiation Through Matter, pp. 141–297. Foreign Literature Publishing House, Moscow (1955)
25. Konobeevekij, E.T.: Effect of Radiation on Material. Atomizdat, Moscow (1967)
26. Mackrodt, W.C., Stewart, R.F.: Defect properties of ionic solids. I. point defects at the surfaces of face-centred cubic crystals. J. Phys. C Solid State Phys. **10**(9), 1431 (1977)
27. Roux, A., Elston, J.: Energie des fefants crees dans MgO par irradiation neutronique. Comptes Rendus de l'Académie des Sci. **270**, 505–508 (1970)
28. Wertz, J.E., Auzins, P., Weeks, R.A., Silsbee, R.H.: Electron spin resonance of F-centres in magnesium oxide; confirmation of the spin of magnesium-25. Phys. Rev. **107**(6), 1535–1537 (1957)
29. King, R.D., Henderson, B.: Zero phonon lines unaxial stress in magnesium oxid. Proc. Phys. Soc. **89**(563), 153–164 (1966)
30. Norgett, M.J.: The electronic levels of the F_t centre in MgO and CaO. J. Phys. C Solid State Phys. **4**(11), 1289–1298 (1971)
31. To, K.-C., Stoneham, A.M., Henderson, B.: Electron spin resonance from a vacancy pair centre in MgO. Phys. Rev. **181**(3), 1237–1240 (1969)
32. Henderson, B.: Optical pumping cycle of exchange-coupled F^+-centre Pairs in MgO and CaO. J. Phys. C Solid State Phys. **9**(11), 2185–2195 (1967)
33. Wertz, J.E., Saville, G.S., Hall, L., Auzins, P.: Point defects in Magnezium Oxid. Proc. Br. Ceram. Soc. **1**, 59–70 (1964)
34. Henderson, B., King, R.D.: Dose dependence of F-centre production by fast neutrons in magnesium oxide. Phil. Mag. **13**, 1149–1153 (1966)
35. Kemp, J.C., Ziniker, W.M., Glass, J.A.: Microwave-sensitive faraday rotation in the MgO F-band. Phys. Lett. **22**(1), 37–39 (1966)
36. Bessent, R.G., Cavenett, B.C., Hunter, I.C.: Faraday rotation studies of F-centres in Alkaline Earth Oxides. J. Phys. Chem. Solids **29**(9), 1523–1530 (1968)
37. Chen, Y., Sibley, F.D., Weeks, R.A., Hensley, E.B.: Negative-ion vacancies in irradiated MgO. J. Phys. Chem. Solids **29**(6), 863–865 (1968)
38. Kemp, J., Neeley, V.: Wave function for F-centres in MgO. Phys. Rev. **132**(1), 215–223 (1963)
39. Wood, R.F., Wilson, T.M.: Electronic structure of the F-centre in CaO and MgO. Solid State Commun. **16**(5), 545–548 (1975)
40. Kappers, L.A., Kroes, R.L., Hensley, E.B.: F^+ and F-centres in magnesium oxide. Phys. Rev. B **1**(10), 4151–4157 (1970)
41. Kemp, J.C., Ziniker, W.M., Hensley, E.B.: Evidence for the photoreaction F^+
42. Chea, Y., Koiopus, J.L., Sibley, W.A.: Luminescence of the F^+-centre in MgO. Phys. Rev. **186**(3), 865–870 (1969)
43. Chen, Y., Williams, R.T., Sibley, W.A.: Defect cluster centres in MgO. Phys. Rev. **182**(3), 960–964 (1969)
44. Wertz, J.E., Auzins, P., Griffithg, J.H.E., Orton, J.W.: Spin resonance studies of defects in Magnesium Oxide. Discuss. Faraday Soc. **28**, 136–141 (1959)
45. Wertz, J.E., Savilly, G., Auzins, P., Orton, J.W.: Studies of point defects in Magnesium Oxide. J. Phys. Soc. Jpn. **18**(2), 305–311 (1963)
46. Chen, Y., Sibley, W.A.: Study of ionization-induced radiation damage in MgO. Phys. Rev. **154**(3), 842–850 (1967)

47. Wertz, J.E., Auzins, P.: Trapped hole centre containing fluorine in Magnesium Oxide. Phys. Rev. A **139**(5), 1645–1647 (1965)
48. Izen, E.H., Mazo, R.L., Kemp, J.C.: Electron paramagnetic resonance and magnetic circular dichroism double resonance of V-centre in MgO. J. Phys. Chem. Solids **34**(8), 1431–1440 (1973)
49. Henderson, B., Bowen, D.H., Briggs, A., King, R.D.: Radiation damage Magnesium Oxide. II. Effect of Pre-irradiation Annealing in Hydrogen. J. Phys. C Solid State Phys. **4**(12), 1496–1504 (1971)
50. Kappers, L.A., Wertz, J.E.: Thermal decay of the Vqh centres in MgO. Solid State Commun. **9**(20), 1755–1758 (1971)
51. Henderson, B., Kolopus, J.L., Unruh, W.P.: Studies of OH- and OD-ions in Magnesium Oxide. The structure of the Vqd centre. J. Chem. Phys. **55**, 3519–3524 (1971)
52. O'Mara, W.C., Davies, J.J., Wertz, J.E.: Structure of the fluorine-containing trapped hole centre in Magnesium Oxide. Phys. Rev. **179**(3), 816–818 (1968)
53. Schoenlerg, A., Suss, J.T., Szapiro, S., Luz, Z.: Oxigen-17 hyperfine interaction of the V_F centre in MgO. Phys. Rev. Lett. **24**, 1641–1643 (1971)
54. Kelli, B.: Radiation Damage to Solids. Atomizdat, Moscow (1970)
55. Unruh, W.P., Chen, Y., Abraham, M.M.: V_{a1} and V^- centres in MgO. Phys. Rev. Lett. **30**(10), 446–449 (1973)
56. Abraham, M.M., Chen, Y., Unruh, W.P.: Formation and stability of V^- and V_{Al} centres in MgO. Phys. Rev. B **9**, 1842–1852 (1974)
57. DuVarney, R.C., Garrison, A.K.: Electron-nuclear-double-resonance of the V_{Al} centres in MgO. Solid State Commun. **12**(11), 1235–1237 (1973)
58. Henderson, B.: Trapped hole centre in the Alkaline Earth Oxides. J. Phys. C Solid State Phys. **9**, 1579–1583 (1976)
59. Abraham, M.M., Chen, Y., Unruh, W.P.: Electron-nuclear-double-resonance investigation of $[Li]^0$ and $[Na]^0$ centres in MgO, CaO, and SrO. Phys. Rev. B **10**, 3540–3545 (1974)
60. Abraham, M.M., Chen, Y., Kolopus, J.L., Tohver, H.T.: Radiation-induced $[Na]^0$ centres in MgO and CaO. Phys. Rev. B **5**, 4945–4951 (1972)
61. Kappers, L.A., Dravnieks, F., Wertz, J.E.: Electron spin resonance and optical studies of the double hole (V0) centre in MgO. J. Phys. C Solid State Phys. **7**(7), 1387–1399 (2001)
62. Kappers, L.A., Dravnieks, F., Wertz, J.E.: Optical absorption of the V_{0H} centre in MgO. Solid State Commun. **10**(12), 1265–1269 (1972)
63. Sibley, W.A., Kolopus, J.L., Mallard, W.C.: A study of the effect of deformation on the E.S.R., luminescence and absorption of MgO single crystals. Basic Solid State Phys. **31**(1), 223–231 (1969)
64. Chen, Y., Abraham, M.M., Templeton, L.C., Sounder, E.: Effect of plastic deformation on hole-defect formation in MgO. Solid State Commun. **18**, 61–65 (1976)
65. Abraham, M.M., Chen, Y., Boother, L.A., Reynolds, R.W.: Stable [Li]° defect in MgO single crystals. Phys. Rev. Lett. **37**(13), 849–852 (1976)
66. Modin, F.A.: Stress-induced optical dichroism of [Li]° defects in MgO. Phys. Rev. B **16**(12), 5528–5534 (1977)
67. Kyarner, T.H., Sorokin, B.A.: Hole processes in MgO crystals during photostimulated luminescence and electron emission. Russ. Phys. J. **20**(9), 2698–2699 (1978)
68. Chen, Y., Tohner, H.T., Narayan, J., Abraham, M.M.: High-temperature and ionization-induced effects in lithium-doped single inter crystals. Phys. Rev. B **16**(12), 5535–5542 (1977)
69. Kalder, K.L., Kyarner, T.N., Lushchik, Ch.B., Malysheva, A.V., Milenina, R.V.: Korotkovol-novaya lyuminescenciya kristallov MgO. J. Appl. Spectrosc. **25**(1), 639–644 (1976)
70. Searle, TM, Glass, A.M.: The thermal decay of the V' centre in MgO. J. Phys. Chem. Solids **29**(4), 609–614 (1968)
71. Halliburton, L.E., Kappers, L.A.: Radiation-included oxygen interstates in MgO. Solid State Commun. **26**(2), 111–114 (1978)

72. Kyarner, T.N.: Recombination luminescence and paramagnetic centers in irradiated MgO crystals. The thesis, Estonia, Tartu (1979)
73. Blazey, K.W.: Optical absorption of MgO: Fe. J. Phys. Chem. Solids **38**, 671–675 (1974)
74. Jones, G.D.: Jan-teller splitting in the optical absorption spectra of divalent iron compounds. Phys. Rev. **155**(2), 259–261 (1967)
75. Modin, F.A., Sender, E: Weeks RA Determination of the Fe^{+3} and Fe^{+2} concentration in MgO. J. Appl. Phys. **48**(8), 3514–3518 (1977)
76. Soshea, R.W., Dekker, A.J., Strutz, J.P.: X-ray colour centers in MgO. J. Phys. Chem. Solids **5**(1–2), 23–33 (1958)
77. Cheng, J.C., Kemp, R.D.: Magnetic-optical study of the spin-lattice relaxation of Fe^{3+} in MgO. Phys. Rev. B **4**(9), 2841–2846 (1971)
78. Henderson, B., King, R.D., Stoneham, A.M.: The temperature dependence of the F-band in Magnesium Oxide. J. Phys. C Solid State Phys. **1**(3), 586–593 (1968)
79. Evans, B.D.: Spectral study of Ne^{+} bombarded crystalline MgO. Phys. Rev. B **9**(12), 5222–5235 (1974)
80. Lushchik, C.B., Kuusman, I.L., Kyarner, T.N. et al.: Electronic excitations and luminescence of magnesium oxide. Academy of Sciences of the Estonian SSR, Institute of Physics, Estonia, Tartu (1977)
81. Kyarner, T.N.: Thermal stability of hole centers and hole recombination luminescence of Mg, SaO, and SrO with various impurities. Academy of Sciences of the Estonian SSR, Institute of Physics, Estonia, Tartu (1977)
82. Mollencopf, H.C., Halliburton, L., Kohnke, E.E.: Initiation of exoelectron emission by thermally released holes in single crystal MgO. Phys. Status Solidi (a) **1**, 243–250 (1973)
83. Sibley, W.A.: Radiation damage in oxide and other materials. IEEE Trans. Nucl. Sci. **18**(6), 273–280 (1971)
84. Kuznetsov, A.S., Yaek, I.V.: Stabilization of radiation atomic Frenkel defects in MgO crystals by Fe^{+} ions. Mezhdunarodnaya Kniga **18**(11), 3522–3525 (1976)
85. Rius, C, Cox, R.: Mise on evidence D'un lon molecular $(OF)^{2-}$ Dans la magnesia irradiee aux neutrons. Phys. Lett. **27A**(2), 76–77 (1968)
86. Rius, C., Cox, R., Freund, P., Owen, J.: An electron spin resonance study of the $(OF)^{2-}$ molecular ion in neutron- irradiated ^{17}O-enriched MgO. J. Phys. C Solid State Phys. **7**(3), 581–588 (2001)
87. Seman, B.O., Rejfman, S.P., Lekhto, T.P.: Electron paramagnetic resonance of O_2- centers in SrO crystals. Russ. Phys. J. **22**(8), 2244–2249 (1980)
88. Hall, TPP: Studies of neutron irradiation damage in CaO. J. Phys. C Solid State Phys. **8**(12), 1921–1927 (1975)
89. Bowen, D.H., Klaekr, F.J.P.: The growth of neutron irradiated Magnesium Oxide. Phil. Mag. **9**(9), 413–421 (1964)
90. Kuznetsov, A.S., Kil'k, A.V.: Formation of intrinsic defects in MgO crystals under the influence of X-ray radiation. Technical. Phys. **17**(2), 607–609 (1977)
91. Tyapunina, N.A., Tselebrovskyi, A.N.: Vliyanie plasticheskoj deformacii na koncentraciyu tochechnyh defektov v kristallah KBr. Sov. Phys. Crystallogr. **21**(1), 221–222 (1976)
92. Baubekova, G., Lushchik, A., Asylbaev, R., Akilbekov, A.: Creation of radiation defects in MgO crystals irradiated with swift heavy ions. Bulletin of L.N. Gumilyov Eurasian National University. Phys. Astron. Ser. **128**, 41–48 (2019). 10.32523/2616-68-36-2019-128-3-41-48
93. Wertz, J.E., Orton, J.W., Auzins, P: Spin resonance of point defect in MgO. J. Appl. Phys. **33**(1), 320–328 (1962)
94. Sosin, A., Neely, H.H.: Influence of foreign solute atoms on stage I. 94. Recovery in electron-irradiated copper. Phys. Rev. **127**, 1465–1470 (1962)
95. Chen, Y., Trueblood, D.L., Schow, O.E., Tohver, H.I.: Colour centers in electron irradiated MgO. J. Phys. C Solid State Phys. **3**(12), 2501–2508 (1979)
96. Tompson, M.: Defects and Radiation Damage in Metals. Mir, Moscow (1971)
97. Pooley, D.: F-center production in Alkali Halides by electron-hole recombination and subsequent 110 replacement sequence: a discussion of the electron-hole recombination. Proc. Phys. Soc. **87**, 245–256 (1966)

98. Evans, B.D., Comas, J., Malberg, P.R.: Coloration induced in MgO by MeV $^{20}Ne^{+}$ Bombardment. Phys. Rev. B **6**(6), 2453–2462 (1972)
99. Turner, T.A.: Study of the effect of deformation on optical absorption of MgO single crystals. Phys. Status Solidi **58**, 843–857 (1973)
100. Peria, W.T.: Optical absorption and photoconductivity in Magnesium Oxide crystals. Phys. Rev. J. **112**(2), 423–433 (1958)
101. Clarke, F.P.: Irradiation damage in single crystals of Magnesium Oxide. Philos. Mag. Phil. Mag. **17**, 607–627 (1957)
102. Lushchik, C.B., Vale, G.K., Elango, M.A.: Electronic excitations of ionic crystals and elementary mechanisms for the creation of color centers. Bull. Acad. Sci. USSR. Phys. Ser. **31**(5), 820–828 (1967)
103. Lushchik, C.B.: Intrinsic electronic excitations and defects of ionic crystals. Academy of Sciences of the Estonian SSR, Institute of Physics, Estonia, Tartu, 54–63 (1978)
104. Lushchik, Ch.B., Lnid'ya, G.G., Elango, M.A.: Electron-hole mechanism for creating color centers in ionic crystals. Russ. Phys. J. **6**, 2256–2262 (1964)
105. Kuusman, I.L., Lushchik, Ch.B. Intrinsic luminescence of ionic crystals with self-trapped excitons. **40**(9), 1785–1791 (1976)
106. Hughes, AE: Production of Oxygen vacancies by elastic collisions in Alkaline Earth Oxides. J. Phys. C Solid State Phys. **34**(11–12), 515–518 (1973)
107. Peercy, P.S.: Photon-induced X-ray measurements in ion implanted MgO. Defect in insulating crystals. In: Proceedings of the international conference on defects in insulating crystals, p. 335; Gatlinburg, TN, USA (1977)
108. Hersh, H.: Proposed excitonic mechanism of color center formation in Alkali Halides. Phys. Rev. **148**, 928–932 (1966)
109. Sharp, J.V., Rumsby, D.: Electron irradiation damage in Magnesium Oxide. Radiat. Eff. **17**(1–2), 65–68 (1973)
110. Chen, Y., Abraham, M.M., Templeton, L.C., Unruh, W.P.: Role of hydrogen and deuterium on the V^{-} -center formation in MgO. Phys. Rev. B **11**(2), 881–890 (1975)
111. Chen, Y., Abraham, M.M., Tohver, H.T.: Radiation-induced diffusion of hydrogen and deuterium in MgO. Phys. Rev. Lett. **37**(26), 1557–1560 (1976)
112. Dergobuzov, K.A., Puhov, A.M., Yakovleva, A.V., et al.: Intense electron beam spectrometer. Instrum. Exp. Tech. **1**, 29–30 (1975)
113. Epshtejn, M.I.: Izmerenie Opticheskogo Izlucheniya m Elektronike. Energiya, Moscow (1975)
114. Gol'danskij, V.I., Kuznetsov, A.V., Podgorodeckij, M.I.: Statistics of Reports When Registering Nuclear Particles. Fizmatizdat, Moscow (1959)
115. Hudson, D.: Statistics for Physicists. Mir, Moscow (1970)
116. Akkerman, A.F., Nikitushev, Yu.M., Botvin, V.A.: Solving the Problems of Fast Electron Transfer in Matter Using the Monte Carlo Method. Nauka, Alma-Ata (1972)
117. Baranov, V.F.: Electron Radiation Dosimetry. Atomizdat, Moscow (1974)
118. Vavilov, B.C., Uhin, H.A.: Radiation Effects in Semiconductors. Atomizdat, Moscow (1969)
119. Sveshnikov, A.A. (ed.): Collection of Problems on Probability Theory, Mathematical Statistics and the Theory of Random Fluctuations. Nauka, Moscow (1970)
120. Hensli, V.F., Dzhonson, Yu.S.: Radiation Chemistry. Atomizdat, Moscow (1974)
121. Kozlov, V.F., Troshkin, Yu.S.: Radiation Safety Handbook. Atomizdat, Moscow (1967)
122. Gusev, N.G., Kimel', L.R., Mashkovich, V.P., et al.: Physical Basis of Radiation Protection. Atomizdat, Moscow (1969)
123. Pikaev, A.K.: Dosimetry in Radiation Chemistry. Atomizdat, Moscow (1975)
124. Gol'danskij, V.I.: Physical Chemistry of Positron and Positronium. Nauka, Moscow (1968)
125. Deans, J., Vinyard, J.: Radiation Effects in Solids. Inostrannaya literatura, Moscow (1960)
126. Lejman, K.: Interaction of Radiation with a Solid and the Formation of Elementary Defects. Atomizdat, Moscow (1979)
127. Kyarner, T.N., Malysheva, A.F., Maaros, A.A., et al.: Thermally stimulated luminescence of MGU single crystals in the temperature range 4.2–600 K. Tech. Phys. **22**(4), 1178–1183 (1980)

128. Annenkov, Yu.M., Pritulov, A.M., Frangul'yan, T.S., et al.: Photoluminescence of MgO crystals. Russ. Phys. J. **9**, 130–132 (1981)
129. Rozhanskij, V.N., Velednickaya, M.A., Shrajber, I., et al.: Local violation of the stoichiometry of the MgO crystal resulting from plastic deformation. Tech. Phys. **19**(7), 1980–1982 (1977)
130. Newton, R.D., Sibley, W.A.: Deformation induced damage in MgO. Phys. Status Solidi (a) **41**, 569–572 (1977)
131. Velednitskaya, M.A., Roshansku, V.N., Comolova, L.F., et al.: Investigation of the deformation mechanism of MgO crystals affected by concentrated load. Phys. Status Solidi (a) **32**, 123–132 (1975)
132. Starodubtsev, S.B., Romanov, A.M.: Passage of Charged Particles Through Matter. Bulletin of the Academy of Sciences of the Uzbekistan SSR, Tashkent (1962)
133. Rumshinskij, L.Z.: Mathematical Processing of Experimental Results. Nauka, Moskow (1971)
134. Spitsin, V.I., Ionova G.V., Barsova, L.I.: Possible structures of the hole center in irradiated magnesium oxide. Bulletin of the Academy of Sciences of the USSR. Chem. Ser. **6**, 1209–1214 (1976)
135. Henderson, B, Bowen, D.H.: Radiation damage in Magnesium Oxide. I dose dependence of reactor damage. J. Phys. C Solid State Phys. **4**(12), 1487–1495 (1971)
136. Spitsin, V.I., Barsova, L.I., Polova, G.B., et al.: Paramagnetic centers in v-irradiated magnesium oxide. Bull. Acad. Sci. USSR. Chem. Ser. **5**, 963–970 (1976)
137. Mallard, W.C., Crawford, J.H.: Thermostimulated currents and thermoelectric power in irradiated MgO. Solid State Commun. **7**, 1767–1770 (1969)
138. Mallard, W.C., Crawford, J.H.: Thermostimulated conductivity and trapping centers in irradiated MgO. J. Appl. Phys. **43**(5), 2060–2066 (1972)
139. Aduev, B.P., Vaisburd, D.I.: Creation and destruction of F^{2+} centers in life crystals under pulse irradiation with dense electron beams. Phys. Solid State **23**(6), 1869–1871 (1981)
140. Vorob'ev, A.A., Lisitsyn, V.M.: Radiation resistance of ionic crystalline materials. Russ. Phys. J. **8**, 85–90 (1977)
141. Mesyat, G.A. (ed.): High-power Nanosecond Pulsed Electron Sources. Nauka, Novosibirsk (1973)
142. Annenkov, Yu.M., Pritulov, A.M.: Formation of F-centers in MgO crystals upon irradiation with protons. Russ. Phys. J. **23**(4), 1065–1068 (1981)
143. Whitwort, R.W.: Charged dislocations in ionic crystals. Adv. Phys. **24**, 203–304 (1975)
144. Urusovskaya, A.A.: Electrical effects associated with plastic deformation of ionic crystals. Phys. Usp. **96**(1), 39–60 (1968)
145. Hirt, D.: Dislocation theory. Atomizdat, Moscow (1972)
146. Cantor, S.: Lattice energies of cubic alkaline-earth oxide. Affinity of oxygen for two electrons. J. Chem. Phys. **59**(9), 5189–5194 (1973)
147. Granzer, F., Wagner, G.: Eisen blatter S. atomistische berechnung der Core-Struktur, Core-Energie und Peierls-Spannung einer Stufenversetzung in NaCl. Phys. Status Solidi **30**(2), 587–600 (1968)
148. Arefiev, V.P., Etin, G.I.: Determination of the momentum density of electrons of matter using the positron annihilation method. Tech. Phys. **18**(11), 3532–3534 (1976)
149. Arefiev, V.P., Vorobiev, S.A., Etin, G.I.: Positron states in defective alkali halide crystals. Russ. Phys. J. **12**, 152–153 (1975). (In Russian)
150. Surzhikov, A.P., Pritulov, A.M.: Enhanced packing of ceramic ferrite mouldings during the sintering by a beam of accelerated electrons. J. Adv. Mater. **2**, 48–56 (1998). (in Russian)
151. Lysenko, E.N., Surzhikov, Vlasov, V.A., Malyshev, A.V., Nikolaev, E.V.: Thermal analysis study of solid-phase synthesis of zinc- and titanium-substituted lithium ferrites from mechanically activated reagents. J. Therm. Anal. Calorim. **122**, 1347–1353 (2015). 10.1007/s10973-015-4849-9
152. Surzhikov, A.P., Ghyngazov, S.A., Lysenko, E.N., Frangylyan, T.S.: Grain boundary diffusion in polycrystalline ferrites with different intergranular potential barrier. Russ. Phys. J. **47**(3), 319–323 (2004). https://doi.org/10.1023/B:RUPJ.0000038751.02769.1a

153. Lysenko, E., Nikolaev, E., Vlasov, V., Surzhikov, A.: Microstructure and reactivity of Fe_2O_3–Li_2CO_3–ZnO ferrite system ball-milled in a planetary mill. Thermochim. Acta **664**, 100–107 (2018). https://doi.org/10.1016/j.tca.2018.04.015
154. Lysenko, E.N., Malyshev, A.V., Vlasov, V.A., Nikolaev, E.V., Surzhikov, A.P.: Microstructure and thermal analysis of lithium ferrite pre-milled in a high-energy ball mill. J. Therm. Anal. Calorim. **134**(1), 127–133 (2018). https://doi.org/10.1007/s10973-018-7549-4
155. Surzhikov, A.P., Pritulov, A.M., Lysenko, E.N., Sokolovskiy, A.N., Vlasov, V.A., Vasendina, E.A.: Calorimetric investigation of radiation-thermal synthesized lithium pentaferrite. J. Therm. Anal. Calorim. **101**(1), 11–13 (2010). https://doi.org/10.1007/s10973-010-0788-7
156. Surzhikov, A.P., Frangulyan, T.S., Ghyngazov, S.A., Lisenko, E.N., Galtseva, O.V.: Physics of magnetic phenomena: investigation of electroconductivity of lithium pentaferrite. Russ. Phys. J. **49**(5), 506–510 (2006). https://doi.org/10.1007/s11182-006-0133-6
157. Surzhikov, A.P., Peshev, V.V., Pritulov, A.M., Gyngazov, S.A.: Grain-boundary diffusion of oxygen in polycrystalline ferrites. Russ. Phys. J. **42**(5), 490–495 (1999). https://doi.org/10.1007/BF02508222
158. Surzhikov, A.P., Lysenko, E.N., Malyshev, A.V., Vasiljeva, O.G., Pritulov, A.M.: Influence of mechanical activation of initial reagents on synthesis of lithium ferrite. Russ. Phys. J. **55**(6), 672–678 (2012). https://doi.org/10.1007/s11182-012-9865-7
159. Surzhikov, A.P., Lysenko, E.N., Vlasov, V.A., Vasendina, E.A.: Analysis of the phase composition and homogeneity of ferrite lithium-substituted powders by the thermomagnetometry method. J. Therm. Anal. Calorim. **112**(2), 739–746 (2013). https://doi.org/10.1007/s10973-012-2618-6
160. Surzhikov, A.P., Lysenko, E.N., Malyshev, A.V., Vlasov, V.A., Suslyaev, V.I., Zhuravlev, V.A., Korovin, E.Y., Dotsenko, O.A.: Study of the radio-wave absorbing properties of a lithium-zinc ferrite based composite. Russ. Phys. J. **57**(5), 621–626 (2014). https://doi.org/10.1007/s11182-014-0284-9
161. Lysenko, E.N., Surzhikov, A.P., Vlasov, V.A., et al.: Synthesis of substituted lithium ferrites under the pulsed and continuous electron beam heating. Nucl. Instrum. Methods Phys. Res. Sect. B **392**, 1–7 (2017). https://doi.org/10.1016/j.nimb.2016.11.042
162. Surzhikov, A.P., Frangulyan, T.S., Ghyngazov, S.A., Lysenko, E.N.: Investigation of oxidation processes in non-stoichiometric lithium-titanium ferrites using TG analysis. J. Therm. Anal. Calorim. **102**(3), 883–887 (2010). https://doi.org/10.1007/s10973-010-0912-8
163. Surzhikov, A.P., Lysenko, E.N., Vasendina, E.A., Sokolovskii, A.N., Vlasov, V.A., Pritulov, A.M.: Thermogravimetric investigation of the effect of annealing conditions on the soft ferrite phase homogeneity. J. Therm. Anal. Calorim. **104**(2), 613–617 (2011). https://doi.org/10.1007/s10973-010-1074-4.doi:10.1007/s10973-010-1074-4
164. Surzhikov, A.P., Pritulov, A.M., Lysenko, E.N., et al.: Dependence of lithium–zinc ferrospinel phase composition on the duration of synthesis in an accelerated electron beam. J. Therm. Anal. Calorim. **110**(2), 733–739 (2012). https://doi.org/10.1007/s10973-011-1947-1
165. Surzhikov, A.P., Lysenko, E.N., Vlasov, V.A., Malyshev, A.V., Nikolaev, E.V.: Investigation of the process of ferrite formation in the Li_2CO_3–ZnO–Fe_2O_3 system under high-energy actions. Russ. Phys. J. **56**(6), 681–685 (2013). https://doi.org/10.1007/s11182-013-0085-6
166. Surzhikov, A.P., Galtseva, O.V., Vasendina, E.A., Vlasov, V.A., Nikolaev, E.V.: Processing line for industrial radiation-thermal synthesis of doped lithium ferrite powders. IOP Conf. Ser. Mater. Sci. Eng. **110**(123), 012002 (2015). https://doi.org/10.1088/1757-899X/110/1/012002
167. Surzhikov, A.P., Frangylyan, T.S., Ghyngazov, S.A.: A dilatometric study of the effect of pressing on the kinetics of compression of ultrafine zirconium doxide powders under thermal annealing. Russ. Phys. J. **55**(4), 345–352 (2012). https://doi.org/10.1007/s11182-012-9818-1
168. Surzhikov, A.P., Ghyngazov, S.A., Frangulyan, T.S., Vasil'ev, I.P., Chernyavskii, A.V.: Investigation of sintering behavior of ZrO2 (Y) ceramic green body by means of non-isothermal dilatometry and thermokinetic analysis. J. Therm. Anal. Calorim. **128**(2), 787–794 (2017). 10.1007/s10973-016-5966-9

169. Kalytka, V., Baimukhanov, Z., Neshina, Y., et al.: Influence of quantum effects on dielectric relaxation in functional electrical and electric energy elements based on proton semiconductors and dielectrics. Appl. Sci. **13**, 8755 (2023). https://doi.org/10.3390/app13158755
170. Bordunov, S., Fedorchuk, Y., Galtseva, O., Narimanova, G.: Technology of gold extraction from clay ore and technogenic raw materials. Eng. Mater. **F1222**, 61–70 (2023). https://doi.org/10.1007/978-3-031-38964-1_4
171. Atyaksheva, A., Sarsikeyev, Y., Atyaksheva, A., Galtseva, O., Rogachev, A.: The study of the dependence of optimal structure of composite materials containing hollow aluminosilicate microspheres on humidity. Micro Nanosystems **13**(4), 385–392 (2021). https://doi.org/10.2174/1876402912999201109204218
172. Kuzmina, L., Gazenaur, E., Krasheninin, V., Galtseva, O., Gazenaur, N.: Combined treatment of energy-saturated materials in external fields. J. Phys. Conf. Ser. **1499**(1), 012040 (2020). https://doi.org/10.1088/1742-6596/1499/1/012040
173. Wang, S., Rogachev, AA, Yarmolenko, M.A, et al.: Structure and properties of polyaniline nanocomposite coatings containing gold nanoparticles formed by low-energy electron beam deposition. Appl. Surf. Sci. **428**, 1070–1078 (2018). https://doi.org/10.1016/j.apsusc.2017.09.225
174. Lysenko, E.N., Nikolaev, E., Surzhikov, A., Minina, J. Magnetization study of Li0.5Fe2.5O4 ferrite synthesized by the electron-beam heating of mechanically activated Fe_2O_3–Li_2CO_3 mixture. Eng. Mater. F1222, 71–80 (2023). 10.1007/978-3-031-38964-1_5
175. Nikolaev, E., Lysenko, E.N., Surzhikov, A., Bobuyok, S.: The influence of thermomagnetometric measurement conditions on the recorded curie temperature of cobalt-zinc ferrite. Eng. Mater. **F1222**, 1–10 (2023). https://doi.org/10.1007/978-3-031-38964-1_1
176. Surzhikov, A.P., Pritulov, A.M., Lysenko, E.N., Sokolovskii, A.N., Vlasov, V.A., Vasendina, E.A.: Influence of solid-phase ferritization method on phase composition of lithium-zinc ferrites with various concentration of zinc. J. Therm. Anal. Calorim. **109**(1), 63–67 (2012). https://doi.org/10.1007/s10973-011-1366-3